

Title	Studies on the electrode reactions of molybdenum(VI) in aqueous acidic solutions
Author(s)	Yokoi, Kunihiko
Citation	大阪大学, 1984, 博士論文
Version Type	VoR
URL	<a href="https://hdl.handle.net/11094/34856">https://hdl.handle.net/11094/34856</a>
rights	
Note	

*Osaka University Knowledge Archive : OUKA*

<https://ir.library.osaka-u.ac.jp/>

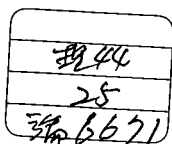
Osaka University

Studies on the electrode reactions of  
molybdenum(VI) in aqueous acidic solutions

by  
Kunihiko YOKOI

Osaka Kyoiku University

1984



## Contents

Chapter I.	General introduction	- - - - -	1
	References	- - - - -	5
Chapter II.	Direct current polarographic study of		
	Mo(VI) in acidic solution	- - - - -	9
II-1.	Introduction	- - - - -	9
II-2.	Experimental	- - - - -	10
II-3.	Results	- - - - -	11
II-4.	Discussion	- - - - -	34
II-4-1.	Reduction mechanisms	- - - - -	34
II-4-2.	Species of reactants	- - - - -	36
II-4-3.	Catalytically active species	- - - - -	40
II-5.	References	- - - - -	42
Chapter III.	Differential pulse and alternating		
	current polarographic study of Mo(VI)		
	in acidic solution	- - - - -	44
III-1.	Introduction	- - - - -	44
III-2.	Experimental	- - - - -	44
III-3.	Results	- - - - -	45
III-4.	Discussion	- - - - -	55
III-4-1.	Adsorption of Mo complexes	- - - - -	55
III-4-2.	Effect of ionic surfactants	- - - - -	57

III-4-3.	Species of reactants	- - - - -	57
III-5.	References	- - - - -	59
Chapter IV.	The analysis of the character of catalytically active electrogenerated Mo(V)	- - - - -	60
IV-1.	Introduction	- - - - -	60
IV-2.	Experimental	- - - - -	61
IV-3.	Results	- - - - -	62
IV-3-1.	Polarographic catalytic current	- - -	62
IV-3-2.	Absorption spectra of Mo(V)	- - - - -	65
IV-3-3.	Dimer-dimer-monomer equilibria of Mo(V)		68
IV-3-4.	Oxidation of monomeric Mo(V) with perchlorate	- - - - -	72
IV-4.	Discussion	- - - - -	76
Appendix 1.	Koutecky's treatment for the polarographic catalytic reaction		81
IV-5.	References	- - - - -	84
Chapter V.	The analysis of wave 4	- - - - -	86
V-1.	Introduction	- - - - -	86
V-2.	Experimental	- - - - -	86
V-3.	Results	- - - - -	87
V-4.	Discussion	- - - - -	99
Appendix 2.	The rotating ring-disc electrode and the collection efficiency	- - - - -	106

V-5.	References	- - - - -	108
Chapter VI.	Summary	- - - - -	109
	Acknowledgement	- - - - -	111
	Papers relevant to the present study	- -	112

## I General introduction

There have been many investigations about the polarography of hexavalent molybdenum ion in aqueous solution [1-32]. For analytical purposes various procedures were proposed for the quantification of Mo(VI) in solutions [1-16]. In neutral or alkaline solutions, molybdenum species exists in the form of monomeric anion,  $\text{MoO}_4^{2-}$ , and this species gives no polarographic reduction waves. While in acidic solutions, different kinds of polarographic reduction behavior of Mo(VI) were observed as the functions of the acidity, the concentration of Mo(VI) and of the coexisting anion. It is also well known that the polarographic catalytic wave is observed in the presence of nitrate or perchlorate [4,6-12,17-19] and this phenomena could be applied to the determination of trace amounts of molybdenum ( $2 \times 10^{-9}\text{M}$  [10]). In about 0.1M hydrochloric or sulfuric acid solutions, three reduction waves were observed for Mo(VI) solution. The first (most easily reducible) wave has been conclusively assigned to be due to the reduction of Mo(VI) to Mo(V). As for the second wave, five different mechanisms have been proposed so far: (1) reduction of Mo(VI) to Mo(IV) [20,21]; (2) of Mo(V) to Mo(IV) [7]; (3) of Mo(V) to Mo(III) [8,22-26]; (4) of Mo(VI) to Mo(III) and then Mo(III) reacts with Mo(VI) to produce Mo(V) [27,29]; (5) of Mo(VI) to Mo(II),

reacting successively with Mo(VI) to produce Mo(V) [30]. The interpretation of the third wave was dependent on analytical results of the reaction product introduced by the second wave and the following three reaction mechanisms have been proposed so far, that is, the reduction of Mo(V) to Mo(III), of Mo(V) to Mo(II) or of Mo(IV) to Mo(III). The existing of so many dispersed conclusions in the interpretation of electrode reactions of Mo(VI) is the evidence of the misunderstandings of the reduction mechanism due to the development of complicated phenomena as the functions of the acidity, the concentration of the depolarizer and of coexisting anion.

In the polarographic investigations of molybdenum, there has been few reports referring to the characteristic of the electroactive species for each reduction step. When the acidity of the solution is increased from neutral, the dissolved species is transformed from  $\text{MoO}_4^{2-}$  to  $\text{Mo}_7\text{O}_{24}^{6-}$  [33-35],  $\text{Mo}_8\text{O}_{26}^{4-}$  [36-38],  $\text{Mo}_6\text{O}_{19}^{2-}$  [39] and cationic monomer or dimer [40.41]. These species have been identified by potentiometry, Raman spectroscopy and spectrophotometry. In hydrochloric acid solution the chloro complex of molybdenum ion is considered to be the main species [38,42,43] and the first polarographic reduction wave is overlapped with the oxidation wave of Hg to  $\text{Hg}_2\text{Cl}_2$ , so hydrochloric acid media is not suitable for the polarographic investigation of the

characteristics of the electroactive oxomolybdenum species. In nitric acid or perchloric acid solution little complex forming is to be expected, but these acid promote the catalytic enhancement of the second reduction wave, and then sulfuric acid media seems to be most suitable.

In biological chemistry molybdenum is known to act as a redox catalyst in some enzymes [44], and electrochemical techniques have often been used for the investigation of the redox behavior of molybdenum in model-compounds of enzymes [45-50]. Concerning to the polarographic catalytic reduction of nitrate or perchlorate ion in the presence of Mo(VI) in aqueous acidic solution, no precise analysis of the active species molybdenum at the electrode has been reported.

As described above, polarographic reduction waves of Mo(VI) show complex behavior depending on the composition of solutions. When a chemical reaction is involved in the process of electrode reaction, it is probable that the electrochemical behavior is easily affected by the change of the composition of solutions. Some authors have described the chemical reaction in the process of the electrode reaction of Mo(VI) [27-30], however, their interpretation was qualitative and not conclusive. So it is necessary to investigate the chemical reactions in detail to elucidate the electrode reaction mechanism.



Consequently, the objects of this work are: (1) to examine the polarographic behavior of Mo(VI) in sulfuric acid media and to analyze the reduction mechanism; (2) to obtain information about the electroactive species; (3) to establish the polarographic catalytic reaction mechanism of molybdenum in the presence of nitrate or perchlorate; (4) to elucidate the reaction mechanism of the chemical reaction involved in the electrode reaction.

In addition to polarography, other voltammetric technique, such as cyclic voltammetry or voltammetry with a rotating ring-disc electrode, may be useful. With these voltammetry, it is possible to study the oxidation reaction or the transformation of the electrode reduction product [51].

## References

1. J.B.Hedridge and D.P.Hubbard, *Analyst*, 90 (1965) 173.
2. D.L.Manning, R.G.Ball and O.Menis, *Anal.Chem.*, 32 (1960) 1247.
3. E.P.Parry and M.G.Yakubik, *Anal.Chem.*, 26 (1954) 1294.
4. P.L.Buldini and D.Ferri, *Anal.Chim.Acta*, 124 (1981) 233.
5. R.L.Pecsok and R.M.Parkhurst, *Anal.Chem.*, 27 (1955) 1920.
6. P.Lanza, D.Ferri and P.L.Buldini, *Analyst*, 105 (1980) 379.
7. G.P.Haight, Jr., *Anal.Chem.*, 23 (1951) 1505.
8. M.G.Johnson and R.J.Robinson, *Anal.Chem.*, 24 (1952) 366.
9. G.D.Christian, J.L.Vandenbalck and G.J.Patriarche, *Anal.Chim.Acta*, 108 (1979) 149.
10. T.E.Edmonds, *Anal.Chim.Acta*, 116 (1980) 323.
11. P.Jost, P.Lagrange, M.Wolff and J.P.Schwing, *J.Less-Common Met.*, 36 (1974) 169.
12. A.T.Violanda and W.D.Cooke, *Anal.Chem.*, 36 (1964) 2287.
13. L.Meites, *Anal.Chem.*, 25 (1953) 1753.
14. K.Ogura, Y.Enaka and K.Morimoto, *Electrochim.Acta*, 23 (1978) 289.
15. V.S.N.Rao and S.B.Rao, *Talanta*, 26 (1979) 502.
16. P.Bosserman, D.T.Sawyer and A.L.Page, *Anal.Chem.*, 50 (1978) 1300.

17. E.W.Zahnow and R.J.Robinson, *J.Electroanal.Chem.*,  
3 (1962) 263.
18. I.M.Kolthoff and I.Hodara, *J.Electroanal.Chem.*, 5 (1963) 2.
19. G.P.Haight,Jr., *Acta Chem.Scand.*, 15 (1961) 2012.
20. G.P.Haight,Jr., *J.Inorg.Nucl.Chem.*, 24 (1962) 673.
21. J.J.Wittick and G.A.Rechnitz, *Anal.Chem.*, 37 (1965) 816.
22. C.M.Gupta and J.K.Gupta, *J.Ind.Chem.Soc.*, 44 (1967) 526.
23. M.N.Hull, *J.Electroanal.Chem.*, 51 (1974) 57.
24. Von G.Henrion, F.Scholtz, R.Stösser and U.Ewert,  
*Z.Anorg.Allg.Chem.*, 467 (1980) 23.
25. R.Höltje and R.Geyer, *Z.Anorg.Allg.Chem.*, 246 (1941) 258.
26. I.M.Kolthoff and I.Hodara, *J.Electroanal.Chem.*,  
4 (1962) 369.
27. P.Souchay, *Talanta*, 12 (1965) 1187.
28. M.Lamache and P.Souchay, *J.Chim.Phys.*, 2 (1973) 384.
29. M.Lamache-Duhameaux, M.Cadiot and P.Souchay, *J.Chim.Phys.*,  
65 (1968) 1921.
30. M.Wolter, D.O.Wolf and M.Von Stackelberg, *J.Electroanal.*  
*Chem.*, 22 (1969) 221.
31. K.Ogura, Y.Enaka and T.Yosino, *Electrochim.Acta*,  
22 (1977) 509.
32. G.Elinany and D.S.Veselinović, *J.Electroanal.Chem.*,  
32 (1971) 437.

33. Y.Sasaki and L.G.Sillen, *Arkiv Kemi*, 29 (1968) 253.
34. Y.Sasaki and L.G.Sillen, *Acta Chem.Scand.*, 18 (1964) 1014.
35. Y.Sasaki, I.Lindqvist and L.G.Sillen, *J.Inorg.Nucl.Chem.*, 9 (1959) 93.
36. E.Pungor and A.Halasz, *J.Inorg.Nucl.Chem.*, 32 (1970) 1187.
37. W.P.Griffith and P.J.B.Lensniak, *J.Chem.Soc. (A)*, (1969) 1066.
38. J.Aveston, E.W.Anacker and J.S.Johnson, *Inorg.Chem.*, 3 (1964) 735.
39. K.Murata and S.Ikeda, *Spectrochim.Acta*, 39A (1983) 787.
40. J.J.Cruywagen, J.B.B.Heyns and E.F.C.H.Rohwer, *J.Inorg.Nucl.Chem.*, 40 (1978) 53.
41. J.F.Ojo, R.S.Taylor and A.G.Sykes, *J.Chem.Soc., Dalton*, (1975) 500.
42. W.P.Griffith and T.D.Wickins, *J.Chem.Soc. (A)*, (1967) 675.
43. H.M.Newmann and N.C.Cook, *J.Am.Chem.Soc.*, 79 (1957) 3026.
44. R.A.D.Wentworth, *Coord.Chem.Rev.*, 18 (1976) 1.
45. A.F.Isbell, Jr. and D.T.Sawyer, *Inorg.Chem.*, 11 (1971) 2449.
46. J.K.Howie and D.T.Sawyer, *ibid*, 15 (1976) 1892.
47. V.R.Ott, D.S.Swieter and F.A.Schultz, *ibid*, 16 (1977) 2538.
48. F.A.Schultz, V.R.Ott, D.S.Rolison, D.C.Bravard, J.W.McDonald and W.E.Newton, *ibid*, 17 (1978) 1758.
49. L.M.Charney and F.A.Schultz, *ibid*, 19 (1980) 1527.

50. L.M.Charney, H.O.Finklea and F.A.Schultz, *ibid*,  
21 (1982) 549.
51. Z.Galus, *Fundamentals of Electrochemical Analysis*,  
John Wiley and Sons Inc., 1976.

## II Direct current polarographic study of Mo(VI) in acidic solution

### II-1 Introduction

Multistep reduction waves are observed in acidic media and the mechanism of the electrode reaction remains subject to continuing arguments. Some authors have already performed the polarographic investigation of Mo(VI) in acidic solutions, but no interpretation of the electrode reduction mechanism of the species has been done clearly, as described in chapter I. A well-known catalytic wave develops in the presence of nitrate or perchlorate ion and is often utilized for the determination of trace amounts of molybdenum, however, this catalytic phenomena has not been understood, either. In dc polarography, the number of electrons in the electrode reaction has often been determined by the comparison of the relative height of each wave, but for Mo(VI) in acidic solution, multistep reduction waves may develop, changing features as a function of both the concentration of the reactant and the acidity of the media. Although polarography is a useful tool for the study of ions existing in solution in very dilute concentration, the additional methods are introduced in this study to obtain detailed information about the electrode reaction. Controlled potential

electrolysis ( CPE ) and spectrophotometric analysis are used to determine the equivalent electron number and reaction products in polarographic studies of Mo(VI) in sulfuric acid solution. In this chapter the precise investigation on the dc polarographic behavior of Mo(VI) in 0.1-5M sulfuric acid is described and the reduction mechanisms and accompanying phenomena are discussed.

## II-2 Experimental

The stock solution of hexavalent molybdenum ion was prepared from ammonium molybdate,  $(\text{NH}_4)_6\text{Mo}_7\text{O}_{24}\cdot 4\text{H}_2\text{O}$ , and its concentration was determined gravimetrically with 8-hydroxyquinoline [1]. Sulfuric acid was used as supporting electrolyte, and its factor was determined volumetrically with potassium hydrogenphthalate. Recrystallized sodium nitrate was used. All chemicals were of analytical reagent grade and used without further purification unless otherwise noted.

Polarographic and coulometric instruments employed in this study consisted of a home made potentiostat, a function generator and a coulometer, a Voltammetric Analyzer, Model P-1000 ( Yanagimoto Mfg. Co. Ltd. ) and an X-Y recorder ( Yokogawa Type 3086 ). For polarographic experiments a saturated calomel electrode ( SCE ) was used as a reference electrode and a platinum wire was used as a counter electrode.

The characteristics of a dropping mercury electrode at a mercury column height of 59.0cm were  $m = 1.40\text{mgs}^{-1}$ ,  $t = 5.76\text{s}$  in 0.1M  $\text{H}_2\text{SO}_4$  at -0.70V vs. SCE. An agar-salt bridge prepared from 0.1M  $\text{Na}_2\text{SO}_4$  solution was used as a junction between the SCE and the sample solution. No maximum suppressor was used. For CPE experiments an H-cell was used in which an Hg-pool working electrode and the Pt-wire counter electrode were separated by an agar-salt ( 0.1M  $\text{Na}_2\text{SO}_4$  ) bridge. An SCE was used as the reference electrode.

All measurements were carried out at  $25 \pm 0.1^\circ\text{C}$ . Dissolved oxygen was removed by bubbling oxygen-free nitrogen through the sample solution for 15min. before each polarographic measurement. During CPE measurements the sample solution was bubbled with nitrogen and stirred by a magnetic stirrer. The polarographic current values in this chapter were measured with no RC damping, i.e. the currents at the end of the drop life were measured unless otherwise noted.

The optical path length of the cell for spectrophotometric measurements was 1cm and a UVIDEC-500 UV/VIS digital spectrophotometer ( Japan Spectroscopic Co. ) was used.

### II-3 Results

The polarogram of 0.5mM Mo (VI) in 0.1M sulfuric acid is shown in Fig.II-1. Four reduction waves ( +0.09, -0.03,



-0.27 and -0.55V vs. SCE) are found. The waves are numbered according to the order of  $E_{1/2}$  (the half-wave potential) from positive to negative.

When the concentration of Mo(VI) ion,  $C_{\text{Mo(VI)}}$ , is 0.3mM, waves 1 and 2 overlap, so that apparently three waves are observed (curve 5 in Fig.II-2). The first wave (originating from waves 1 and 2 which are clearly distinguishable when  $C_{\text{Mo(VI)}}$  is  $> 0.3\text{mM}$ ) has a rounded shape which is different from that normally obtained for a diffusion controlled wave. When  $C_{\text{Mo(VI)}}$  is  $> 1.3\text{mM}$ , waves 2 and 3 overlap and the height of wave 1 is so small in comparison with that of other waves that apparently only two waves are observed in such high concentration of Mo(VI) solution.

The dependence of  $E_{1/2}$  for each wave on  $C_{\text{Mo(VI)}}$  in 0.1M  $\text{H}_2\text{SO}_4$  is shown in Fig.II-3. Wave 1 shows an adsorptive character in the higher  $C_{\text{Mo(VI)}}$  region, and the precise determination of  $E_{1/2}$  is difficult. The  $E_{1/2}$  of wave 2 shows large negative shift with the increase of  $C_{\text{Mo(VI)}}$ . The  $E_{1/2}$  of waves 3 and 4 are almost independent of  $C_{\text{Mo(VI)}}$  in the region of 0.05-2.0mM.

The dependence of wave heights on  $C_{\text{Mo(VI)}}$  in 0.1M  $\text{H}_2\text{SO}_4$  is shown in Fig.II-4. Since the waves overlap each other more or less as  $C_{\text{Mo(VI)}}$  changes, and wave 1 shows the adsorptive character, it is difficult to determine the height of each wave 1, 2 and 3 respectively. But the total

(13)

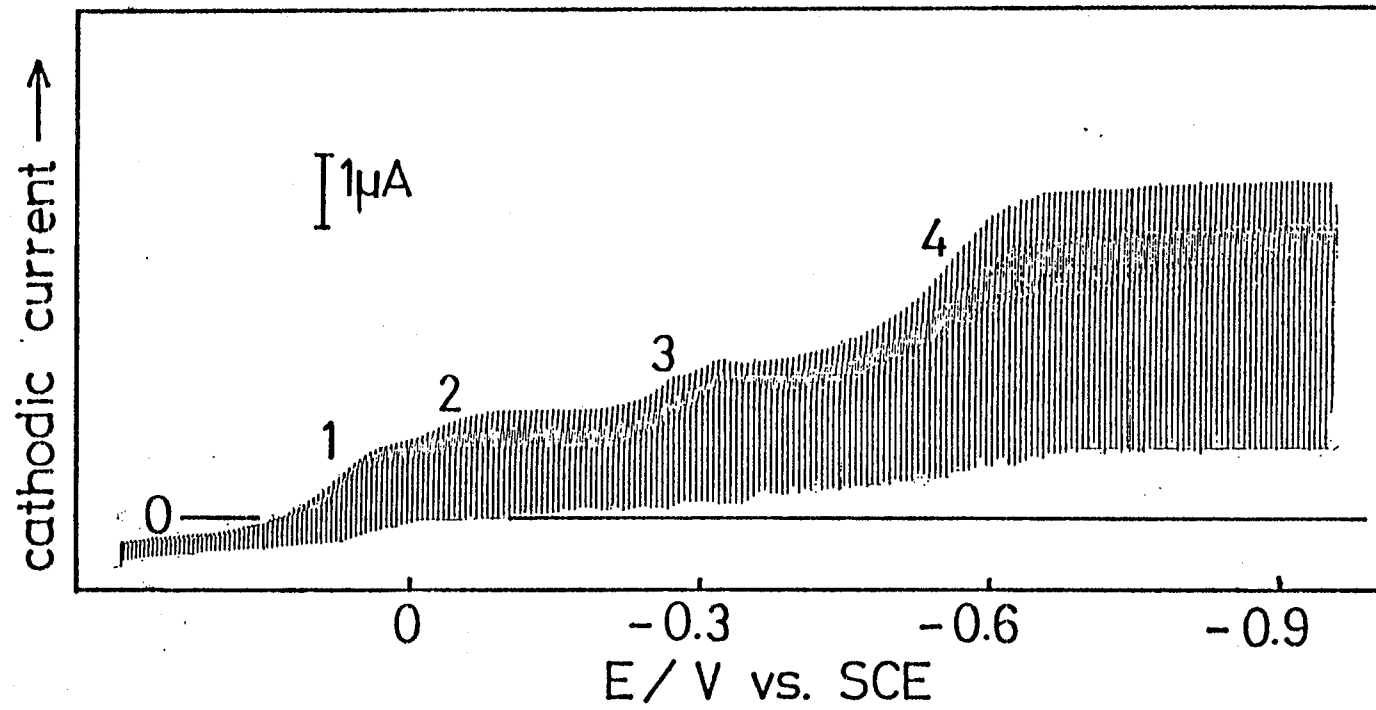


Fig.II-1. Polarogram of 0.5mM Mo(VI) in 0.1M H<sub>2</sub>SO<sub>4</sub>.

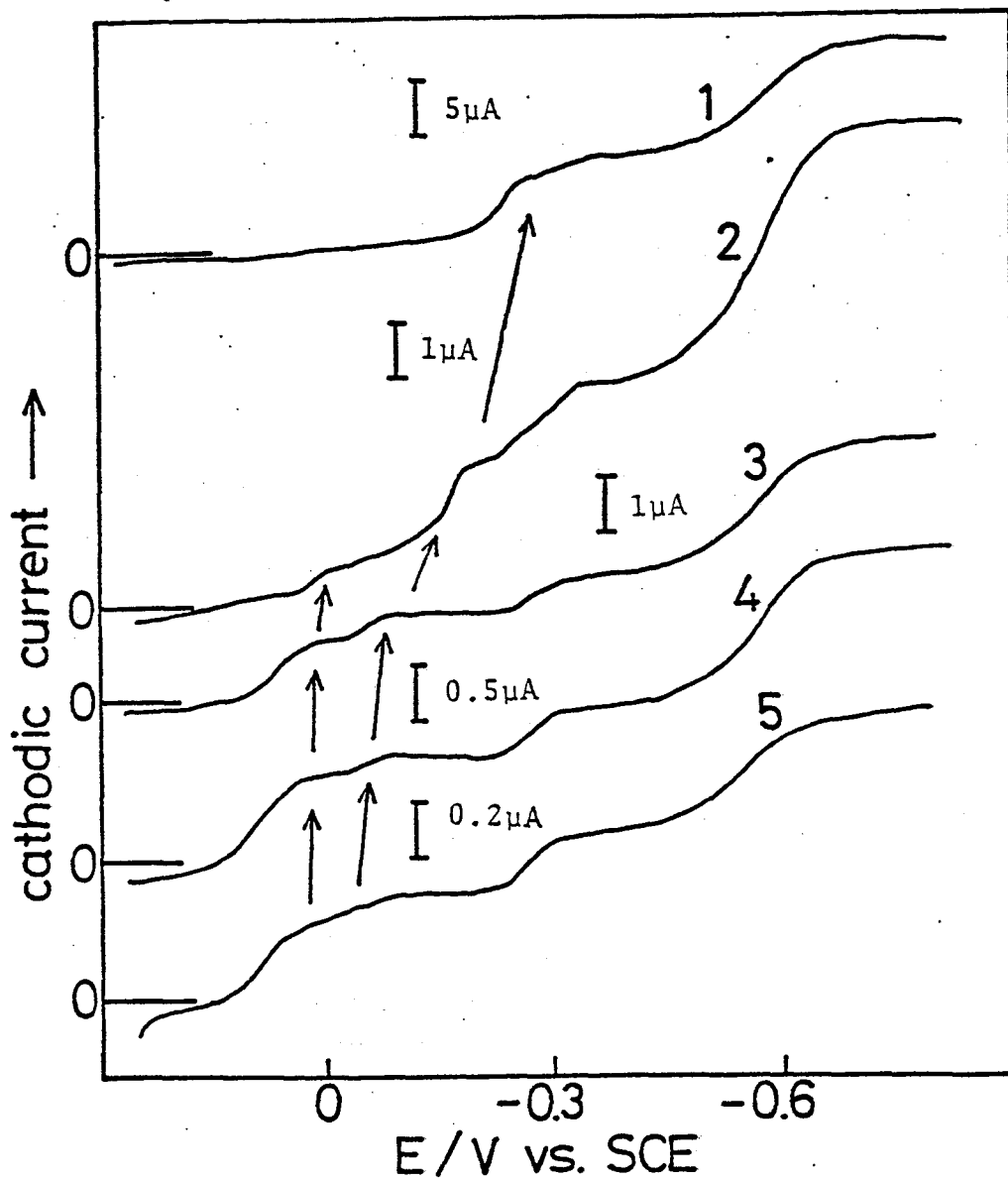


Fig.II-2. Polarograms of Mo(VI) in 0.1M H<sub>2</sub>SO<sub>4</sub>. C<sub>Mo(VI)</sub>:  
 (1) 2.0mM; (2) 0.9mM; (3) 0.5mM; (4) 0.3mM; (5) 0.1mM.

(15)

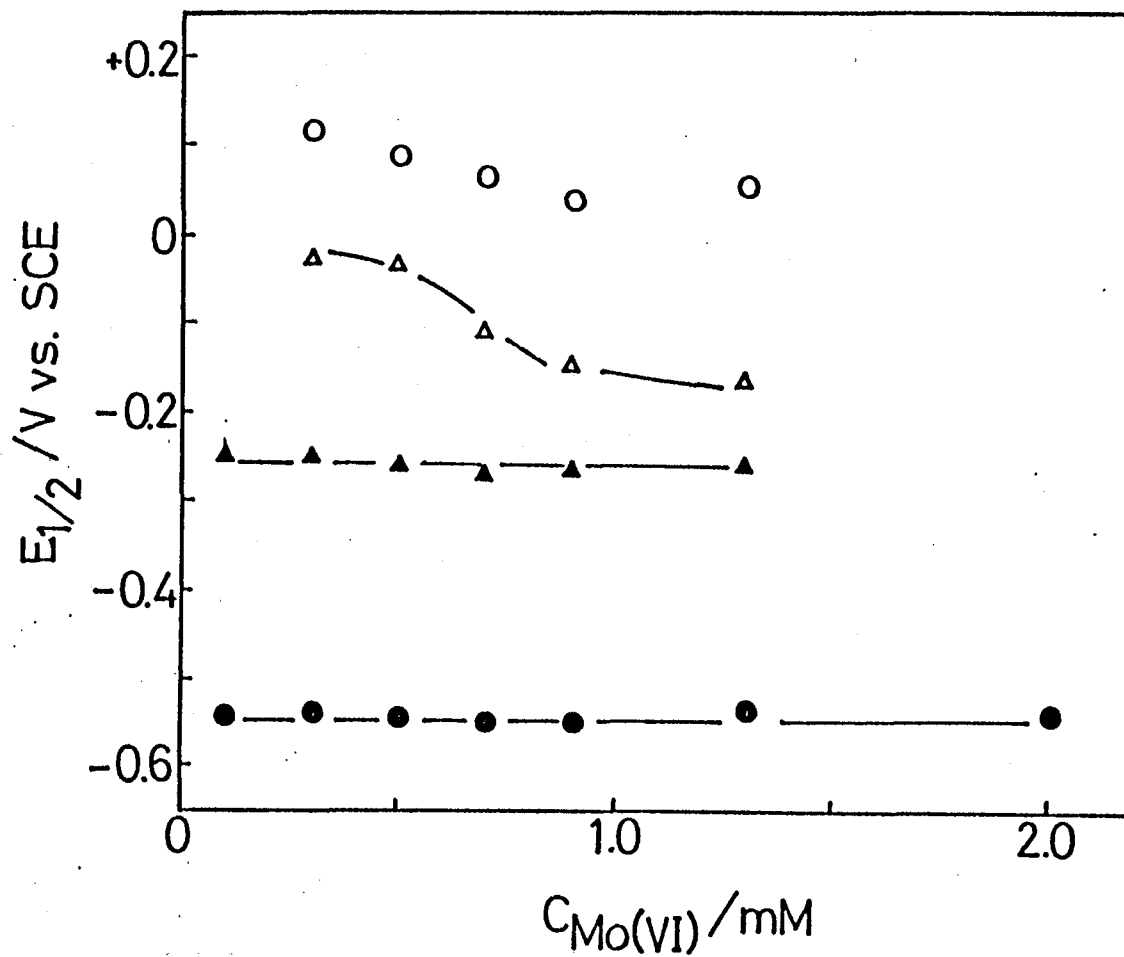


Fig.II-3. Dependence of  $E_{1/2}$  on  $C_{\text{Mo(VI)}}$  in 0.1M  $\text{H}_2\text{SO}_4$ .

(○) Wave 1; (△) wave 2; (▲) wave 3; (●) wave 4.

(16)

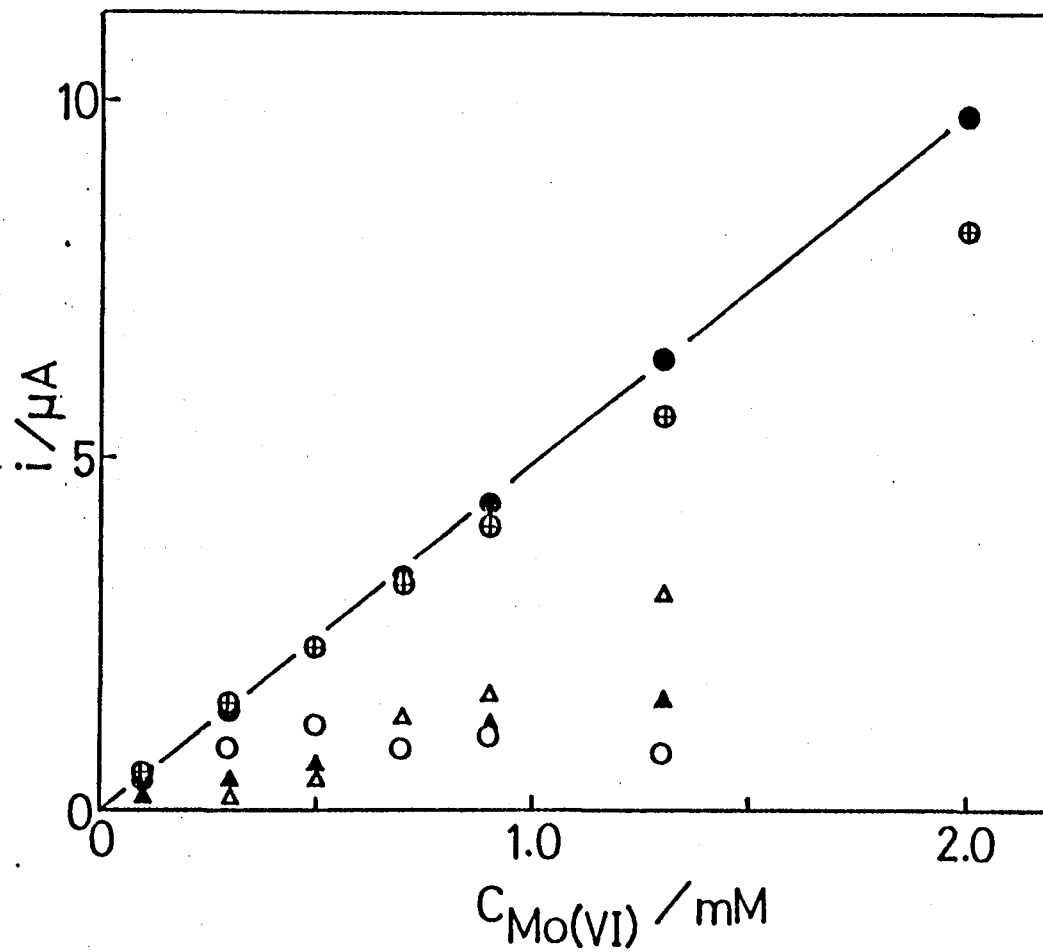


Fig.II-4. Dependence of wave heights on  $C_{\text{Mo(VI)}}$  in 0.1M  $\text{H}_2\text{SO}_4$ .

(○) Wave 1; (△) wave 2; (▲) wave 3; (●) wave 4;

(⊕) wave 1+2+3.

height of waves 1-3 is roughly equivalent to that of wave 4. The height of wave 4 is proportional to  $C_{\text{Mo(VI)}}$  in the region of 0.05-2.0mM.

Current-time curves for single mercury drop at each potential corresponding to the plateau of waves 1-3 are shown in Fig.II-5 for Mo(VI) solutions with three different concentrations. In the higher concentration region of Mo(VI), the current-time curves on waves 1 and 3 show anomalous behavior. Current-time curves which are similar to that of wave 1 have been described when reduction products are adsorbed on the electrode [2]. In the case of wave 3, presumably the electrode-adsorption of reduction products might also take place.

In dc polarography the characteristics of the reduction process is often examined by observing the dependence of the current on the mercury column height,  $h$ . When the reduction process is diffusion controlled, reaction rate controlled and controlled by the adsorption on electroactive species, the current is proportional to  $h^{1/2}$ ,  $h^0$  and  $h$ , respectively [3]. The dependence of each wave height on  $h^{1/2}$  is shown in Fig.II-6. This result is obtained with a solution of 0.5mM Mo(VI) in 0.1M  $\text{H}_2\text{SO}_4$  in which four distinct reduction waves are observed. The height of wave 2 is independent of  $h^{1/2}$ , indicating that wave 2 is reaction rate controlled. The relation for wave 4 is linear and has positive intercept

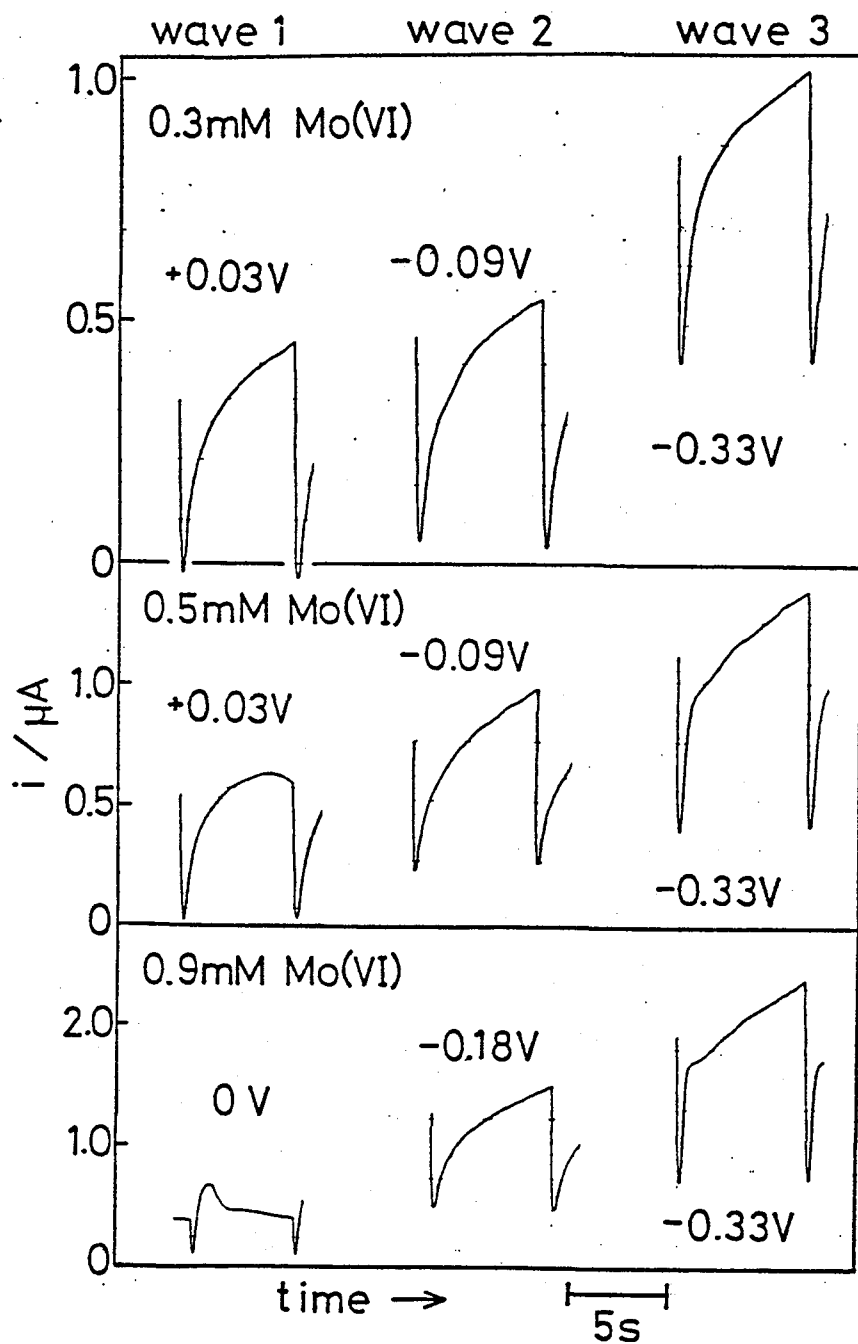


Fig.II-5. Current-time curves on single drop in  $0.1\text{M H}_2\text{SO}_4$   
 (  $m = 0.608\text{mgs}^{-1}$ ,  $t = 6.00\text{s}$  ).

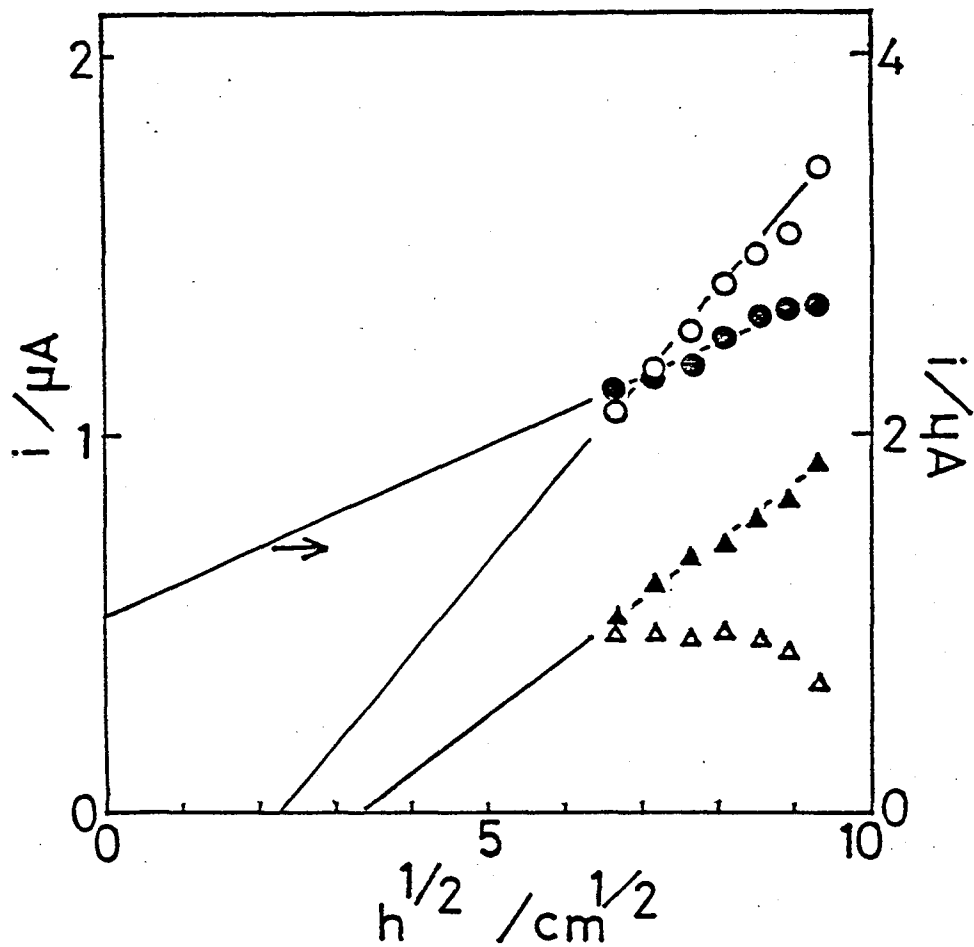


Fig.II-6. Dependence of wave heights on the square root of the mercury column heights. ( $\circ$ ) Wave 1; ( $\triangle$ ) wave 2; ( $\blacktriangle$ ) wave 3; ( $\bullet$ ) wave 4 (right axis).



at  $h^{1/2} = 0$ , which indicates that wave 4 is controlled by the competition of diffusion and reaction rate. In the cases of waves 1 and 3, the relations are linear and have negative intercepts at  $h^{1/2} = 0$ , which indicates that waves 1 and 3 are controlled by the competition of diffusion and adsorption of electroactive species.

Controlled potential electrolysis was carried out on a solution of 0.5mM Mo(VI) in 0.1M H<sub>2</sub>SO<sub>4</sub> which gives four reduction waves clearly. Polarograms and absorption spectra for the solution taken before and after CPE appear in Figs.II-7 and II-8. Curve 2 in Fig.II-7 is the polarogram after CPE carried out at +0.03V vs. SCE, the potential which corresponds to the first section of the plateau of wave 1. The equivalent number of electrons,  $n$ , concerned in the reduction process at this potential, was found to be  $1.03 \pm 0.04$  from the measurement of current consumed. Not only wave 1 but also waves 2 and 3 disappeared as a result of CPE at wave 1 ( curve 2 in Fig.II-7 ); CPEs were also carried out at -0.10 and -0.30V, the potentials which correspond to the first section of the plateaus of waves 2 and 3, respectively. The solutions after CPEs gave the same polarograms as that recorded after the CPE at wave 1 and  $n$  was  $1.06 \pm 0.05$  and  $1.11 \pm 0.01$ , respectively. When CPE was carried out successively on the resulting solutions ( which gave the polarograms of curve 2 in Fig.II-7 ) at -0.70V, i.e. at the potential of wave 4,

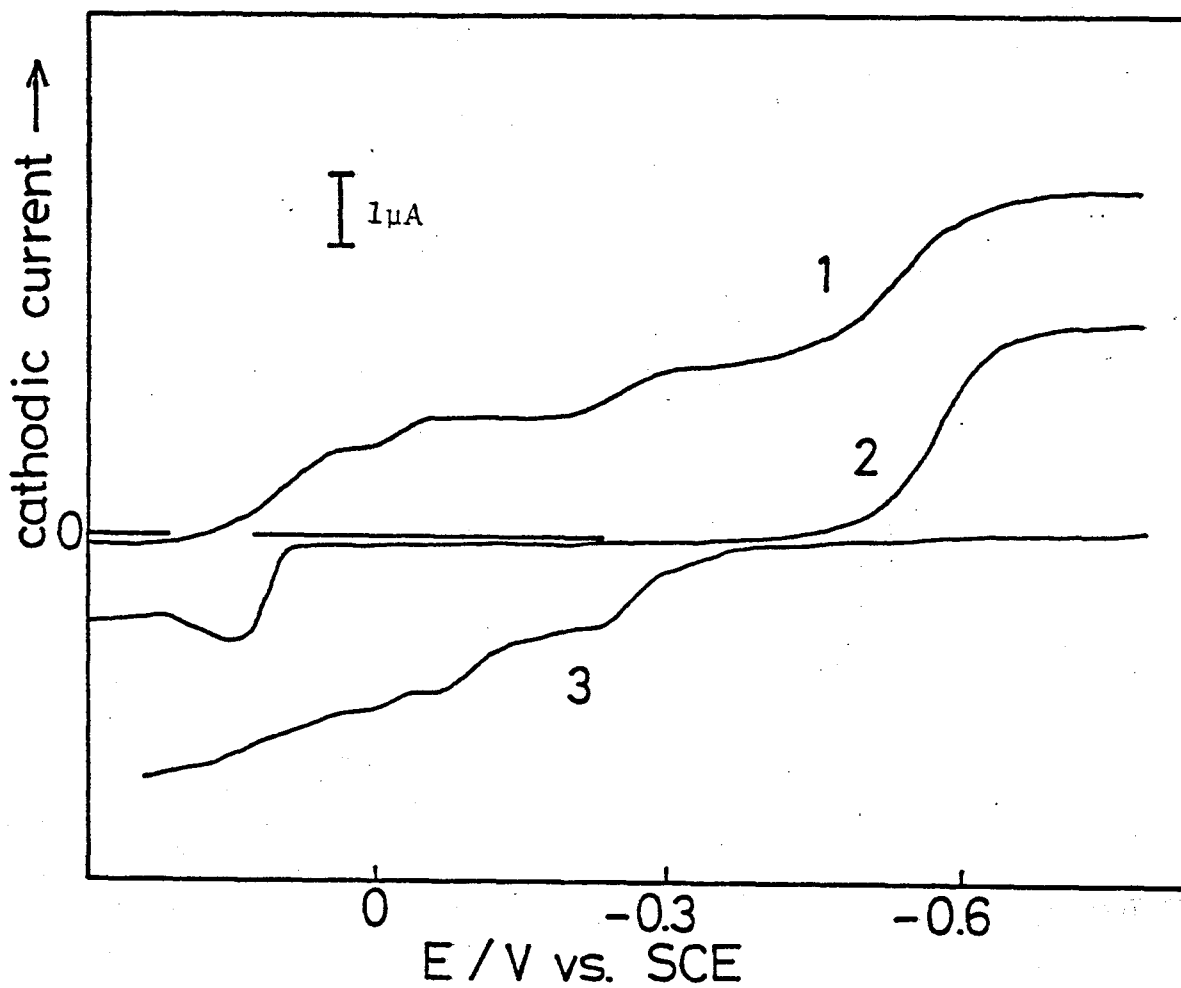


Fig.II-7. Polarograms of Mo solutions in 0.1M  $\text{H}_2\text{SO}_4$ ,  
 (1) 0.5mM Mo(VI); (2) after CPE at +0.03V vs. SCE  
 on (1); (3) after CPE at -0.70V vs. SCE on (2).

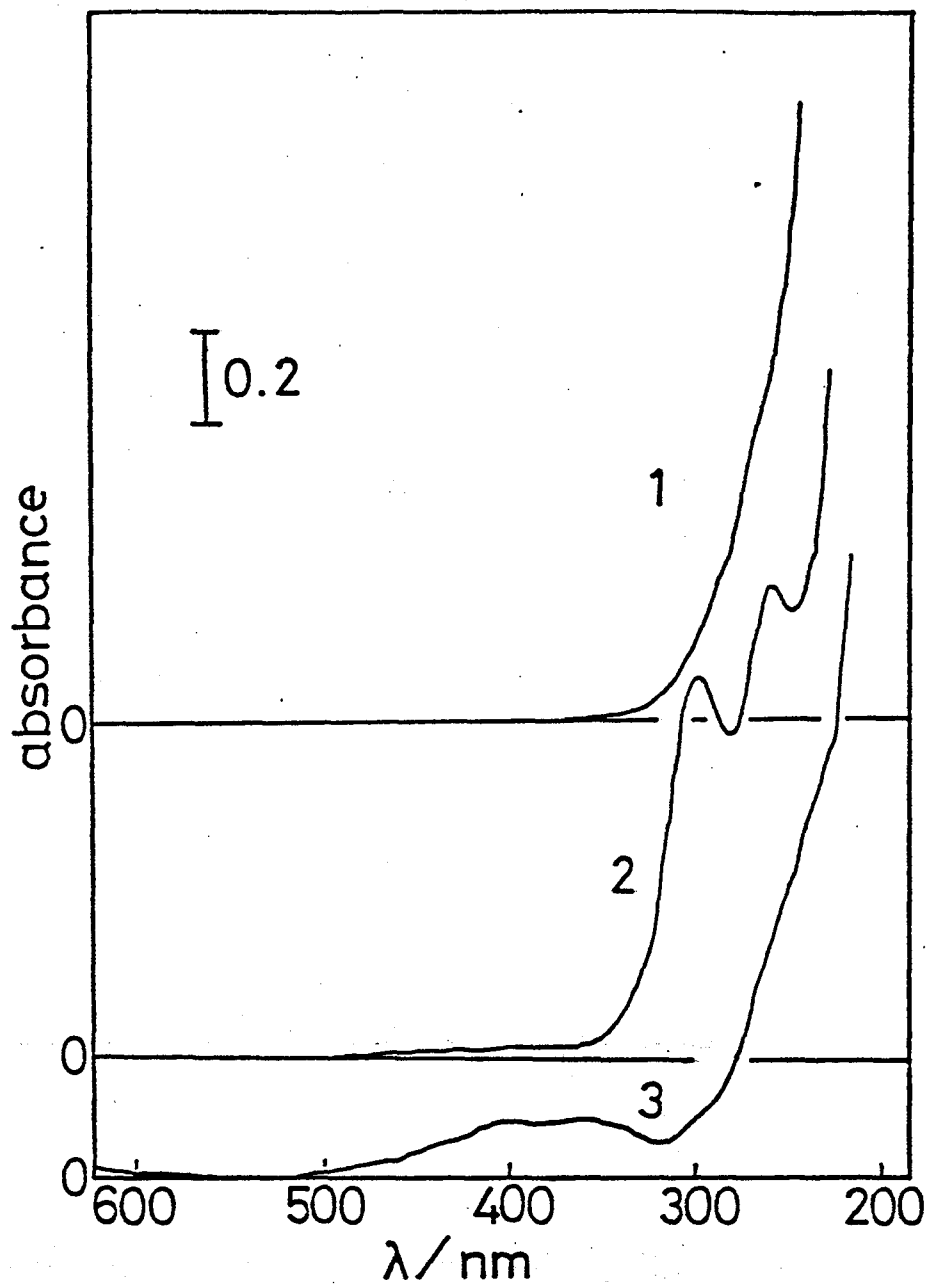


Fig.II-8. Absorption spectra of Mo solutions in 0.1M  $\text{H}_2\text{SO}_4$ ,  
 (1) 0.5mM Mo(VI); (2) after CPE at +0.03V vs. SCE  
 on (1); (3) after CPE at -0.70V vs. SCE on (2).

n was found to be  $2.00 \pm 0.06$ , and the residual solution gave no polarographic reduction wave until the discharge of hydrogen ion ( curve 3 in Fig.II-7 ). Here, Mo(VI) has no absorption band in the visible region in 0.1M H<sub>2</sub>SO<sub>4</sub> solution ( curve 1 in Fig.II-8 ). The solution after the CPEs at waves 1, 2 and 3 ( one-electron reduction) has absorption maxima at 253 and 294nm ( curve 2 in Fig.II-8 ). This spectrum has already been assigned to that of dimeric Mo(V), Mo<sub>2</sub>O<sub>4</sub><sup>2+</sup> [4]. The solution after completion of CPE at the potential of wave 4 is pale green in color and gives a spectrum with two broad maxima at about 360 and 405nm ( curve 3 in Fig.II-8 ). This spectrum is like that for Mo(III) in p-toluensulphonic acid [5].

During CPE on Mo(VI) solution at wave 1 the sample solution becomes blue, and when one-electron reduction at wave 1 is completed, the color disappears. In Fig.II-9, the spectra are shown for the solutions being reduced by 50% at each wave potential. The solution reduced at +0.03V ( curve 1 in Fig.II-9 ) shows broad absorption in the visible region, and solutions reduced at -0.10 and -0.30V ( curves 2 and 3 in Fig.II-9 ) show significantly lower absorptivity.

The presence of nitrate ions enhances the height of wave 3, but the heights of waves 1 and 2 remain constant ( Fig.II-10 ). The height of the enhanced wave is almost independent of  $h^{1/2}$ .

(24)

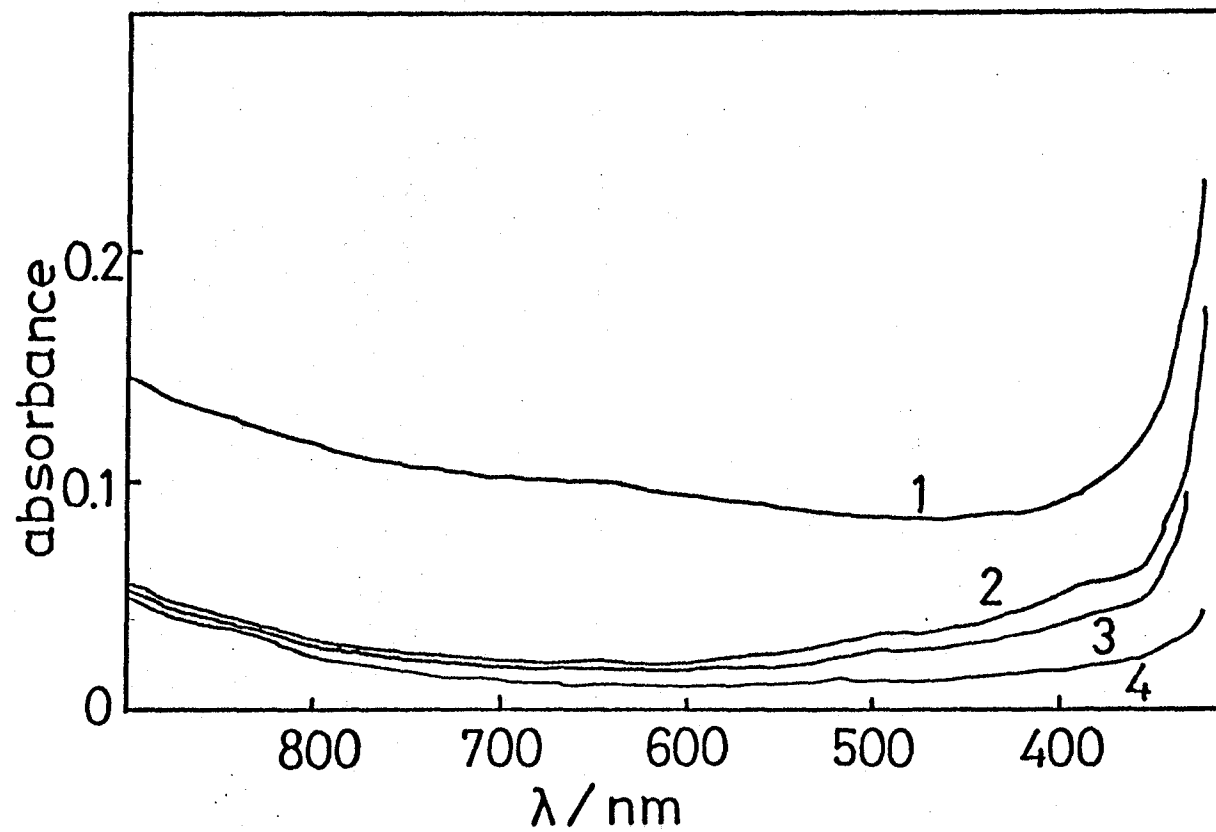


Fig.II-9. Absorption spectra in 0.1M H<sub>2</sub>SO<sub>4</sub>. After half-electron reduction at various potentials vs. SCE on 0.5mM Mo(VI) solution. (1) +0.03V, (2) -0.10V, (3) -0.30V, (4) 0.5mM Mo(VI).

(25)

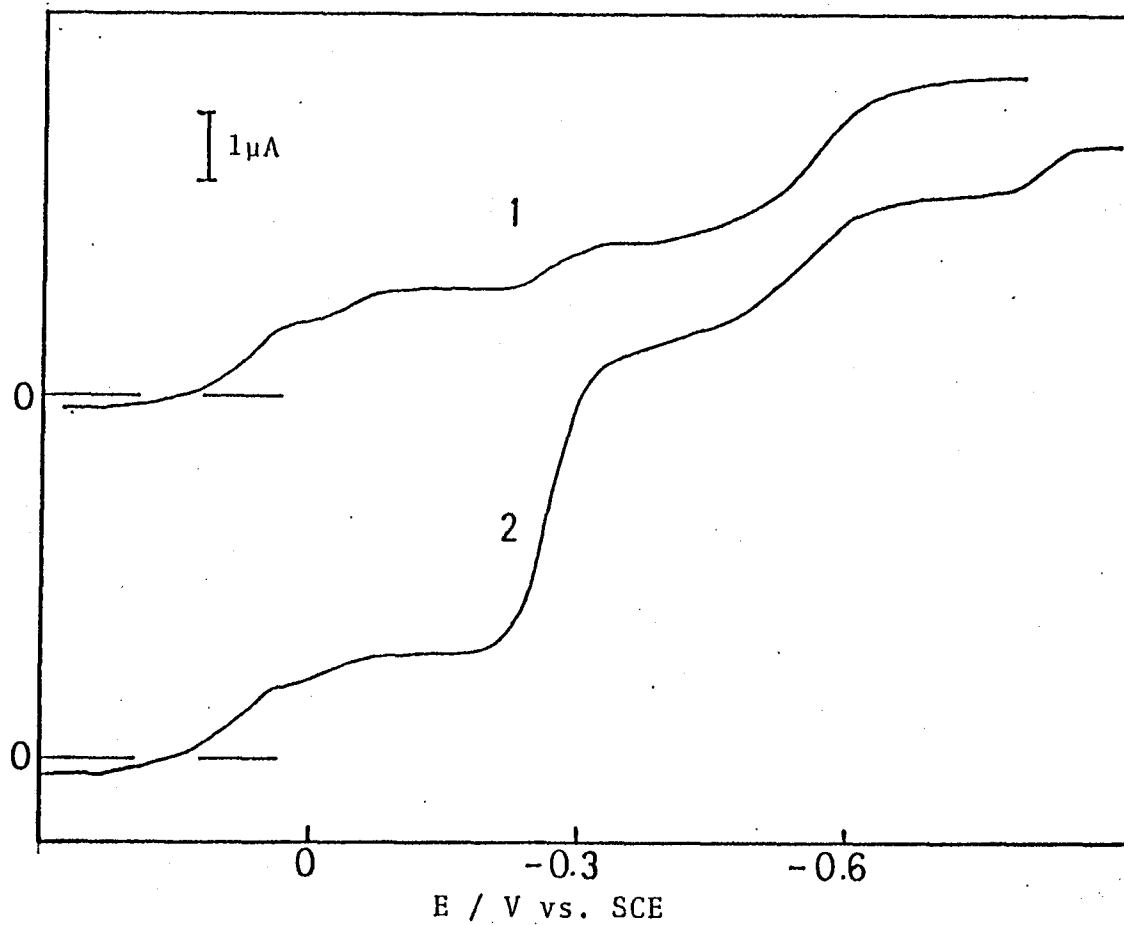


Fig.II-10. Polarograms of Mo(VI) solutions in 0.1M H<sub>2</sub>SO<sub>4</sub>.  
(1) 0.5mM Mo(VI), (2) 0.5mM Mo(VI), 5mM NaNO<sub>3</sub>.

When the sulfuric acid concentration,  $C_{H_2SO_4}$ , is increased from 0.1M, the polarograms of 0.5mM Mo(VI) solution show complex change as shown in Fig.II-11, i.e. wave 1 overlaps with wave 2 and wave 3 with wave 4. In 1M  $H_2SO_4$ , ( curve 3 ), two waves ( +0.11V and -0.29V vs. SCE ) are observed. Further increase of  $C_{H_2SO_4}$  brings about a successive change in the polarograms. In 5M  $H_2SO_4$  ( curve 1 ), three waves ( +0.14V, -0.01V and -0.23V ) are observed. Wave 3' on curve 1 denotes a new wave which appears in the 3-5M  $H_2SO_4$  region. Since the waves overlap each other more or less depending on  $C_{H_2SO_4}$ , it is difficult to determine each  $E_{1/2}$ . As  $C_{H_2SO_4}$  increases, positive shifts of  $E_{1/2}$  are observed. It is also difficult to determine the height of each wave. The total wave height decreases with  $C_{H_2SO_4}$ . In dc polarography, when the concentration of electroactive species is not changed, the value of the diffusion current is practically influenced by the diffusion coefficient,  $D$ , of the electroactive species and the drop time,  $t$ , of the dropping mercury electrode [6]. As the value of  $t$  can be determined in every case, the value of the current,  $i$ , was corrected to correspond to a constant value of  $t$ . Thus the only remaining variable is  $D$ , and since  $i \propto D^{1/2}$  ( Ilkovic equation ) and  $D \propto \eta^{-1}$  ( Stokes-Einstein equation, where  $\eta$  is the viscosity coefficient of the solvent ) it follows that if the variation in the viscosity of the solvent is

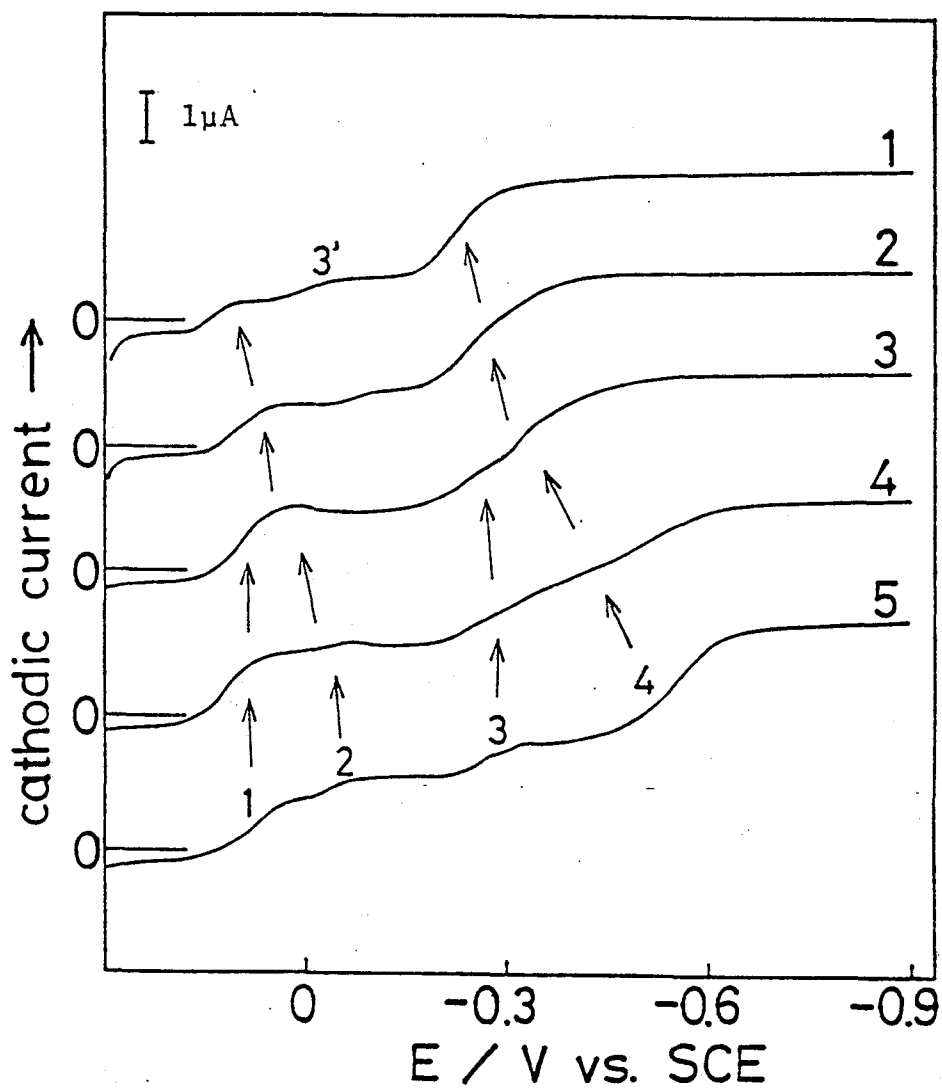


Fig.II-11. Polarograms of 0.5mM Mo(VI) in various concentrations of sulfuric acid.  $\text{CH}_2\text{SO}_4$ : (1) 5M; (2) 3M; (3) 1M; (4) 0.3M; (5) 0.1M.



alone responsible for differences in the value of  $i$ , then  $i$  should be proportional to  $\eta^{-1/2}$ . When the change in the viscosity of the medium with increasing  $C_{H_2SO_4}$  is taken into consideration after Brasher and Jones, the total current is inversely proportional to the square root of the relative viscosity ( $\eta = 1$  in  $0.01N H_2SO_4$  [6] ) of the medium ( Fig.II-12 ). In  $0.1-5M H_2SO_4$ ,  $t^{1/6}$  varies within experimental error ( $< 1\%$  ) so only  $\eta$  was treated as the variable.

Figure II-13 shows the polarograms of Mo(VI) in various  $C_{H_2SO_4}$  in the presence of  $5mM$  nitrate. In  $1M H_2SO_4$  ( curve 3 ), the height of the second wave ( $-0.23V$ ; waves 3 and 4 ) are enhanced catalytically.

The CPE experiments were performed to study the mechanism of the catalytic current and the results are shown in Fig.II-14. Two waves are observed in  $1M H_2SO_4$  solution containing no nitrate before CPE ( curve 1 ). Then, CPE was carried out at  $0V$  vs. SCE ( the potential of the first wave ). After completion of the CPE, the product solution gave the polarogram of curve 2. From the current consumed during the CPE,  $n$  of the first wave determined to be 1. Two polarograms taken on a solution containing  $5mM$  nitrate are also shown in Fig.II-14 before ( curve 3 ) and after ( curve 4 ) the CPE at  $0V$  vs. SCE. After completion of the CPE, the catalytic current, as well as the first wave, disappeared and the polarogram observed

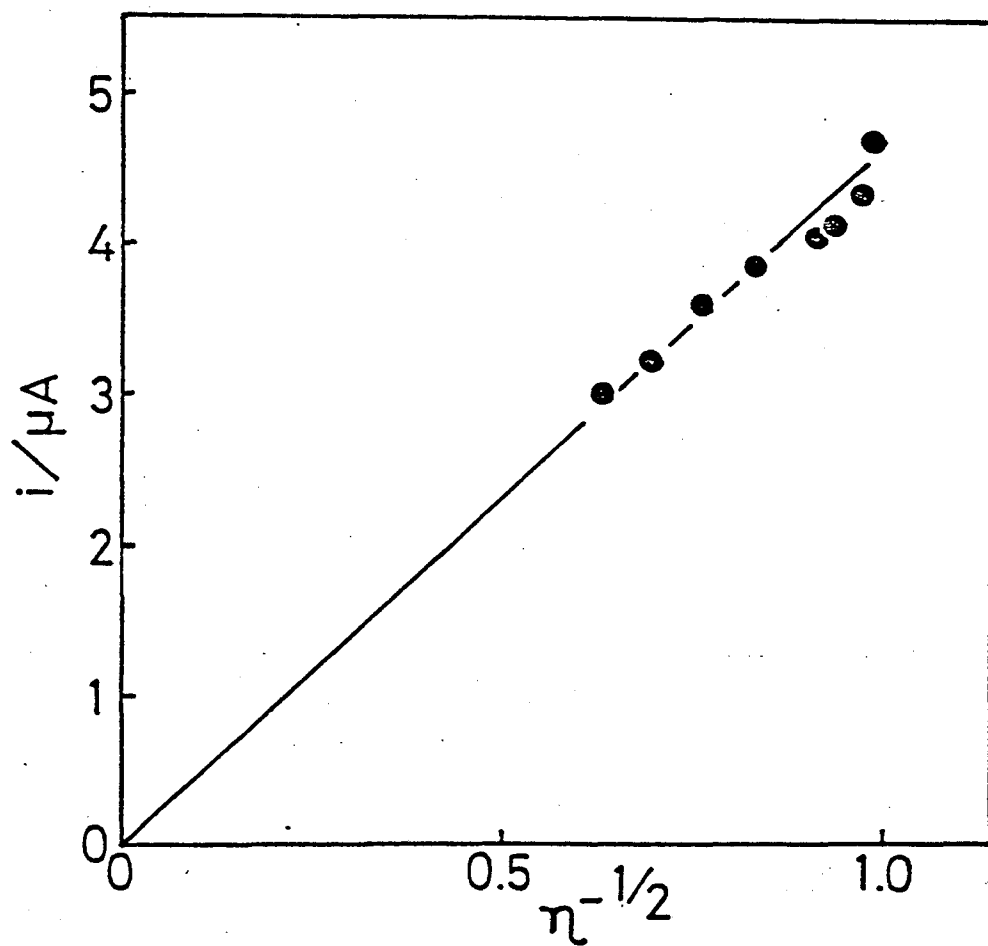


Fig.II-12. Relationship between the total current and the reciprocal of the square root of relative viscosity.

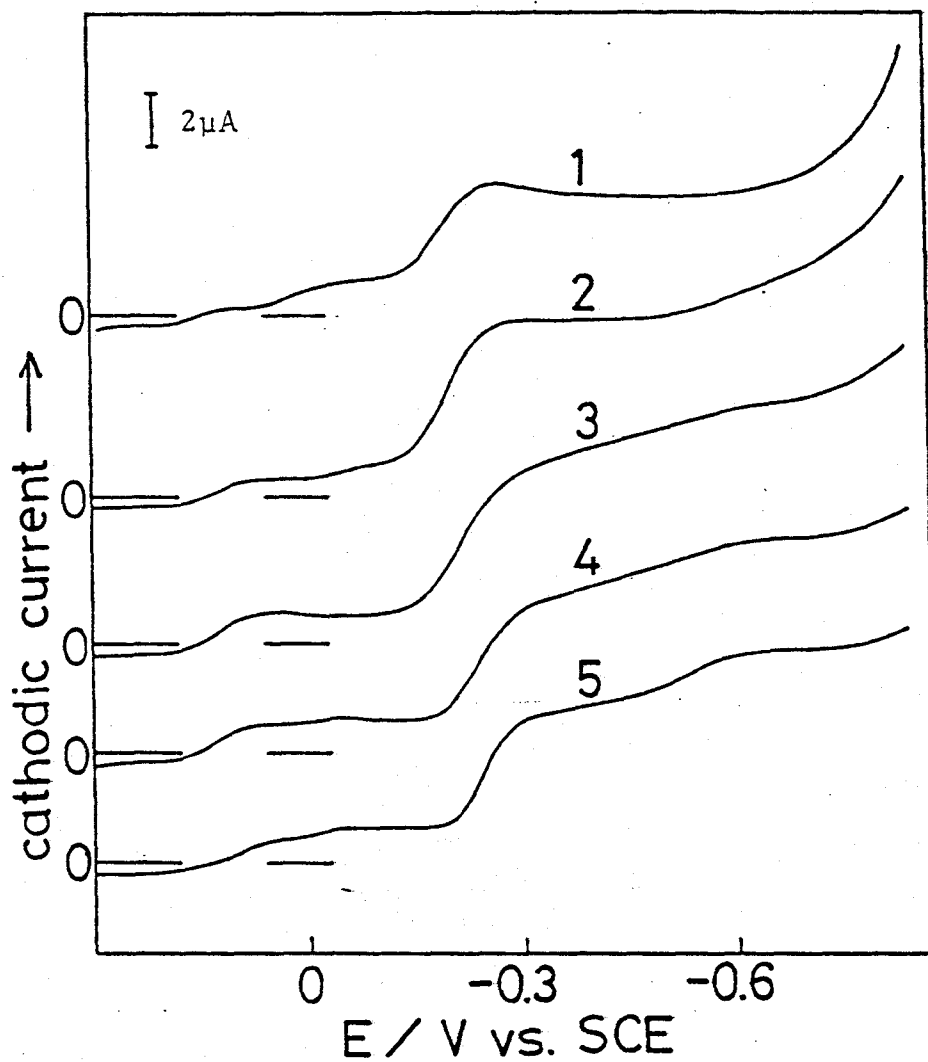


Fig.II-13. Polarograms of 0.5mM Mo(VI) with 5mM NaNO<sub>3</sub> in various concentration of sulfuric acid.  $C_{H_2SO_4}$ :  
 (1) 5M; (2) 3M; (3) 1M; (4) 0.3M; (5) 0.1M.

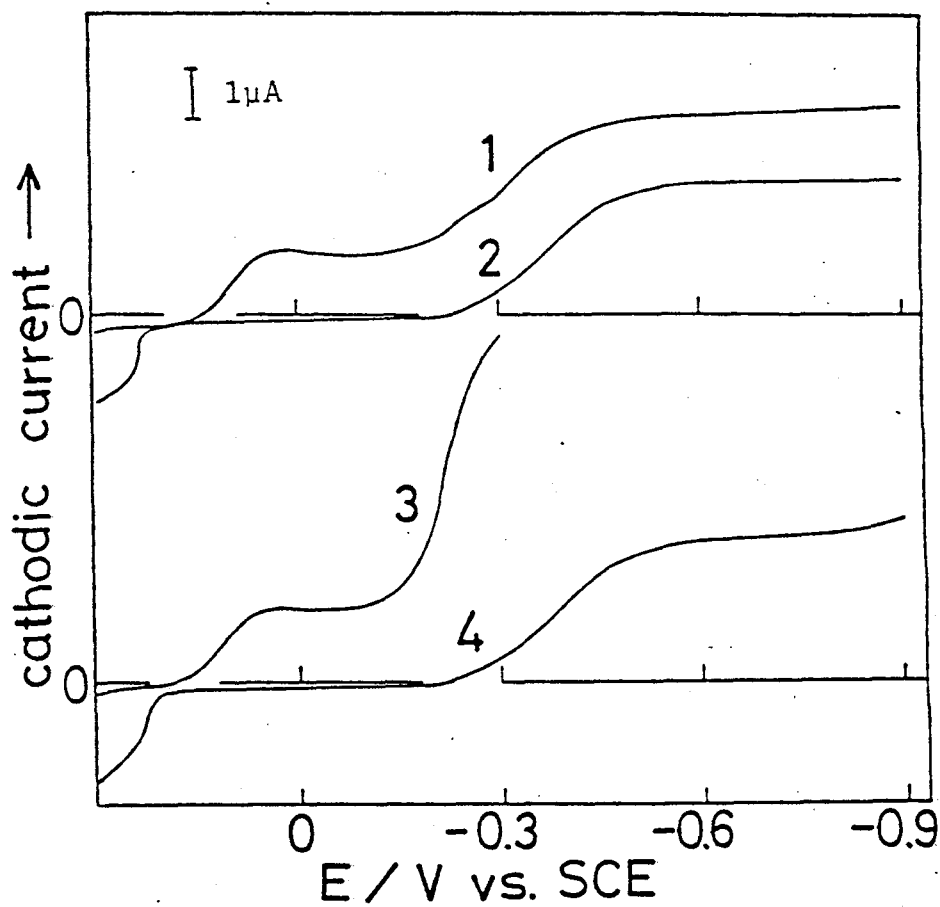


Fig.II-14. Polarograms of Mo solutions in 1M H<sub>2</sub>SO<sub>4</sub>.  
 (1) 0.5mM Mo(VI); (2) after CPE at 0V vs. SCE on (1); (3) 0.5mM Mo(VI) with 5mM NaNO<sub>3</sub>; (4) after CPE at 0V vs. SCE on (3).

( curve 4 ) was identical with curve 2. The  $n$  for the electrolysis was also determined to be 1. In order to elucidate the reduction mechanism of the second wave in 1M  $H_2SO_4$ , CPE was carried out at  $-0.70V$  vs. SCE on the product solution of one-electron reduction ( giving the polarogram of curve 2 in Fig.II-14 ), and  $n$  was determined to be 2.

The same CPE experiments were carried out on 5M  $H_2SO_4$  solutions. After completion of the CPE at  $+0.09V$  vs. SCE ( on the first wave ) the first wave (  $+0.14V$  ) and wave 3' (  $-0.10V$  ) disappeared, and  $n$  was determined to be 1. During the CPE the solution turned out to be yellow.

Three absorption spectra for 5M  $H_2SO_4$  solutions are shown in Fig.II-15 for Mo(VI) ( curve 1 ), its CPE product solution after one-electron reduction ( curve 2 ) and the product solution after further two-electron reduction ( curve 3 ). Although the spectra of curves 1 and 3 in 5M  $H_2SO_4$  ( Fig.II-15 ) are similar to the corresponding spectra in 0.1M  $H_2SO_4$  ( Fig.II-8 ), curve 2 for 5M  $H_2SO_4$  shows a weak and broad absorption in the visible region, having a maximum at about 400nm, which is not observed in 0.1M or in 1M  $H_2SO_4$ . The spectra for 1M  $H_2SO_4$  solutions after the same procedures are very similar to those of Mo(VI), Mo(V) and Mo(III) in 0.1M  $H_2SO_4$ , respectively.

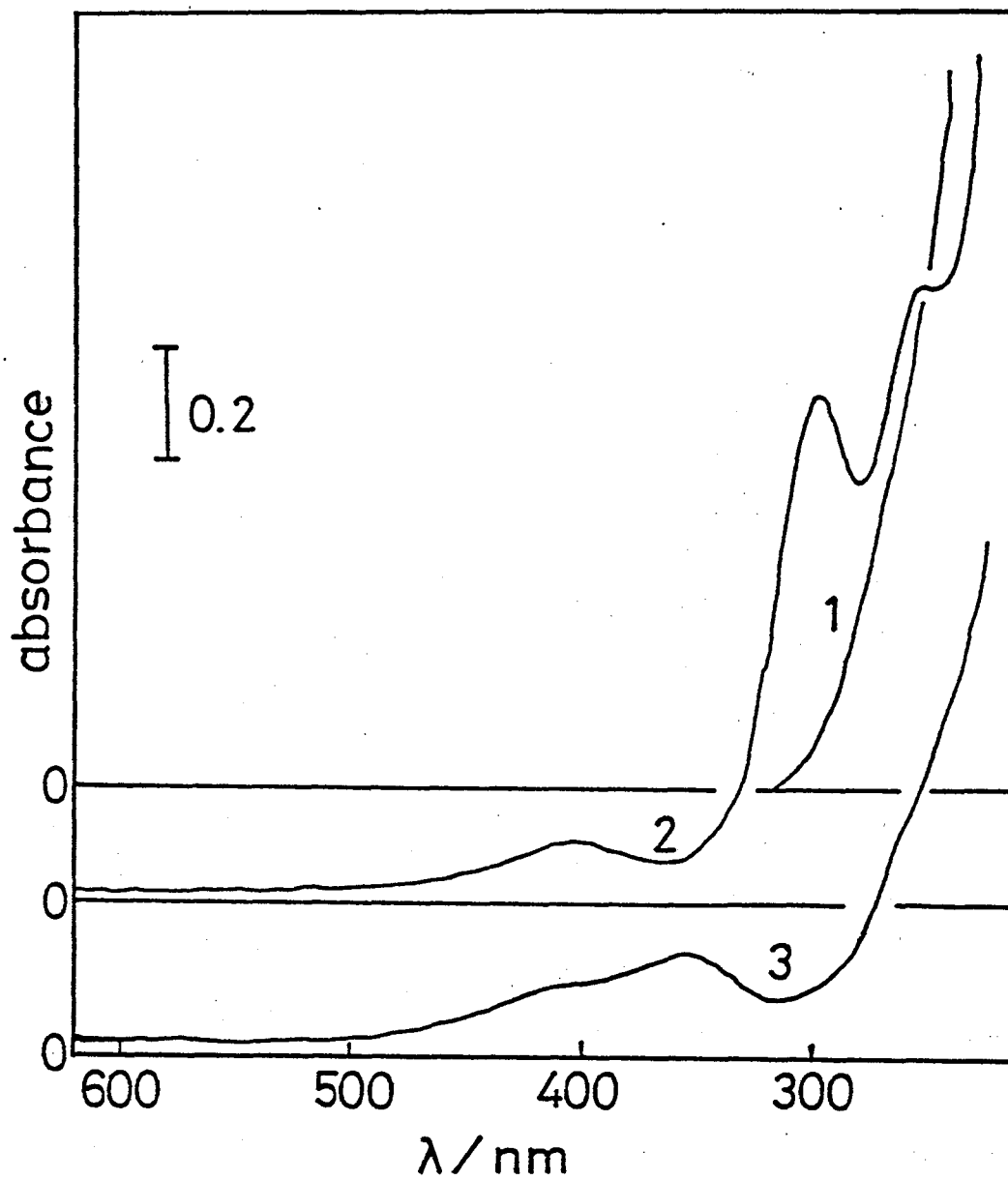


Fig.II-15. Absorption spectra of Mo solutions in 5M H<sub>2</sub>SO<sub>4</sub>.  
(1) 0.5mM Mo(VI); (2) after CPE at +0.09V vs. SCE  
on (1); (3) after CPE at -0.70V vs. SCE on (2).

## II-4 Discussion

### II-4-1 Reduction mechanisms

Kolthoff and Hodara [7] and other workers [8-11] observed only three waves in the polarogram of Mo(VI) in 0.1M H<sub>2</sub>SO<sub>4</sub> or similar acidity of sulfate supporting electrolyte solution. These three waves have been considered to correspond to the reductions of Mo(VI) to Mo(V), Mo(V) to Mo(IV) [8,10] and Mo(V) to Mo(III) [7,9,11], respectively. Four simultaneously appeared reduction waves are observed in this work. The coulometric results indicate that waves 1-3 together correspond to a one-electron reduction and wave 4 corresponds to a two-electron reduction. Further, the spectra taken after completion of CPE at the former three waves and at wave 4 are considered to correspond to those of Mo(V) and Mo(III), respectively. That is, it should be assumed from these data that waves 1-3 are due to the reduction of Mo(VI) to Mo(V) and only wave 4 corresponds to the reduction of Mo(V) to Mo(III). The first wave reported previously by other authors is considered to be the overlapping wave of waves 1 and 2 numbered in the polarogram of 0.5mM Mo(VI) in 0.1M H<sub>2</sub>SO<sub>4</sub>, the second corresponds to wave 3 and the third to wave 4. So it could be concluded that, from previous work the first and the second waves are due to the reduction of

Mo(VI) to Mo(V) and the third to Mo(V) to Mo(III).

As shown in Fig.II-14, the total height of waves 1-3 is almost the same as that of wave 4, while  $n$  for the reduction in the former three waves and at wave 4 is one and two, respectively. The existence of the disproportionation reaction of Mo(IV) is most probable, but further quantitative examination is required in order to elucidate the precise mechanism.

Although it has been reported by other authors that the second wave in 1M  $H_2SO_4$  corresponded only to the reduction of Mo(V) to Mo(III) [7], there are some indications that the particular reduction path of Mo(VI) to Mo(V) corresponding to wave 3 in 0.1M  $H_2SO_4$  occurs at the potential of the second wave in 1M  $H_2SO_4$ :

(1) As shown in Fig.II-11, the second wave in 1M  $H_2SO_4$  ( -0.29V ) is originated from waves 3 and 4.

(2) In the presence of nitrate ion, the catalytic wave appears at the potential of the second wave ( curve 3 in Fig.II-13 ) and disappears after one-electron reduction by CPE ( Fig.II-14 ), i.e. the catalytic electrode reaction involves Mo(VI). ( Note: In 0.1M  $H_2SO_4$  the catalytic wave is observed at the potential of wave 3 )

In 5M  $H_2SO_4$ , three reduction waves have been found and it has been reported that both the first and second waves ( +0.14V and -0.01V ) corresponded to the reduction of Mo(VI)



to Mo(V), and the third wave ( -0.23V ) of Mo(V) to Mo(III) [7]. However, the present experimental result that the third wave is catalytically active ( curve 1 in Fig.II-13 ) indicates that the reduction of Mo(VI) to Mo(V) occurs at the potential of the third wave. Therefore, three different reduction mechanisms of Mo(VI) to Mo(V) are present in 5M H<sub>2</sub>SO<sub>4</sub>.

The coulometric experiments indicate that the reduction of Mo(V) to Mo(III) is involved in the second and the third waves for H<sub>2</sub>SO<sub>4</sub> solutions of 1M and 5M respectively.

#### II-4-2 Species of reactants

Two kinds of mechanism are considered to explain the existence of three waves corresponding to the reduction of Mo(VI) to Mo(V) in 0.1M H<sub>2</sub>SO<sub>4</sub>: (1) a stepwise reduction of a single polymerized Mo(VI) species; (2) a respective reduction of three different Mo(VI) species. In the case of stepwise reduction of a single species, one would not expect the reduction corresponding to waves 2 and 3 when the potential is kept at the lower value ( CPE at wave 1 ), even though the electrolysis would be carried out for a sufficiently long period. The disappearance of the three waves ( waves 1-3 ) after completion of CPE at wave 1 is inconsistent with the concept of a stepwise reduction of a single species.

Figure II-5 shows that adsorptive effects are involved

in the reduction mechanism for waves 1 and 3. Adsorption leads to the possibility of splitting of a reduction wave due to a single kind of depolarizer [2]. This splitting has been explained by the scheme that the reduction product is adsorbed on the electrode at the potential of the first wave and is not adsorbed at the potential of the second wave. The reduction product should be only one species in this case. In the case of Mo(VI), the results obtained by CPE and absorption spectroscopy and the catalytic behavior in the presence of nitrate ions show that the reduction products at the potentials of waves 1-3 are different from each other. Therefore, the three waves of Mo(VI) to Mo(V) are not due only to adsorptive effects. So it is reasonable to suggest that three chemical species of Mo(VI) are present in equilibrium. The reaction which controls the current of wave 2 ( Fig.II-6 ) may be the transformation among these three species.

In 1M and 5M  $H_2SO_4$  there are two and three waves of Mo(VI) to Mo(V) respectively. From the catalytic behavior, the species corresponding to wave 3 in 0.1M  $H_2SO_4$  seems to exist in all the  $C_{H_2SO_4}$  regions investigated. The second wave ( -0.01V ) in 5M  $H_2SO_4$  is slightly catalytic. Therefore, this wave is denoted as wave 3' in the previous section of this chapter. The reduction product on wave 3' in the higher  $C_{H_2SO_4}$  region is different from those on waves 1 and 2 in 0.1M  $H_2SO_4$ , since no catalytic effect is observed

on waves 1 and 2. The reduction product on the first wave in the higher  $C_{H_2SO_4}$  region must also be different from those on waves 1 and 2 in  $0.1M H_2SO_4$ , because the reduction product produced during the CPE on the first wave in  $5M H_2SO_4$  is a yellow species, while in  $0.1M H_2SO_4$  the reduction product on wave 1 is a blue species and the product on wave 2 has no significant color. Therefore, the reduction products on the first wave and wave 3' in the higher  $C_{H_2SO_4}$  region are different from the products on waves 1 and 2 in  $0.1M H_2SO_4$ , which seems to indicate the existence of four different chemical species of Mo(VI). The reactant corresponding to wave 3 is also the species of Mo(VI); then, five different chemical species of Mo(VI) in all are observed in the  $0.1-5M H_2SO_4$  region. The reduction mechanisms discussed here are summarized in Table II-1.

In higher acidic solutions, the presence of cationic species of Mo(VI) has been reported. Cruywagen and Ojo et al. reported the presence of  $HMoO_3^+$  and  $H_xMo_2O_6^{x+}$  ( $x = 1-3$ ) [5,12] and Jones reported  $MoO_2^{2+}$  [13]. It is not yet known what kind of species of Mo(VI) corresponds to each wave. Although each wave is not completely diffusion controlled, the dependences of the rate of the electrode reaction and of the diffusion coefficient upon  $C_{H_2SO_4}$  due to transformation of the Mo(VI) species must be small compared with their dependence upon the viscosity of sample solutions ( Fig.II-12 ).

Table II-1. Reduction mechanisms of Mo(VI) in H<sub>2</sub>SO<sub>4</sub>.

C H <sub>2</sub> SO <sub>4</sub>	0.1M	1M	5M
	wave 1 Mo(VI) → Mo(V) (blue species)	1st wave Mo(VI) → Mo(V)	1st wave Mo(VI) → Mo(V) (yellow species)
	wave 2 Mo(VI) → Mo(V)		2nd wave (wave 3') Mo(VI) → Mo(V) (catalytically active species)
	wave 3 Mo(VI) → Mo(V) (catalytically active species)	2nd wave Mo(VI) → Mo(V) (catalytically active species)	3rd wave Mo(VI) → Mo(V) (catalytically active species)
	wave 4 Mo(V) → Mo(III)	Mo(V) → Mo(III)	Mo(V) → Mo(III)

A 50% CPE ( at wave 1 ) of 0.5mM Mo(VI) in 0.1M H<sub>2</sub>SO<sub>4</sub> solution produced blue species. Molybdenum blue species chemically produced have been considered to be colloidal, and considered to be a mixed-valence ( Mo(VI) and Mo(V) ) compounds [14]. The Mo species produced at the potential of wave 1 would form the blue species, presumably colloidal, with the coexisting Mo(VI) species, adsorb on the electrode, and prevent further electrochemical reaction, as shown in Fig.II-5.

#### II-4-3 Catalytically active species

The catalytic wave of Mo(VI) in the presence of nitrate ions has been generally known, but some arguments still remain about the wave character and/or species which is concerned in the catalysis. In the present investigation the catalytic effect is observed on wave 3. The reduction wave for catalysis has been assigned to the reduction of Mo(V) to Mo(IV) [8,10] or of Mo(V) to Mo(III) [7,9,11]; therefore, the catalytically active species has been postulated inevitably to be Mo(IV) [8,10] or Mo(III) [9,15]. The coulometric results indicate that wave 3 corresponds to the reduction of Mo(VI) to Mo(V). Another interesting fact is that in the solution after completion of one-electron reduction of Mo(VI) to Mo(V) by CPE at the potentials of waves 1-3, no catalytic wave is observed in the

presence of nitrate ions. Therefore, it is concluded that the catalytically active species is neither Mo(IV) nor Mo(III), but Mo(V) which is formed on the surface of the electrode. The catalytically active Mo(V) at the electrode surface has a different character from that Mo(V) in bulk solution and those produced at the potentials of waves 1 and 2. Oxidation of bulk solution of Mo(V) by nitrate has already been investigated [16,17]. Mo(V) is thought to exist as the dimeric form,  $\text{Mo}_2\text{O}_4^{2+}$ , in bulk solution of weak acidity, and this dimer is oxidized only slowly by nitrate. Therefore, the catalytically active species of Mo(V) is not the dimer. It has been postulated that monomeric Mo(V) species is much more redox active than dimeric Mo(V) [17]. These problems will be studied in chapter IV.

## II-5 References

1. F.Umland, *Theorie und Praktische Anwendung von Komplexbildnern*, Akademische Verlagsgesellschaft, Frankfurt am Main, 1971, p.233.
2. R.Brdicka, *Collect.Czech.Chem.Comm.*, 12 (1947) 522.
3. A.A.Vlcek in F.A.Cotton (Ed.), *Progress in Inorganic Chemistry*, Vol.5, John Wiley and Sons, Inc., 1963, p.211.
4. M.Ardon and A.Pernick, *Inorg.Chem.*, 12 (1973) 2484.
5. J.F.Ojo, R.S.Taylor and A.G.Sykes, *J.Chem.Soc., Dalton*, (1975) 500.
6. D.M.Brasher and F.R.Jones, *Trans.Faraday Soc.*, 42 (1946) 775.
7. I.M.Kolthoff and I.Hodara, *J.Electroanal.Chem.*, 4 (1962) 369.
8. T.E.Edmonds, *Anal.Chim.Acta*, 116 (1980) 323.
9. M.G.Johnson and R.J.Robinson, *Anal.Chem.*, 24 (1952) 366.
10. G.P.Haight, Jr., *Anal.Chem.*, 23 (1951) 1505.
11. G.Henrion, F.Scholz, R.Stösser and U.Ewert, *Z.Anorg. Allg.Chem.*, 467 (1980) 23.
12. J.J.Cruywagen, J.B.B.Heyns and E.F.C.H.Rohwer, *J.Inorg. Nucl.Chem.*, 40 (1978) 53.
13. M.M.Jones, *J.Am.Chem.Soc.*, 76 (1954) 4233.
14. A.F.Trotman-Dickenson (Ed.), *Comprehensive Inorganic Chemistry*, Vol.3, Pergamon Press, Oxford, 1st ed.,

1973, p.737.

15. I.M.Kolthoff and I.Hodara, *J.Electroanal.Chem.*, 5 (1963) 2.
16. E.P.Guymon and J.T.Spence, *J.Phys.Chem.*, 70 (1966) 1964.
17. G.R.Cayley, R.S.Taylor, R.K.Wharton and A.G.Sykes, *Inorg.Chem.*, 16 (1977) 1377.



### III Differential pulse and alternating current polarographic study of Mo(VI) in acidic solution

#### III-1 Introduction

In the previous chapter, direct current ( dc ) polarographic reduction mechanisms of Mo(VI) in sulfuric acid solution were investigated. From the results of CPE it was claimed that there are three reduction waves corresponding to the reduction of Mo(VI) to Mo(V) in 0.1M H<sub>2</sub>SO<sub>4</sub>. However, there is little information about the reactants involved in each wave. Few reports dealing with the character of the electroactive Mo(VI) species have appeared in the polarographic studies on Mo(VI), except for the work done by Paffett and Anson [1]. In order to obtain more information about the character of the reactants and the reduction mechanisms, differential pulse ( DP ) and alternating current ( ac ) polarography are introduced in this chapter. Further, the influences of ionic surfactants on DP polarograms are studied and interpreted in terms of electrostatic effect.

#### III-2 Experimental

The stock solution of molybdenum ion was prepared from sodium molybdate. The surfactants used were as follows:

cationic surfactants: n-decylamine ( Wako Pure Chemical Industry ) and dodecyltrimethylammonium chloride ( Tokyo Kasei Kogyo ); anionic surfactants: sodium dodecylsulfate ( Wako Pure Chemical Industry ) and sodium n-dodecylbenzenesulfonate ( Wako Pure Chemical Industry ).

DP polarograms were obtained with a Yanagimoto Model P-1000 voltammetric analyzer. The pulse amplitude was 50mV. A sweep rate of  $2\text{mVs}^{-1}$  was used with a drop time 2.5s. The characteristics of a dropping mercury electrode at a mercury column height of 59.0cm were  $m = 1.42\text{mgs}^{-1}$ ,  $t = 6.10\text{s}$  in 0.1M  $\text{H}_2\text{SO}_4$  at -0.70V vs. SCE. The ac polarographic instrument was the same as reported elsewhere [2]. An oscillator ( Kikusui Electronics Corp., RC Oscillator Model 4045 ) and a lock-in amplifier ( NF Circuit Design Block Co., Model LI 507 ) were used. Applied ac voltage and frequency were 10mV ( rms ) and 50Hz respectively.

Other experimental conditions were the same as described in chapter II.

### III-3 Results

Figure III-1 shows the DP and dc polarograms of 0.5, 0.9 and 2.0mM Mo(VI) in 0.1M  $\text{H}_2\text{SO}_4$ . Four peaks ( +0.16, +0.06, -0.27 and -0.60V vs. SCE ) are observed in the DP polarogram of 0.5mM Mo(VI) ( curve f ). The numbers on the

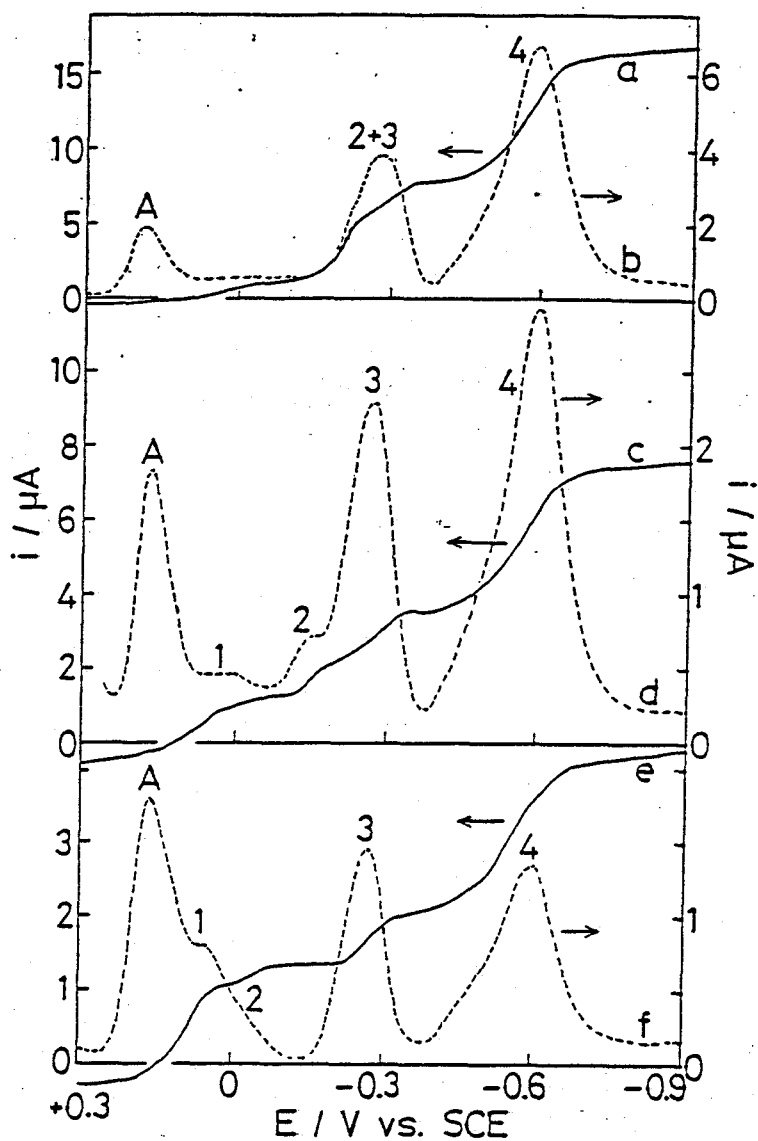


Fig.III-1. Dc (—) and DP (-----) polarograms of Mo(VI) in 0.1M  $H_2SO_4$ . 2.0mM Mo(VI): (a) dc; (b) DP; 0.9mM Mo(VI): (c) dc; (d) DP; 0.5mM Mo(VI): (e) dc; (f) DP.

curves correspond to dc polarographic reduction waves described in chapter II. The peak A ( +0.16V in curve f ) has no corresponding wave in the dc polarogram. Peak 2 is included in the foot of peak 1. When  $C_{\text{Mo(VI)}}$  is  $< 0.3\text{mM}$ , peak A and peak 1 make a single peak. As  $C_{\text{Mo(VI)}}$  increases, peak 2 begins to appear (  $C_{\text{Mo(VI)}} > 0.7\text{mM}$ , curve d ), then peak 2 and 3 overlap and peak 1 is hardly observed (  $C_{\text{Mo(VI)}} > 2.0\text{mM}$  curve b ).

The dependence of each peak height on  $C_{\text{Mo(VI)}}$  in 0.1M  $\text{H}_2\text{SO}_4$  is shown in Fig.III-2. The height of peaks 2, 3 and 4 increase with  $C_{\text{Mo(VI)}}$ , while the height of peak 1 slightly decreases. The height of peak A grows sharply and levels off at 0.5mM.

The ac polarograms of Mo(VI) in 0.1M  $\text{H}_2\text{SO}_4$  are shown in Fig.III-3. Peak 3 ( -0.3V ) seems to consist of two peaks separated by about 30mV. For 0.5mM Mo(VI), the height of the more positive peak ( 3a ) is larger than that of negative peak ( 3b ), while for 2.0mM, these two peaks have almost equivalent heights. The peaks corresponding to peak A or peak 1 shows very complex behavior, and will not be discussed in this chapter.

Figure III-4 shows the DP polarograms of 0.5mM Mo(VI) in sulfuric acid solutions of various concentrations. As  $C_{\text{H}_2\text{SO}_4}$  increases from 0.1M, peak 1 moves toward peak A and peaks 3 and 4 shift to positive potential. Then, two clear peaks ( +0.13

(48)

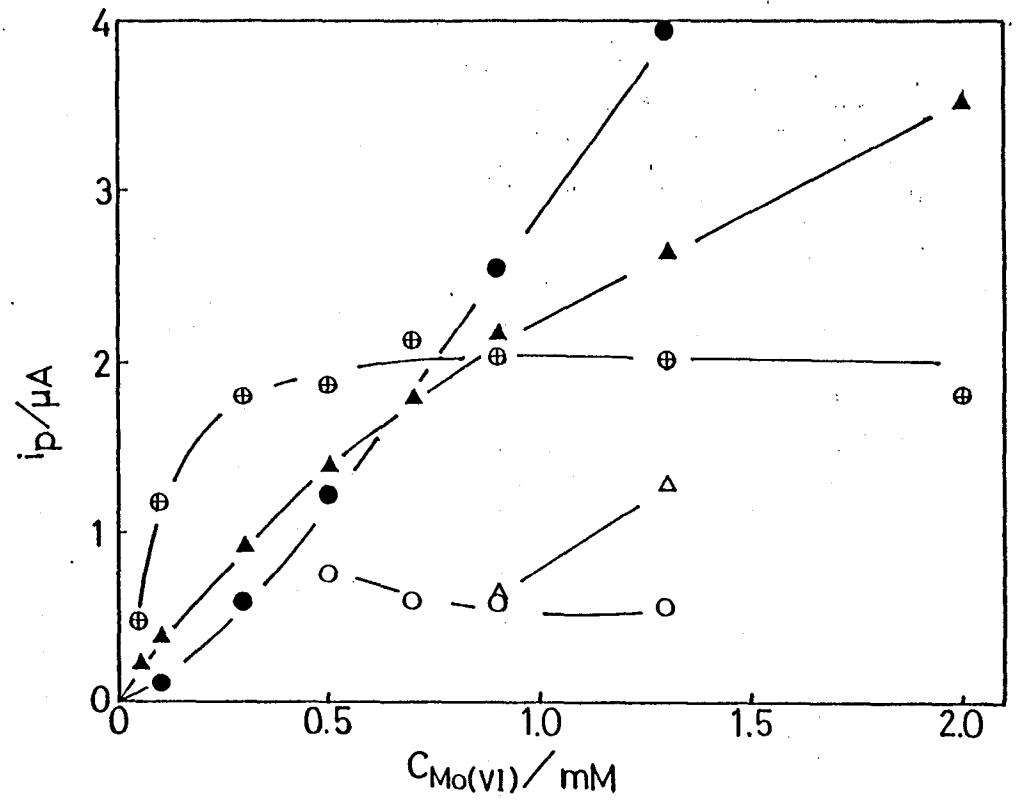


Fig.III-2. Dependence of each peak height in the DP polarogram on  $C_{Mo(VI)}$  in 0.1M  $H_2SO_4$ : ( $\oplus$ ) peak A; ( $\circ$ ) peak 1; ( $\Delta$ ) peak 2; ( $\blacktriangle$ ) peak 3; ( $\bullet$ ) peak 4.

(49)

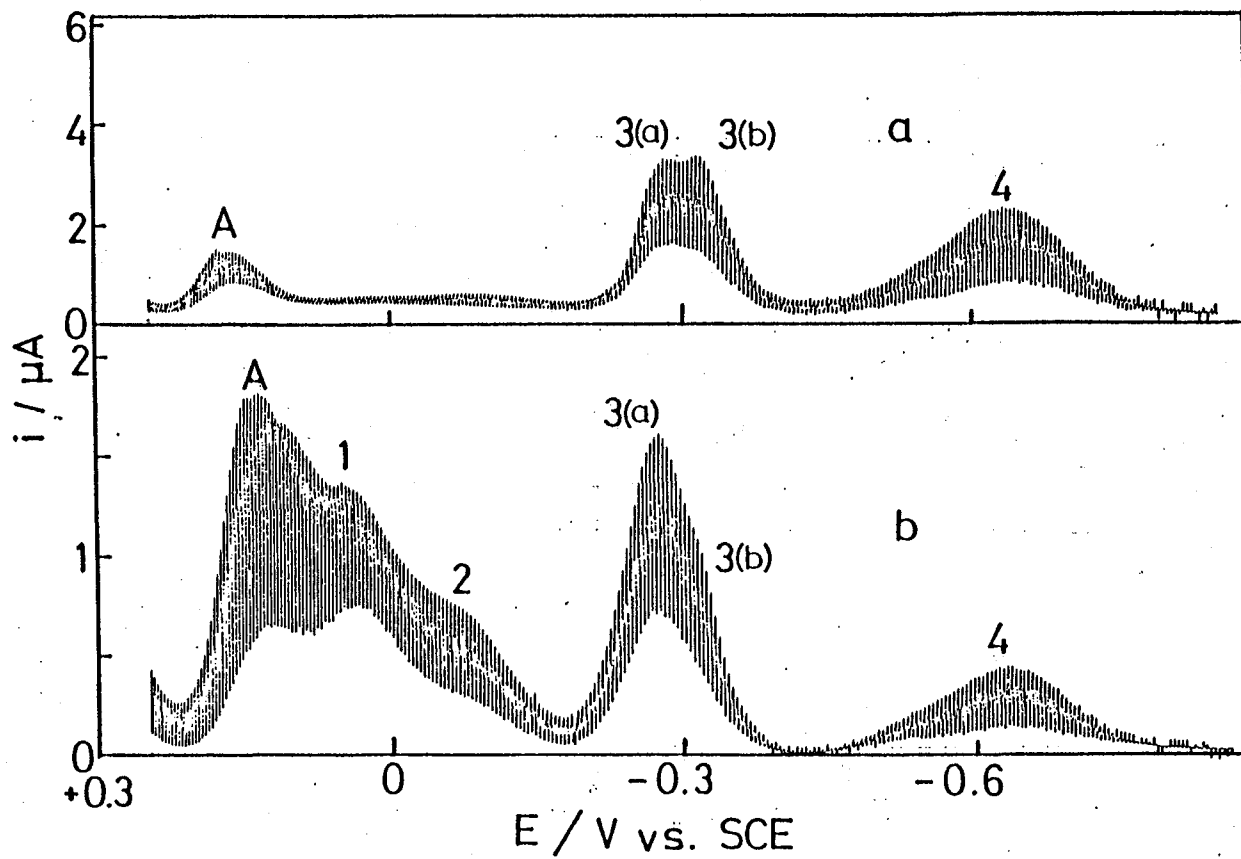


Fig.III-3. Ac polarogram of Mo(VI) in 0.1M  $\text{H}_2\text{SO}_4$  ( 0° component );  $C_{\text{Mo(VI)}}$ : (a) 2.0mM: (b) 0.5mM.

(50)

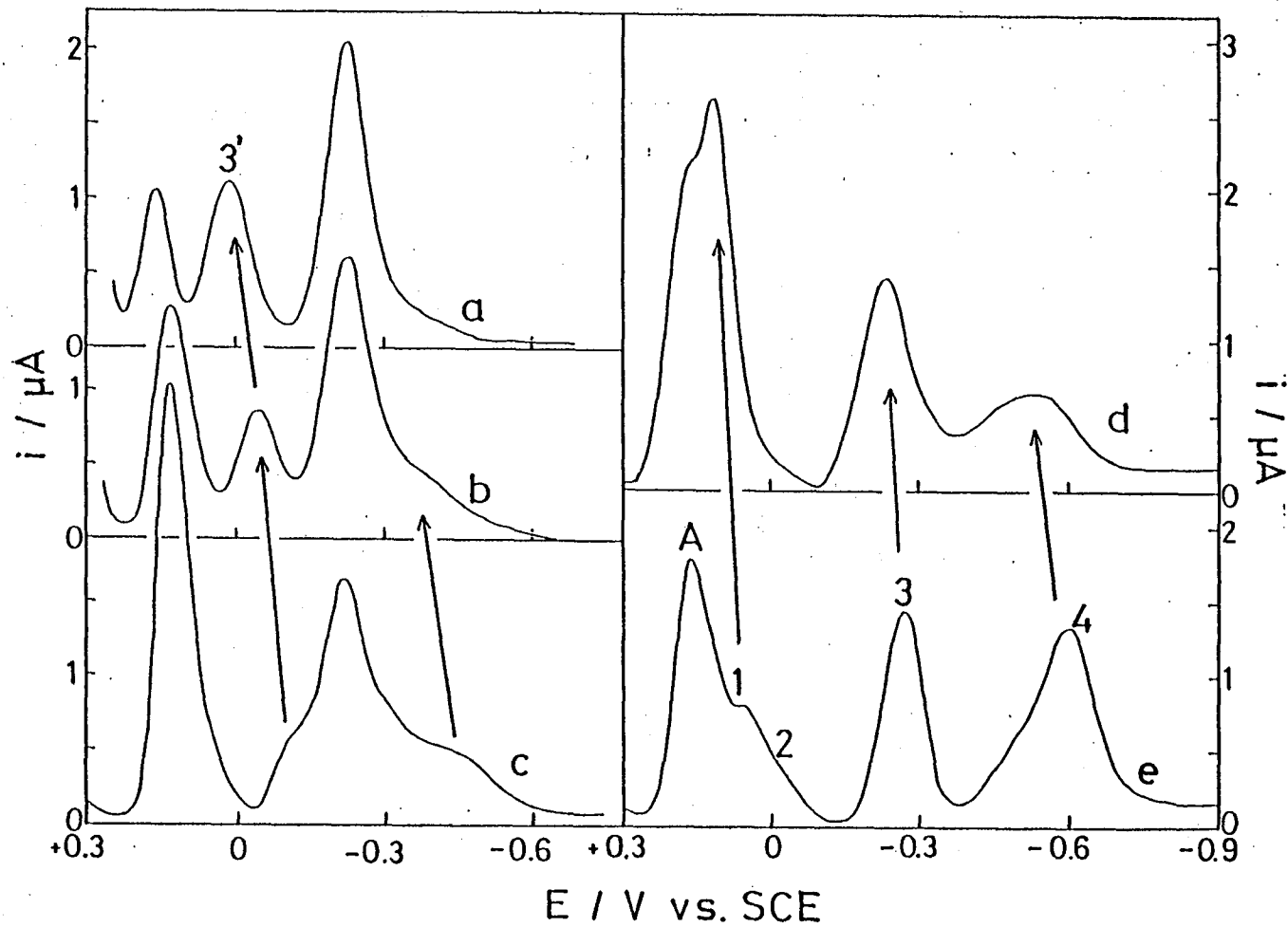


Fig.III-4. DP polarogram of 0.5mM Mo(VI) in various concentration of sulfuric acid;  $\text{CH}_2\text{SO}_4$ : (a) 5M; (b) 3M; (c) 1M; (d) 0.3M; (e) 0.1M.

and  $-0.23\text{V}$  ) and two shoulders ( about  $-0.11$  and  $-0.42\text{V}$  ) are observed in  $1\text{M H}_2\text{SO}_4$ . In  $5\text{M H}_2\text{SO}_4$ , three peaks (  $+0.16$ ,  $+0.02$  and  $-0.23\text{V}$  ) are observed. The second peak (  $+0.02\text{V}$  ) in  $5\text{M H}_2\text{SO}_4$ , which corresponds to wave 3' in the dc polarogram ( chapter II ), is derived from the shoulder (  $-0.11\text{V}$  ) in  $1\text{M H}_2\text{SO}_4$ .

Peak height  $i_p$  and peak potential  $E_p$  in the DP polarogram are influenced by ionic surfactants. Figure III-5 shows the influence of anionic and cationic surfactants on the DP polarogram of  $0.5\text{mM Mo(VI)}$  in  $0.1\text{M H}_2\text{SO}_4$ . Addition of an anionic surfactant, e.g. sodium dodecylsulfate, results in the following phenomena: (1) decrease of  $i_{p(1)}$ ; (2) slight increase of  $i_{p(3)}$ ; (3) positive shift of  $E_{p(3)}$ ; (4) splitting of peak 4 into a peak and a shoulder; (5) no influence on peak A ( curve b ). While addition of cationic surfactant, e.g. n-decylamine, results in the following phenomena: (1) decrease of  $i_{p(3)}$ ; (2) negative shift of  $E_{p(3)}$ ; (3) splitting of peak 4 into two peaks; (4) no influence on peak A and peak 1 ( curve d ).

The dependence of  $i_{p(1)}$  and  $i_{p(3)}$  of  $0.5\text{mM Mo(VI)}$  and  $i_{p(2)}$  of  $0.9\text{mM Mo(VI)}$  in  $0.1\text{M H}_2\text{SO}_4$  on the concentration of ionic surfactants are shown in Figs. III-6 and III-7. When peaks 1 and 2 are too distorted to determine  $E_{p(1)}$  and  $E_{p(2)}$  precisely,  $i_{p(1)}$  and  $i_{p(2)}$  are read at  $+0.06$  and  $-0.15\text{V}$  respectively. As the concentration of sodium dodecylsulfate



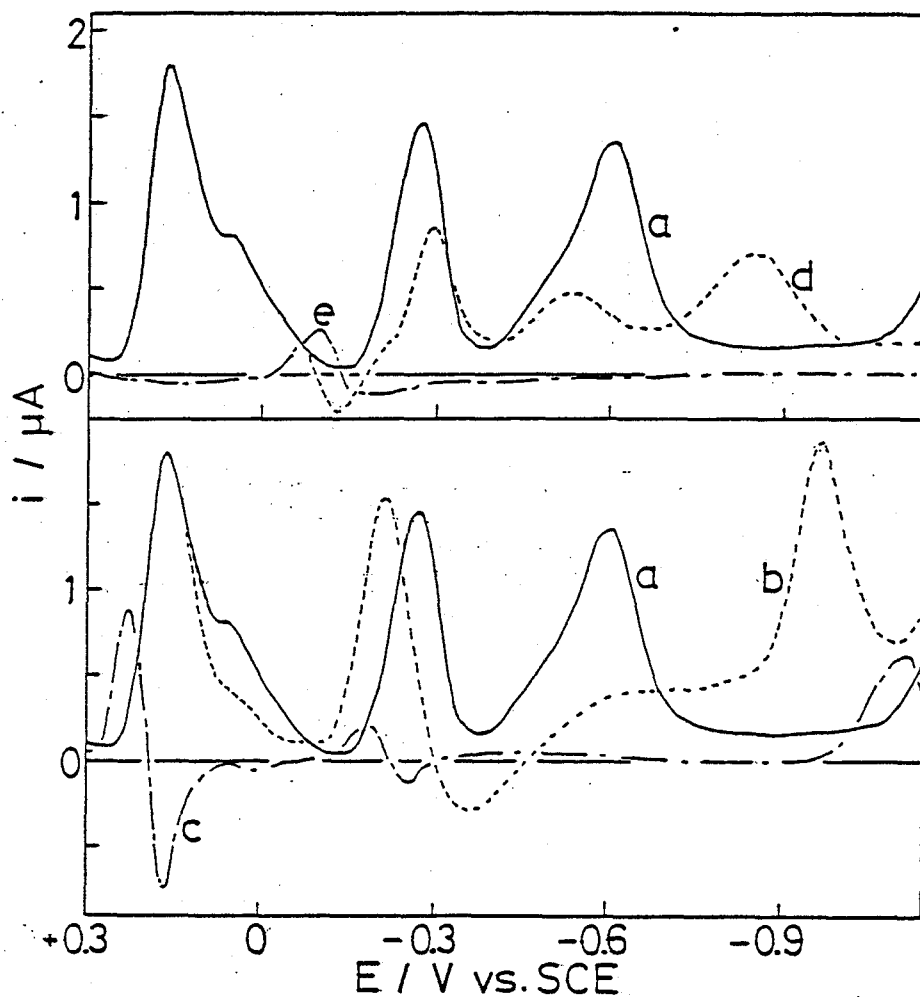


Fig.III-5. DP polarogram of 0.5mM Mo(VI) in the absence and the presence of ionic surfactants in 0.1M  $H_2SO_4$ . (a) (—) Mo(VI) only; (b) (-----) Mo(VI) with 0.01% sodium dodecylsulfate; (c) (---) 0.01% sodium dodecylsulfate only; (d) (-----) Mo(VI) with 0.01% n-decylamine; (e) (---) 0.01% n-decylamine only.

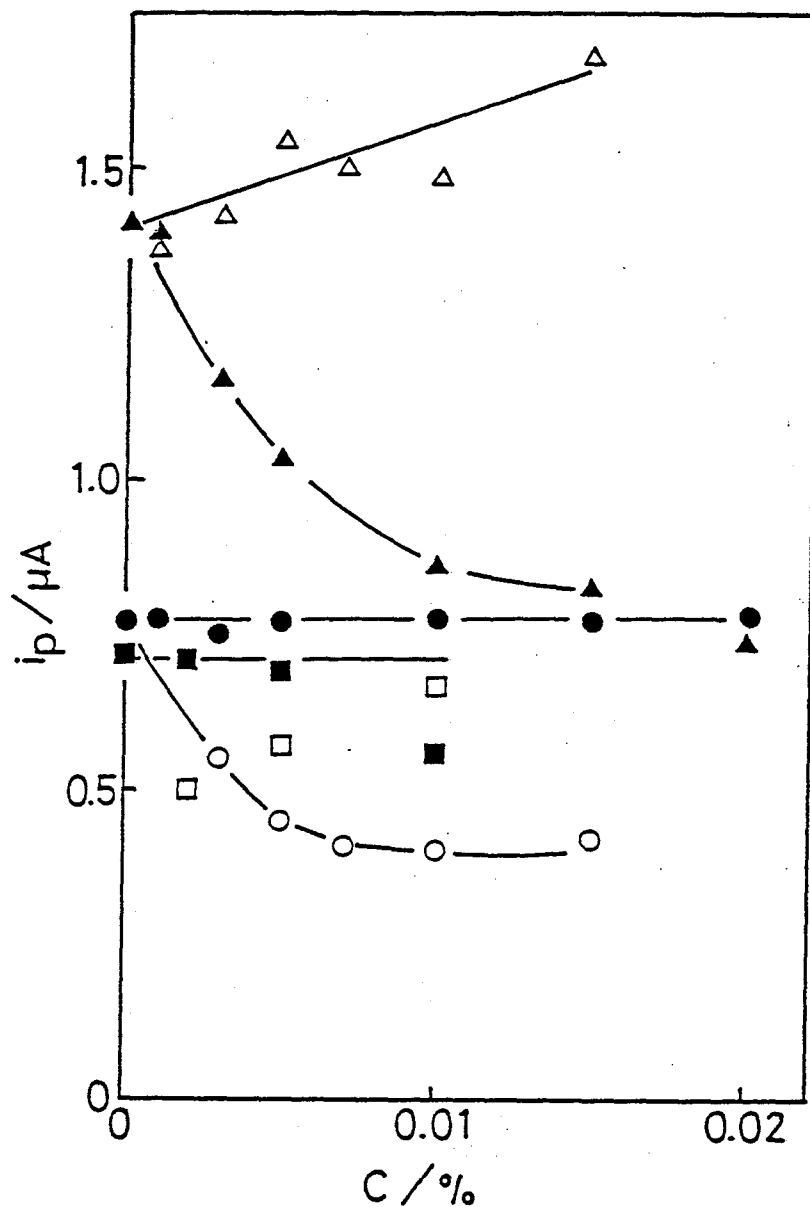


Fig.III-6. Dependence of peak heights on the concentrations of surfactants ( the heights of peak 1 and 3 were measured for 0.5mM Mo(VI) and that of peak 2 was measured for 0.9mM Mo(VI). Sodium dodecylsulfate ( anionic ): ( ○ ) peak 1; ( □ ) peak 2; ( △ ) peak 3. n-Decylamine ( cationic ): ( ● ) peak 1; ( ■ ) peak 2; ( ▲ ) peak 3.

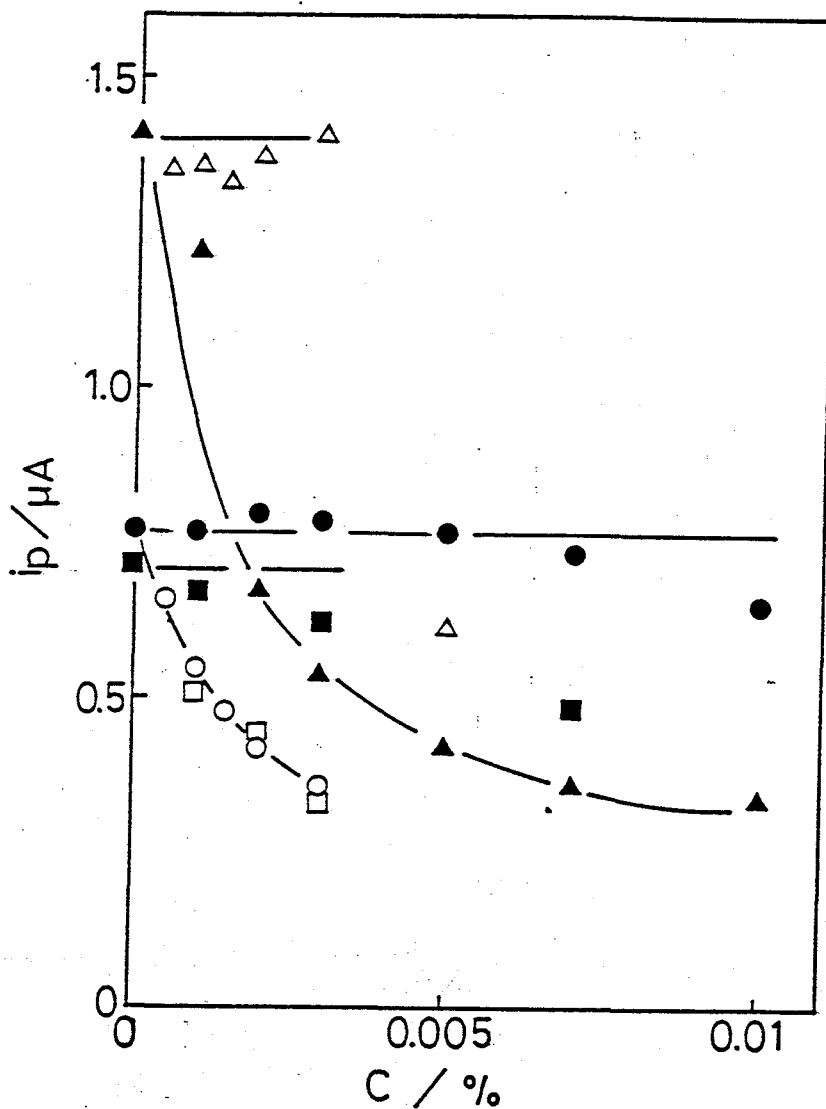


Fig.III-7. Dependence of peak heights on the concentration of surfactants ( $C_{Mo(VI)}$  are as those in Fig.III-6 ). Sodium n-dodecylbenzenesulfonate ( anionic ): (○) peak 1; (□) peak 2; (△) peak 3. Dodecyltrimethylammonium chloride ( cationic ): (●) peak 1; (■) peak 2; (▲) peak 3.

( anionic ) is increased,  $i_{p(1)}$  decreases while  $i_{p(3)}$  increases slightly. As the concentration of n-decylamine ( cationic ) is increased,  $i_{p(1)}$  shows little change while  $i_{p(3)}$  decreases. Similar phenomena are observed in the case of sodium n-dodecylbenzenesulfonate ( anionic ) and of dodecyltrimethylammonium chloride ( cationic ). The effect of the surfactant on  $i_{p(2)}$  is almost the same as that on  $i_{p(1)}$ , except that as the concentration of surfactant is increased,  $i_{p(2)}$  is influenced by the change of  $i_{p(3)}$ .

#### III-4 Discussion

##### III-4-1 Adsorption of Mo complexes

As shown in Fig.III-1, there is no dc wave corresponding to peak A. Further,  $i_{p(A)}$  is independent of  $C_{Mo(VI)}$  in the region of  $C_{Mo(VI)} > 0.3mM$  ( Fig.III-2 ). In ac or DP polarography, a peak current is observed when the differential capacity of the electrode double layer is changed because of the adsorption or desorption of electroinactive species. This nonfaradaic peak current in ac or DP polarogram is called tensammetric peak current [3,4]. Therefore, peak A is concluded to be a tensammetric peak which arises from the adsorption of Mo(VI) ions. This tensammetric peak is also observed in the ac polarogram ( Fig.III-3 ). Adsorptive

behavior of molybdenum ions has been reported by Paffett and Anson [1] on the study with cyclic staircase voltammetry and chronocoulometry in trifluoromethanesulfonic acid and by Hull [3] with a rotating ring-disk electrode in aqueous solutions. Paffett and Anson reported that the adsorption of Mo(VI) at concentration below ca. 0.1mM appeared to be negligible and that the adsorption became significant at 0.2-0.3mM. As shown in Fig.III-2, the behavior of peak A, which is concluded to be a tensammetric wave, is the same as the adsorptive nature of the Mo(VI) complex observed by them. The current-time curve for a single mercury drop at the potential of wave 1 or 3 in the dc polarogram in 0.1M H<sub>2</sub>SO<sub>4</sub> ( chapter II ) shows little adsorptive nature at low concentration of Mo(VI) (  $C_{\text{Mo(VI)}} < 0.3\text{mM}$  ).

In ac polarograms, two adjacent peaks were observed at the potential region of peak 3 in the DP polarogram ( Fig.III-3 ). This phenomenon seems to show that the electrode reaction on wave 3 involves a two-step charge-transfer reaction [6], and/or adsorption of reactant and product [7]. Current-time curves for wave 3 at concentrations of Mo(VI) > 0.5mM in 0.1M H<sub>2</sub>SO<sub>4</sub> also show adsorptive behavior, however, detailed information about the two-step charge-transfer reaction is not obtained.

### III-4-2 Effect of ionic surfactants

As described in chapter II, all the peaks 1-3 correspond to the reduction of Mo(VI) to Mo(V) and peak 4 to the reduction of Mo(V) to Mo(III). The presence of three reduction waves of Mo(VI) to Mo(V) indicates a respective reduction of three different Mo(VI) species. Since there has been little information on the character of these reactants, the effect of ionic surfactants on the DP polarogram was investigated. Jacobsen and co-workers investigated the effects of ionic surfactants on dc [8], ac [9] and DP [10] polarographic waves of some complexes, and observed electrostatic effects. They observed that the surfactant with the same charge as the reactant acted as an electrochemical masking agent. If the results shown in Fig. III-6 and III-7 are interpreted with respect to the electrostatic effect, the electroactive species of Mo(VI) for peaks 1 and 2 are anionic, while that for peak 3 is cationic.

### III-4-3 Species of reactants

Paffett and Anson [1] studied the catalytic reduction of perchlorate by Mo(V) and deduced that the catalytically active species was monomeric Mo(V),  $\text{MoO(OH)(OH)}_2$ , formed by the reduction of cationic Mo(VI),  $\text{MoO}_2(\text{OH})(\text{OH})_2^+$ , in

trifluoromethanesulfonic acid. In sulfuric acid solutions, the catalytic reduction of nitrate was observed at the potential of wave 3 ( chapter II ). Another experiment on the solution containing perchlorate exhibited the same catalytic wave. Therefore, the electroactive species of Mo(VI) at the potential of wave 3 seems to be of the cationic form and this conclusion is consistent with that obtained in this work.

The reduction product of Mo(VI) at the potential of wave 1 is blue species. It is well known that the reduction of certain heteropoly anions, such as  $\text{PMo}_{12}\text{O}_{40}^{3-}$ , makes mixed-valence heteropoly blues [11-13]. Pope [14] reported that in molybdate solutions, the isopoly anions which are the predominant solute species at pH 3-5, viz.,  $\text{Mo}_7\text{O}_{24}^{6-}$  and  $\text{Mo}_8\text{O}_{26}^{4-}$ , are not reducible, although more acidic solutions of Mo(VI) are easily reduced to blue species. The anion responsible for blue color in such solutions have been formulated as  $\text{Mo}_6\text{O}_{19}^{2-}$ . It is not known whether or not the reactant on wave 1 is  $\text{Mo}_6\text{O}_{19}^{2-}$ , however, the reactant is likely to be a large isopoly anion.

### III-5 References

1. M.T.Paffett and F.C.Anson, *Inorg.Chem.*, 20 (1981) 3967.
2. N.Ogawa, I.Watanabe and S.Ikeda, *Anal.Chim.Acta*, 141 (1982) 123.
3. R.Parsons in P.Delahay (Ed.), *Advances in Electrochemistry and Electrochemical Engineering*, Vol.1, Interscience Publishers, Inc., 1961, p.71.
4. D.R.Canterford and R.J.Taylor, *J.Electroanal.Chem.*, 98 (1979) 25.
5. M.N.Hull, *J.Electroanal.Chem.*, 51 (1974) 57.
6. D.E.Smith in A.J.Bard (Ed.), *Electroanalytical Chemistry*, Vol.1, Marcel Dekker, New York, 1966, p.71.
7. T.Kakutani and M.Senda, *Bull.Chem.Soc.Jpn.*, 53 (1980) 1942.
8. E.Jacobsen and G.Kalland, *Anal.Chim.Acta*, 30 (1964) 240.
9. E.Jacobsen and G.Tandberg, *J.Electroanal.Chem.*, 30 (1971) 161.
10. E.Jacobsen and H.Lindseth, *Anal.Chim.Acta*, 86 (1976) 123.
11. S.R.Crouch and H.V.Malmstadt, *Anal.Chem.*, 39 (1967) 1084.
12. M.T.Pope, *Heteropoly and Isopoly Oxometalates*, Springer-Verlag, 1983.
13. G.A.Parker, in I.M.Kolthoff and P.J.Elving (Eds.), *Treatise on Analytical Chemistry*, Part II, Vol.10, John-Wiley and Sons, Inc., 1978, p.341.
14. M.T.Pope, *Inorg.Chem.*, 11 (1972) 1973.



## IV The analysis of the character of catalytically active electrogenerated Mo(V)

### IV-1 Introduction

In the previous chapter II, the catalytic behavior of wave 3 was described. It is well known that the polarography of Mo(VI) gives the catalytic waves in the presence of nitrate or perchlorate ion [1-5], and has been used for the quantitative analysis for Mo(VI) [3,6,7]. Some conflicting arguments have been on the reduction mechanism of Mo(VI) and whether the catalytically active species is Mo(III) or Mo(IV) [2-5]. However, the investigation with coulometry has indicated that the catalytically active species is Mo(V) ([8] and chapter II).

It is known that the Mo(V) species is so stable in hydrochloric acid solution that the dimer-dimer-monomer equilibria can be studied [9,10]. Whereas no similar investigation has been reported in sulfuric acid solution. The investigations in this chapter is carried out ; (1) to obtain the rate constant for the polarographic catalytic reaction, i.e. the oxidation of electrogenerated Mo(V) at mercury electrode with nitrate or perchlorate; (2) to obtain the rate constant for the homogeneous oxidation reaction of Mo(V) in bulk solution with perchlorate to compare the rate with the catalytic one; (3) to establish the equilibrium of

Mo(V) in sulfuric acid solution.

#### IV-2 Experimental

All chemicals were of analytical reagent grade and used without further purification. Nitrogen monoxide was prepared by mixing sodium nitrate and sulfuric acid [11]. Polarographic and coulometric instruments employed in this study were the same as described in chapters II and III. Hitachi 124 spectrophotometer was used for the spectrophotometric measurements. Electron spin resonance spectra were recorded on a JEOL MODEL JES-FE 1X ESR spectrometer with a 100kHz modulator [12].

The polarographic current values in this report were measured with RC damping, i.e. the average current during the drop life was measured unless otherwise noted. The catalytic current  $i_c$  was taken from the difference between the currents measured in the presence and the absence of nitrate or perchlorate at around  $-0.36V$  vs. SCE. It was so determined in each measurement that the potential was 95mV less than the half-wave potential of wave 3 of Mo(VI) solution without nitrate or perchlorate ( chapter II ).

The Mo(V) solutions were prepared by reducing  $2.5 \times 10^{-3}$  -  $5 \times 10^{-3}M$  Mo(VI) in  $0.1M$   $H_2SO_4$  electrolytically using Hg-pool electrode. Oxidation reaction of Mo(V) was initiated

by mixing Mo(V) and perchlorate solutions. Polarographic and spectrophotometric measurements were carried out at  $25 \pm 0.2^\circ\text{C}$ , whereas esr measurements were carried out at room temperature.

### IV-3 Results

#### IV-3-1 Polarographic catalytic current

Polarograms and reduction mechanisms for Mo(VI) in sulfuric acid solutions were in the previous chapters. There are three waves corresponding to the reduction of Mo(VI) to Mo(V) in the polarogram of 0.5mM Mo(VI) in 0.1M  $\text{H}_2\text{SO}_4$ . The presence of nitrate or perchlorate enhances the height of the third wave only. Figure IV-1 shows the relationship between the catalytic current  $i_c (= i - i_3)$ , and the height of the third wave  $i_3$ , which should be proportional to the concentration of the species giving the third wave. When the concentration of Mo(VI) is lower than 0.5mM, the plot is linear. At the higher concentration range, it deviates from the linearity because of adsorptive behavior of Mo(VI) or Mo(V) at higher concentration. The current amplification by catalytic reaction depends on the concentration of the oxidants as shown in Fig. IV-2. The ratio of  $i/i_3$  taken at low concentration of Mo(VI) ( $5 \times 10^{-5}\text{M}$ ) proportional to the square root of the concentration of nitrate

(63)

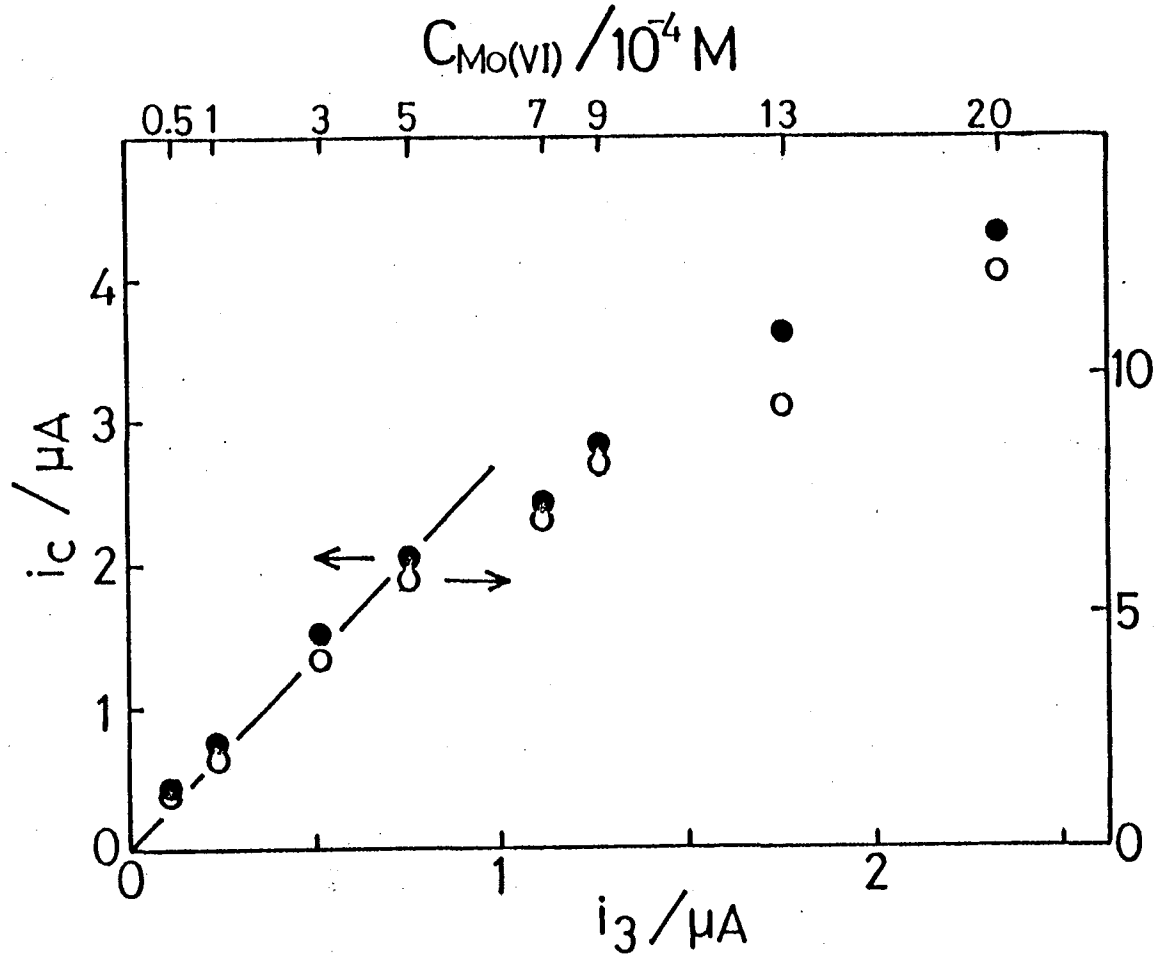


Fig.IV-1. Dependence of the catalytic current on the height of the third wave in 0.1M H<sub>2</sub>SO<sub>4</sub>: (○) with 20mM NaNO<sub>3</sub>; (●) with 50mM NaClO<sub>4</sub>.

(64)

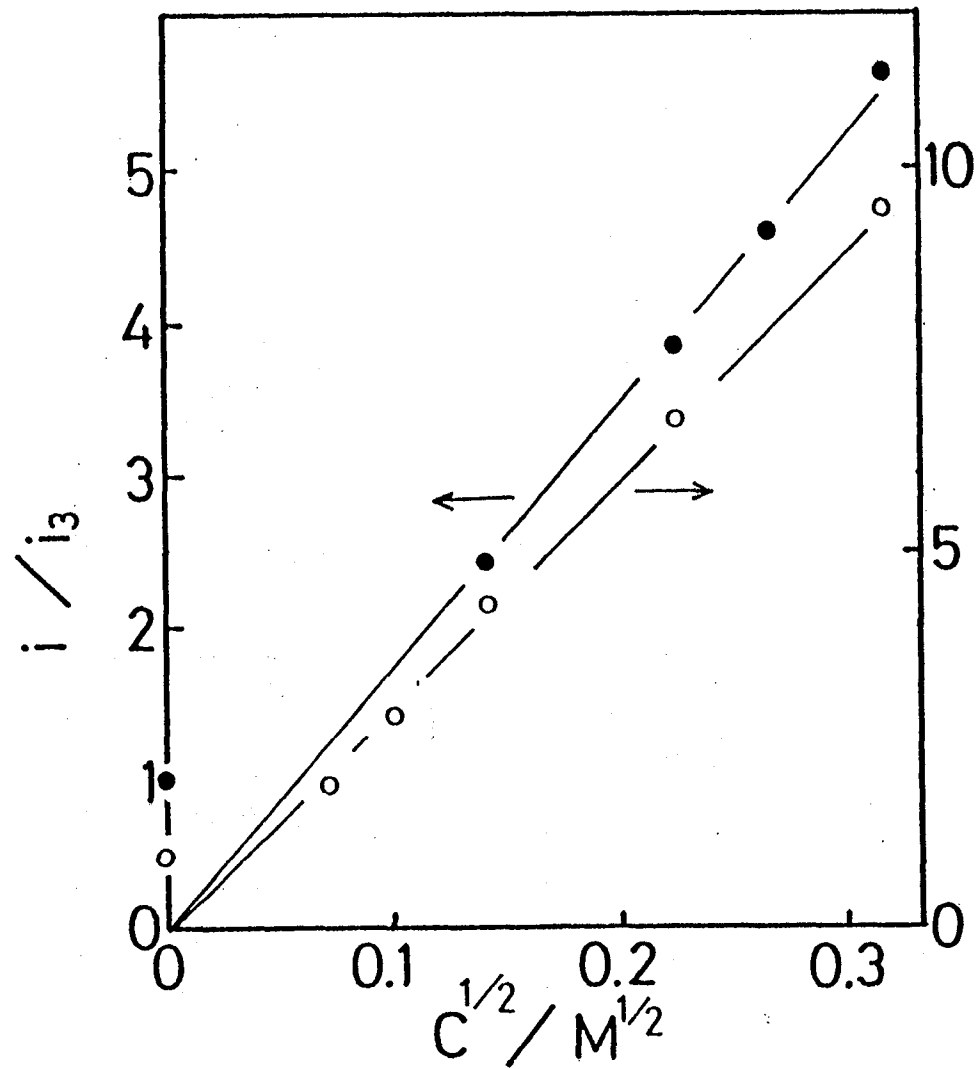


Fig.IV-2. Dependence of  $i/i_3$  on the square root of the concentration of nitrate (O) and perchlorate (●).  $C_{Mo(VI)} = 5 \times 10^{-5}M$ .

or perchlorate, therefore the second-order rate constants  $k_c$  for the catalytic reduction of nitrate and perchlorate by Mo(V) are obtained by using Koutecky's treatment ( [13], Appendix 1 ). Results are listed in Table IV-1.

In the presence of nitrate, the reduction wave of reduction product of nitrate is observed at about -0.9V vs. SCE ( Fig.II-10 ). Same reduction wave is observed for the 0.1M  $H_2SO_4$  solution after bubbling with nitrogen monoxide. Therefore, the reduction product for the catalytic reduction of nitrate is considered to be nitrogen monoxide. In the presence of perchlorate, the solution after CPE at -0.3V ( the potential at which the catalytic reaction is observed ) shows the oxidation of the mercury electrode at more negative potential than that for the solution before CPE, indicating the reduction product of perchlorate in the process of the catalytic reaction is considered to be chloride ion.

#### IV-3-2 Absorption spectra of Mo(V)

Absorption spectra of  $2.5 \times 10^{-4}$  M Mo(V) in various concentration of sulfuric acid solution are shown in Fig.IV-3. In 0.1M  $H_2SO_4$ , the absorption maxima are observed at 254nm and 293nm. This spectrum has been already assigned to be that of dimeric Mo(V),  $Mo_2O_4^{2+}$  [14,15]. When the concentration of sulfuric acid is higher than 3M, the peak at 405nm appears.

Table IV-1. Second-order rate constants for the  
 polarographic catalytic reaction in  
 0.1M H<sub>2</sub>SO<sub>4</sub>. C<sub>Mo(VI)</sub> = 5 x 10<sup>-5</sup>M

		$k_c / M^{-1}s^{-1}$
C <sub>NaNO<sub>3</sub></sub>	5 x 10 <sup>-3</sup> - 1 x 10 <sup>-1</sup> M	(2.1 ± 0.4) x 10 <sup>3</sup>
C <sub>NaClO<sub>4</sub></sub>	2 x 10 <sup>-2</sup> - 1 x 10 <sup>-1</sup> M	(1.9 ± 0.1) x 10 <sup>2</sup>

(67)

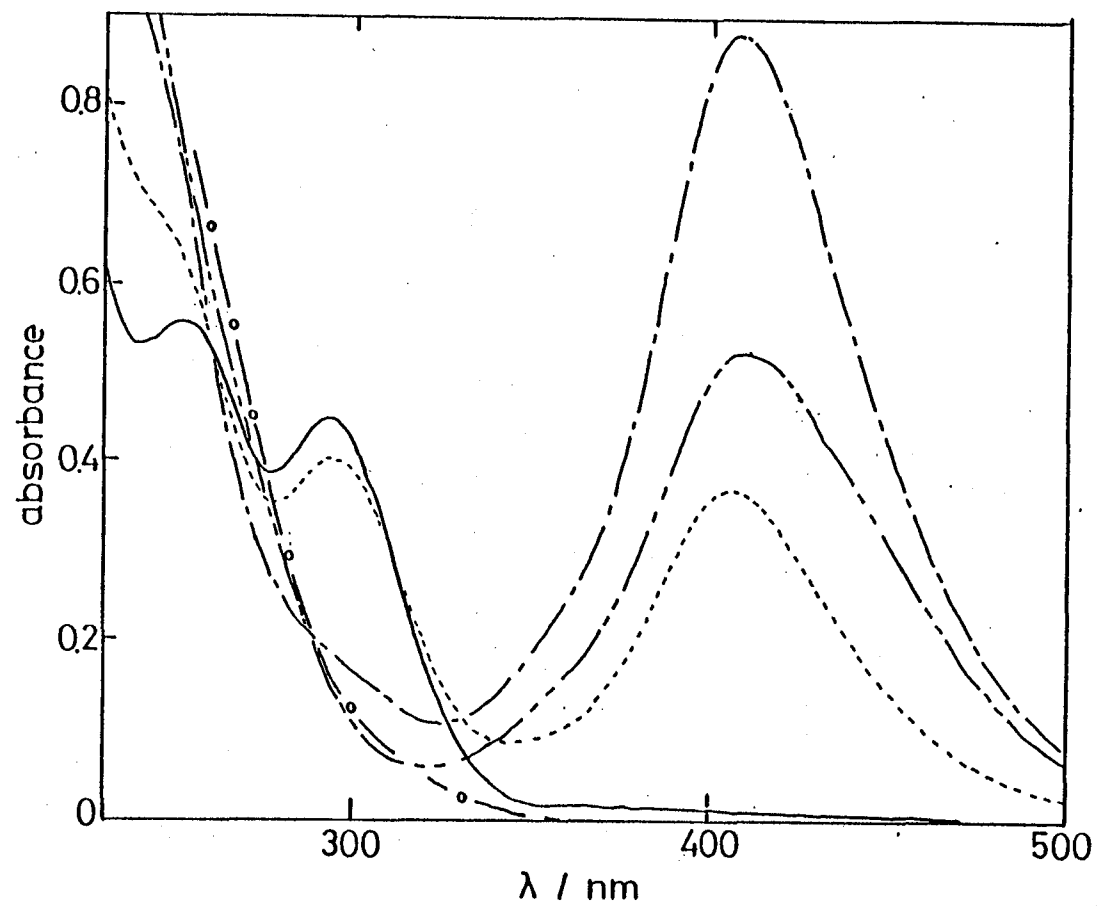


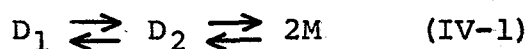
Fig.IV-3. Absorption spectra of  $2.5 \times 10^{-4} \text{ M Mo(V)}$  in various concentration of  $\text{H}_2\text{SO}_4$ : (—) 0.1M; (.....) 7M; (-.-) 9M; (- - -) 11M; (-o-) 15M.  $l = 1\text{cm}$ .



When  $C_{H_2SO_4}$  is increased to 9M, the absorption maxima at 254nm and 293nm disappear, and the absorbance of the peak at 407nm reaches to its maximum and the solution looks green yellow. In 15M  $H_2SO_4$ , there is no absorption in the visible region. The absorbances at 254nm, 293nm and 407nm vary with  $C_{H_2SO_4}$  as shown in Fig.IV-4. The change of absorbance at 407nm suggests that three different species of Mo(V) present in the  $C_{H_2SO_4}$  region studied.

#### IV-3-3 Dimer-dimer-monomer equilibria of Mo(V)

In hydrochloric acid solution, dimer-dimer-monomer equilibria of chloro complex of Mo(V) have been reported [9,10]. However, there has been no study of such equilibria in sulfuric acid solution. It is well characterized that the predominant species of Mo(V) in 0.1M  $H_2SO_4$  is of dimeric form,  $Mo_2O_4^{2+}$  [14,15]. From the analogy of the equilibria of Mo(V) in hydrochloric acid solution, we expect the dimer ( $Mo_2O_4^{2+}$ )-dimer-monomer equilibria of Mo(V) in sulfuric acid solution as follows:



$$K_1 = [D_2]/[D_1] \quad (IV-2)$$

$$K_2 = [M]^2/[D_2] \quad (IV-3)$$

$$C_t = 2[D_1] + 2[D_2] + [M] \quad (IV-4)$$

where  $D_1$  is the dimer,  $Mo_2O_4^{2+}$ ,  $D_2$  is the other dimer and

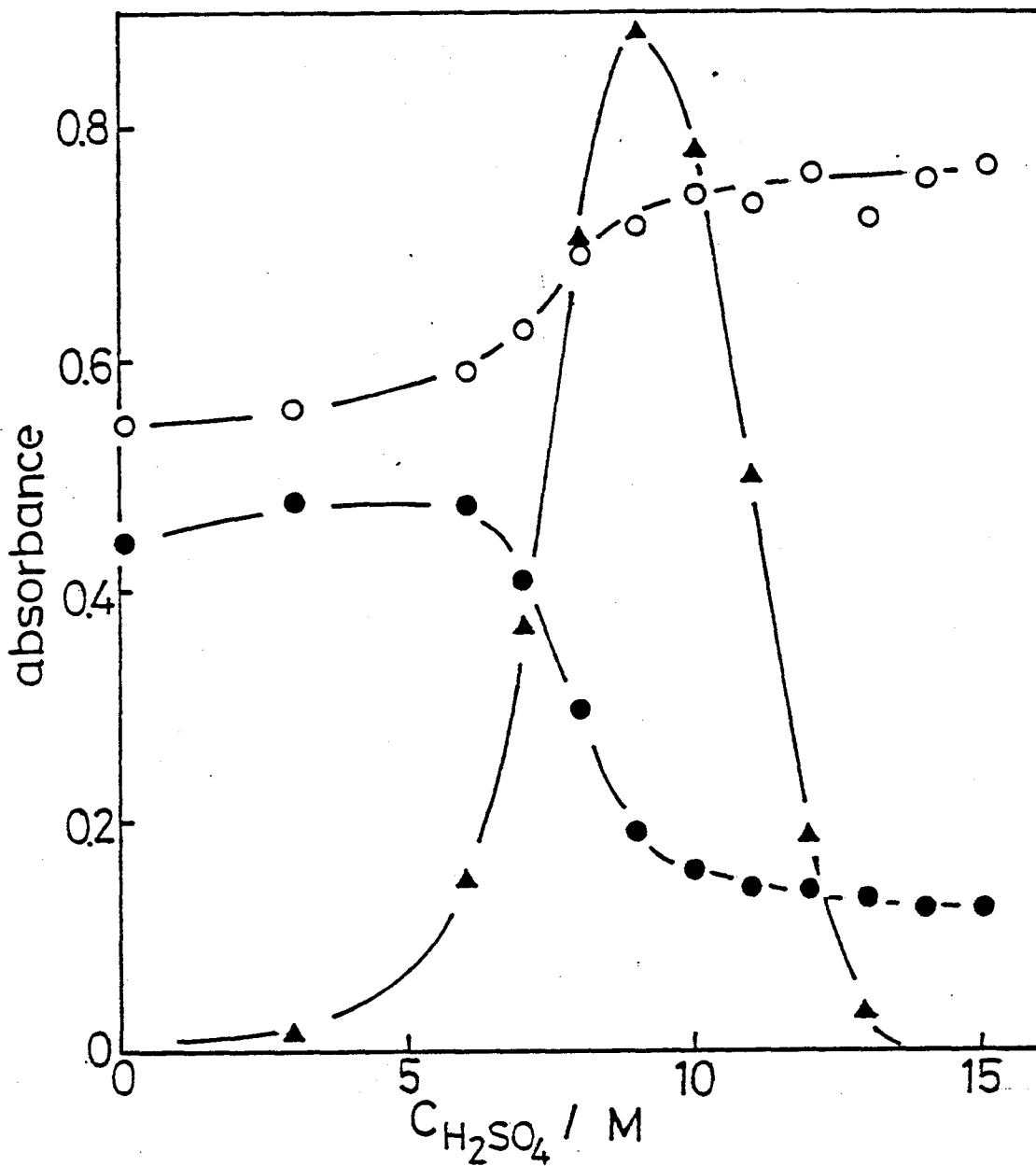


Fig.IV-4. Effect of the concentrations of H<sub>2</sub>SO<sub>4</sub> on absorbances of  $2.5 \times 10^{-4} M$  Mo(V) solution at 254nm (○), 293nm (●) and 407nm (▲).  $l = 1cm$

M is a monomer,  $K_1$  and  $K_2$  are the ratios of the concentration and  $C_t$  is the total concentration of Mo(V). Spectrophotometric data were treated by using Haight's procedure [9]. When  $C_{H_2SO_4}$  is lower than 9M,  $D_1 - D_2$  equilibrium should be predominant. From the result of Fig.IV-4, one can conclude that at 407nm only the species of  $D_2$  absorbs and the absorption intensity at 407nm is expressed as follows:

$$A_{407} = \epsilon_2 [D_2] \quad (IV-5)$$

where  $\epsilon_2$  is the molar absorption coefficient of  $D_2$ .

From the equations (IV-2), (IV-4) under the condition of  $[M] = 0$  and (IV-5),

$$A_{407} = \epsilon_2 K_1 C_t / 2(1 + K_1) \quad (IV-6)$$

Therefore, if  $K_1$  is really a constant which is independent of  $C_t$ ,  $A_{407}$  should be proportional to  $C_t$  when  $C_{H_2SO_4}$  is lower than 9M. The dependence of  $A_{407}$  on  $C_t$  in 7.5M and 8M  $H_2SO_4$  is shown in Fig.IV-5. From the result of Fig.IV-5 it is ascertained that  $D_2$  is also of dimeric form.

When  $C_{H_2SO_4}$  is higher than 9M,  $D_2 - 2M$  equilibrium should exist predominantly. In this case

$$C_t = 2[D_2] + [M] \quad (IV-7)$$

and from the equations (IV-3), (IV-5) and (IV-7),

$$A_{407}/C_t = \epsilon_2/2 - (\epsilon_2 K_2/4)^{1/2} A_{407}^{1/2}/C_t \quad (IV-8)$$

Therefore, a plot of  $A_{407}/C_t$  vs.  $A_{407}^{1/2}/C_t$  should give a straight line of slope  $-(\epsilon_2 K_2/4)^{1/2}$  and intercept of  $\epsilon_2/2$ .

The plots of  $A_{407}/C_t$  vs.  $A_{407}^{1/2}/C_t$  taken at 9, 10, 11 and

(71)

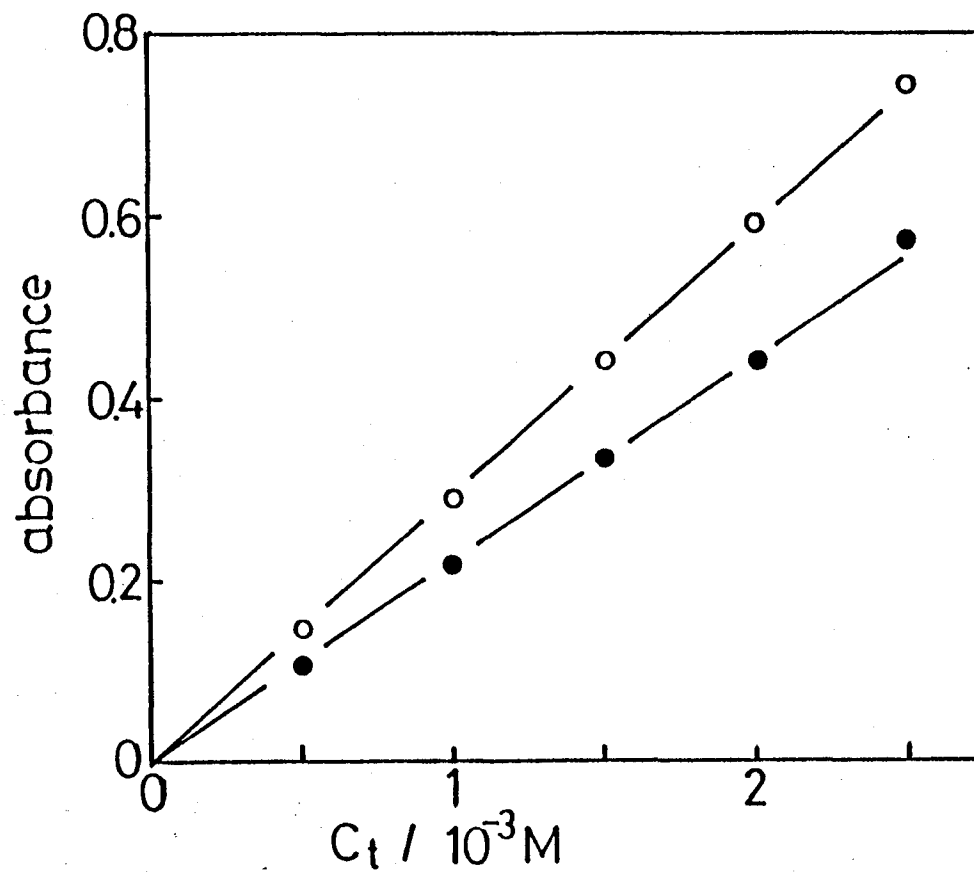


Fig.IV-5. Dependence of  $A_{407}$  on  $C_t$  in 7.5M (●) and 8M (○)  $H_2SO_4$ .

12M H<sub>2</sub>SO<sub>4</sub> are shown in Fig.IV-6. From the average value of  $\epsilon_2$  (  $8.17 \times 10^3 \text{M}^{-1}\text{cm}^{-1}$  ) obtained,  $K_1$  and  $K_2$  are calculated for various C<sub>H<sub>2</sub>SO<sub>4</sub></sub> and are listed in Table IV-2. When C<sub>H<sub>2</sub>SO<sub>4</sub></sub> is higher than 13M, monomeric Mo(V) is a predominant species. Figure IV-7 shows esr spectra of monomeric ( in 14M H<sub>2</sub>SO<sub>4</sub> ) and dimeric ( in 9M H<sub>2</sub>SO<sub>4</sub> ) Mo(V). Esr spectra for monomeric ( in 9.6N HCl ) and dimeric ( in 5N HCl [9] ) Mo(V) are also shown in Fig.IV-7. Both of the species in H<sub>2</sub>SO<sub>4</sub> gives esr signals with different shape and the signals are quite different from those in HCl. No esr signal was observed for the dimer, Mo<sub>2</sub>O<sub>4</sub><sup>2+</sup>, in 0.1M H<sub>2</sub>SO<sub>4</sub>.

#### IV-3-4 Oxidation of monomeric Mo(V) with perchlorate

The reaction was studied by conventional spectrophotometry in the presence of the excess perchlorate in 14M H<sub>2</sub>SO<sub>4</sub>. The decrease in absorption at 260nm was used to monitor the reaction. Absorbance at 260nm, A<sub>260</sub>, can be described as follows:

$$A_{260} = \epsilon_M[M] + \epsilon_{VI}[\text{Mo(VI)}] \quad (\text{IV-9})$$

and

$$C = [M] + [\text{Mo(VI)}] \quad (\text{IV-10})$$

where  $\epsilon_M$  (  $2.57 \times 10^3 \text{M}^{-1}\text{cm}^{-1}$  ) and  $\epsilon_{VI}$  (  $1.10 \times 10^3 \text{M}^{-1}\text{cm}^{-1}$  ) are the molar absorption coefficients of M and Mo(VI), respectively. From the equations (IV-9) and (IV-10), [M] is

$$[M] = (A_{260} - \epsilon_{VI}C) / (\epsilon_M - \epsilon_{VI}) \quad (\text{IV-11})$$

(73)

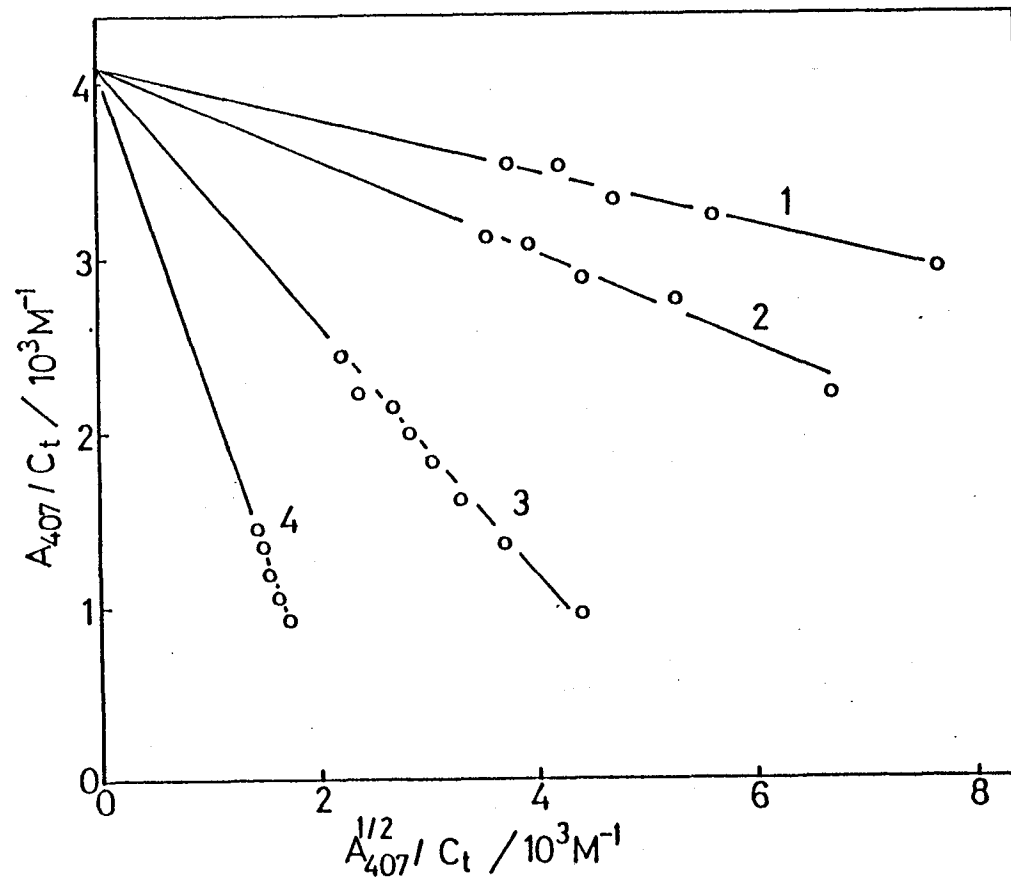


Fig. IV-6. Dependence of  $A_{407}/C_t$  on  $A_{407}^{1/2}/C_t$  in  $H_2SO_4$ .

$C_{H_2SO_4}$ : (1) 9M; (2) 10M; (3) 11M; (4) 12M.

Table IV-2. Equilibrium constants for dimer(D<sub>1</sub>)-  
 dimer(D<sub>2</sub>)(K<sub>1</sub>) and dimer(D<sub>2</sub>)- monomer  
 (M)(K<sub>2</sub>) in various concentration of  
 H<sub>2</sub>SO<sub>4</sub>.

C <sub>H<sub>2</sub>SO<sub>4</sub></sub> / M	K <sub>1</sub>	C <sub>H<sub>2</sub>SO<sub>4</sub></sub> / M	K <sub>2</sub> / M
3	1.80 x 10 <sup>-2</sup>	9	1.17 x 10 <sup>-5</sup>
6	1.71 x 10 <sup>-1</sup>	10	3.97 x 10 <sup>-5</sup>
7	5.71 x 10 <sup>-1</sup>	11	2.28 x 10 <sup>-4</sup>
7.5	1.28	12	1.71 x 10 <sup>-3</sup>
8	2.24		

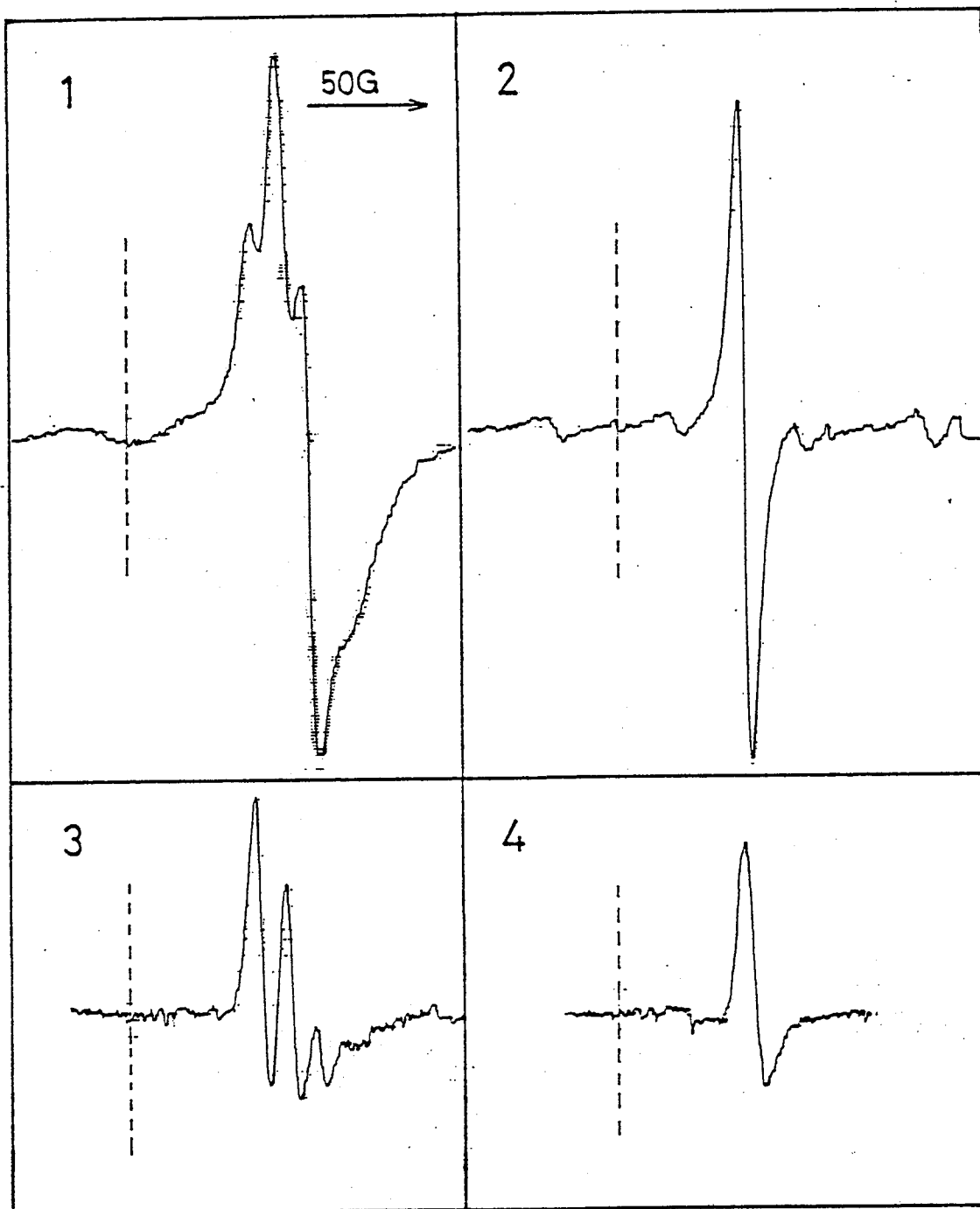


Fig.IV-7. First- derivative esr spectra of  $1 \times 10^{-3} \text{M Mo(V)}$  :  
 (1) in 14M  $\text{H}_2\text{SO}_4$ ; (2) in 9.6N  $\text{HCl}$ ; (3) in 9M  $\text{H}_2\text{SO}_4$ ;  
 (4) in 5N  $\text{HCl}$ . Dotted line indicates the position  
 for the signal of  $\text{Mn}^{2+}$  in  $\text{MgO}$  ( $g = 1.981$ ).



The plot of  $\ln[M]$  against time was linear to > 90% completion. The pseudo-first-order rate constant determined from the plot was linearly dependent on the concentration of perchlorate as shown in Fig.IV-8. Therefore, the rate law is

$$-d[M]/dt = k_{\text{obs}}[M] = k[M][\text{ClO}_4^-] \quad (\text{IV-12})$$

where  $k$  is the second-order rate constant for the oxidation reaction of the monomeric Mo(V) with perchlorate. The value for  $k$  over  $1.67 \times 10^{-2} - 8.33 \times 10^{-2} \text{M}$  perchlorate was  $(1.59 \pm 0.13) \times 10^{-1} \text{M}^{-1} \text{s}^{-1}$  in 14M  $\text{H}_2\text{SO}_4$ . The oxidation with nitrate was not studied, because the large absorbance of nitrate in uv region interferes the monitoring of the reaction. The oxidation of  $\text{Mo}_2\text{O}_4^{2+}$  with perchlorate is extremely slow [17] and of the dimer in 9M  $\text{H}_2\text{SO}_4$  can not be obtained precisely, because the reaction of the monomer is involved simultaneously. However, approximate rate constant obtained in 9M  $\text{H}_2\text{SO}_4$  is about three order smaller than in 14M  $\text{H}_2\text{SO}_4$ .

#### IV-4 Discussion

The catalytic reaction of Mo(VI) in the presence of nitrate or perchlorate ions is a widely known phenomenon. The recent investigations with coulometry concluded that the catalytically active species is Mo(V). ( [8], chapter II ) Paffett and Anson suggested that monomeric Mo(V),  $\text{MoO}(\text{OH})(\text{OH}_2)_4^{2+}$ , is the catalytically active species [1],

(77)

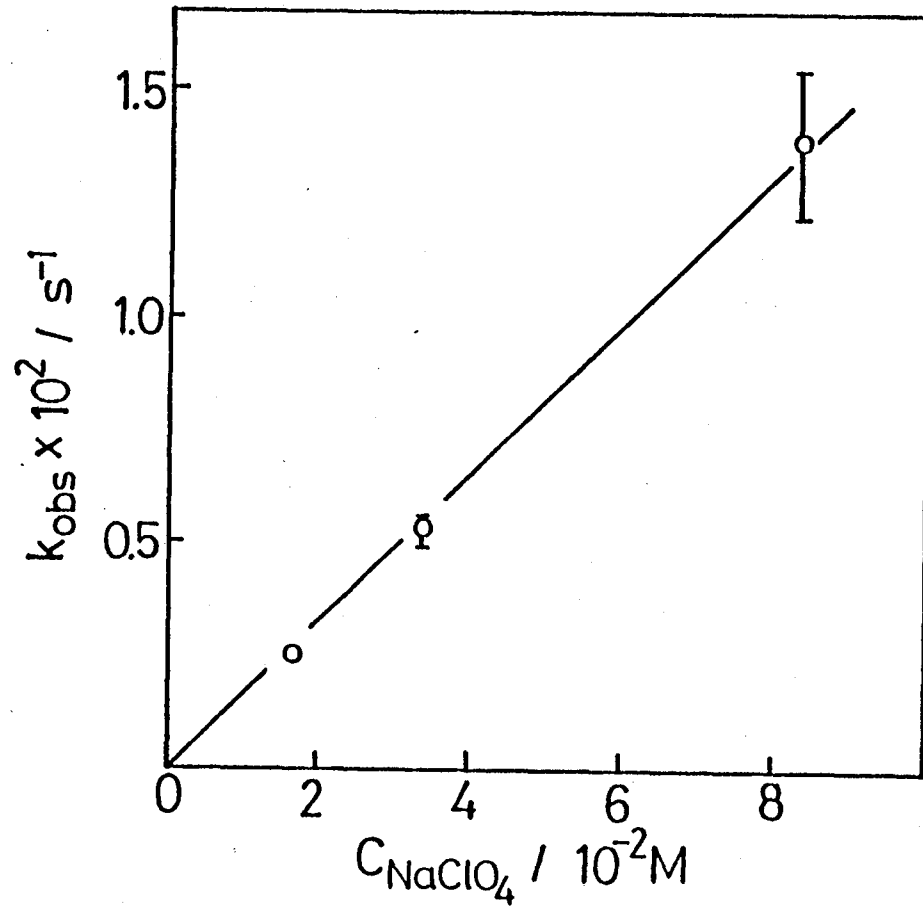


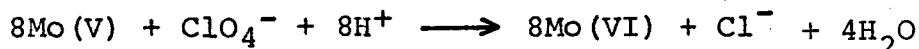
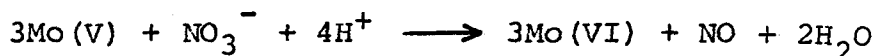
Fig. IV-8. Dependence of  $k_{\text{obs}}$  on the concentration of perchlorate.



however, detailed information can not be obtained in the present stage.

The rate of the reaction involving perchlorate should increase with the activity of hydrogen ion, though the second-order rate constant for the oxidation reaction of monomeric Mo(V) with perchlorate in 14M H<sub>2</sub>SO<sub>4</sub> is found to be about three order smaller than that for the reaction of electrogenerated Mo(V) with perchlorate in 0.1M H<sub>2</sub>SO<sub>4</sub> for 5 x 10<sup>-5</sup> - 5 x 10<sup>-4</sup>M Mo(VI). Therefore, monomeric Mo(VI) in 14M H<sub>2</sub>SO<sub>4</sub> is not the same species as electrogenerated Mo(V) in 0.1M H<sub>2</sub>SO<sub>4</sub>. It has been proposed that monomeric cation of Mo(V) is the catalytically active species, ( [1], chapter III ), however, this electrogenerated monomer is more reactive than the monomer in bulk solution.

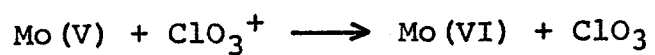
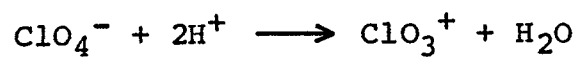
In the catalytic reduction of nitrate and perchlorate, the reduction products are nitrogen monoxide and chloride ion, respectively. Therefore, overall reaction may be as follows:



For the initial reaction, following scheme may be considered [20].



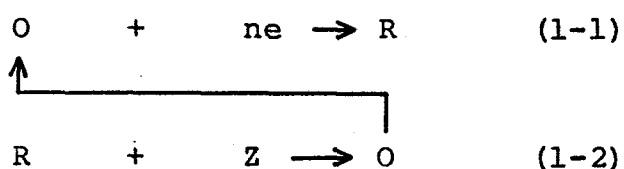
and



but little is known about the successive reduction of nitrate or perchlorate.

Appendix 1 Koutecky's treatment for the polarographic catalytic reaction [13]

Let us think of a reduction of O at an electrode to form R ( equation 1-1 ). If the R is chemically oxydized by a substance Z ( equation 1-2 ), O is regenerated and one should observe catalytic current.



In this case the substance Z should not be reduced at the potential at which the electrolysis is carried out. Because of the regeneration reaction (1-2) the current for reduction of substance O depends on the diffusion rates of the species involved and on the rate of oxidation reaction of substance R by Z. The term, catalytic current, is applicable to all types of currents in which the reactant being consumed in the electrochemical reaction is partially regenerated by a chemical process involving a product of the electrochemical reaction.

If the electrochemical process (1-1) is so rapid that substance O is reduced as soon as it reaches the electrode, the following equations are obtained.

$$\frac{\partial C_O(x,t)}{\partial t} = D_O \frac{\partial^2 C_O(x,t)}{\partial x^2} + k_f C_R(x,t) C_Z(x,t) - k_b C_O(x,t) \quad (1-3)$$

$$\frac{\partial C_R(x,t)}{\partial t} = D_R \frac{\partial^2 C_R(x,t)}{\partial x^2} - k_f C_R(x,t) C_Z(x,t) + k_b C_O(x,t) \quad (1-4)$$

where the  $k$ 's are formal rate constants. In principle the concentration of substance Z is a function of  $x$  and  $t$ , but the bulk concentration  $C_Z^0$  of this substance can be made much larger than that of substance O; the function  $C_Z(x,t)$  can then be replaced by the constant  $C_Z^0$ . Under the condition that backward reaction in (1-2) is extremely slow, Koutecky solved the boundary value problem of equations (1-1) and (1-2) for the dropping mercury electrode. The ratio for average current  $i/i_d$  is derived as follows.

$$i/i_d = 0.812\rho'^{1/2} + 1.92\rho'^{-7/6} \quad (1-5)$$

where

$$\rho' = k_f C_Z^0 \tau \quad (1-6)$$

where  $i$  is the total average current and  $i_d$  is the average diffusion current in the absence of any catalytic effect and  $\tau$  is the drop time. For values of  $\rho'$  larger than 10 the term in  $\rho'^{-7/6}$  becomes rather small in comparison with the

term in  $\rho^{1/2}$ . therefore the ratio  $i/i_d$  is simply equal to  $0.812\rho^{1/2}$ . The units are as follows;  $k_f$  in  $\text{mole}^{-1} \text{cm}^3\text{s}^{-1}$ ,  $C_z^0$  in  $\text{mole cm}^{-3}$  and  $\tau$  in seconds.

The validity of Koutecky's treatment has been verified experimentally for two cases, (1) the reduction of Ti(IV) in the presence of hydroxylamine and (2) the reduction of ferric ion in the presence of hydrogen peroxide.



#### IV-5 References

1. M.J.Paffett and F.C.Anson, *Inorg.Chem.*, 20 (1981) 3967.
2. I.M.Kolthoff and I.Hodara, *J.Electroanal.Chem.*, 4 (1962) 369.
3. T.E.Edmonds, *Anal.Chim.Acta*, 116 (1980) 323.
4. M.G.Johnson and R.J.Robinson, *Anal.Chem.*, 24 (1952) 366.
5. G.P.Haight, Jr., *Anal.Chem.*, 23 (1951) 1505.
6. P.Lanza and D.Ferri, *Analyst*, 105 (1980) 379.
7. G.D.Christian, J.L.Vandenbalck and G.J.Patriorche, *Anal.Chim.Acta*, 108 (1979) 149.
8. P.Chalilpoyil and F.C.Anson, *Inorg.Chem.*, 17 (1978) 2418.
9. G.P.Haight, Jr., *J.Inorg.Nucl.Chem.*, 24 (1962) 663.
10. R.Colton and G.G.Rose, *Aust.J.Chem.*, 21 (1968) 883.
11. Nippon Kagaku Kai (Ed.), *Shin Jikken Kagaku Koza*, Vol.8, Maruzen, 1976, p.224.
12. M.Kamachi, Y.Kuwae and S.Nozakura, *Polym.J.*, 13 (1981) 919.
13. P.Delahay, "New Instrumental Methods in Electrochemistry"; Interscience, New York, 1954.
14. M.Ardon and A.Pernick, *Inorg.Chem.*, 12 (1973) 2484.
15. Y.Sasaki and A.G.Sykes, *J.Chem.Soc., Dalton Trans.*, (1974) 1468.
16. E.P.Guymon and J.T.Spence, *J.Phys.Chem.*, 70 (1966) 1964.
17. G.R.Cayley, R.S.Taylor, R.K.Wharton and A.G.Sykes, *Inorg.Chem.*, 16 (1977) 1377.

18. G.P.Haight and D.R.Boston, *J.Less-Common Met.*,  
36 (1974) 95.
19. J.O.Edwards, *Inorganic Reaction Mechanisms*, W.A.Benjamin  
Inc., New York, 1964.

## V The analysis of wave 4

### V-1 Introduction

In the series of electrochemical investigations of Mo(VI) ( chapters II-IV ), the change of the valence state of each reduction wave is determined by coulometry, and its reduction mechanisms has been proposed. However, one strange phenomena still remains. It is described in chapter II that in 0.1M H<sub>2</sub>SO<sub>4</sub> the total height of waves 1, 2 and 3 is almost the same as that of wave 4, while n for the reduction in the former three waves and n for wave 4 are one and two respectively. The disproportionation reaction of Mo(IV) may exist but the evidence for this deduction could not be obtained ( chapter II ). Then, to investigate the chemical reaction being accompanied by the electrode reaction of wave 4 and the redox behavior of each reduction step, cyclic voltammetry with a hanging mercury drop electrode ( HMDE ) and a rotating ring-disc electrode ( RRDE ) are introduced.

### V-2 Experimental

All chemicals described in this chapter were the same as those in previous chapters.

Hanging mercury drop electrode ( Mitubishi Kasei Kogyo, Co.

ASHMDE, drop area:  $0.042\text{cm}^2$  ) and a Voltammetric Analyzer, Model P-1100 ( Yanagimoto Mfg. Co. Ltd. ) were used for cyclic voltammetry. Rotating ring-disc electrode instrument RRDE-1 and speed controller SC-5 ( Nikko Keisoku Co. ) were used for voltammetric measurements. Rotating ring(Au)-disc(Au) electrode (Nikko Keisoku Co., NKP-2 ) was used and had the dimension  $r_1 = 0.295\text{cm}$ ,  $r_2 = 0.305\text{cm}$  and  $r_3 = 0.415\text{cm}$ . The collection efficiency,  $N$ , for this electrode was calculated to be 0.450. ( appendix 2 ) Amalgamation of the RRDE was performed by slowly rotating ( 400rpm ) the electrode in a pool of mercury for five seconds, and then spinning the electrode at 2000rpm to remove the excess mercury. The characteristics of the dropping mercury electrode at a mercury column height of 59.0cm were  $m = 1.40\text{mgs}^{-1}$ ,  $t = 5.76\text{s}$  in 0.1M  $\text{H}_2\text{SO}_4$  at -0.80V vs. SCE unless otherwise noted. The pulse amplitude in DP polarographic measurement was 50mV.

### V-3 Results

Figure V-1 shows the dc polarogram of 0.5mM Mo(VI) and Mo(V) in 0.1M  $\text{H}_2\text{SO}_4$ . As described in chapter II, the reaction at wave 4 for Mo(VI) is controlled by the competition of diffusion and reaction rate, for the dependence of wave height of wave 4 on  $h^{1/2}$  is linear and has a positive intercept at  $h^{1/2} = 0$  ( Fig.II-6 ). The dependence of the

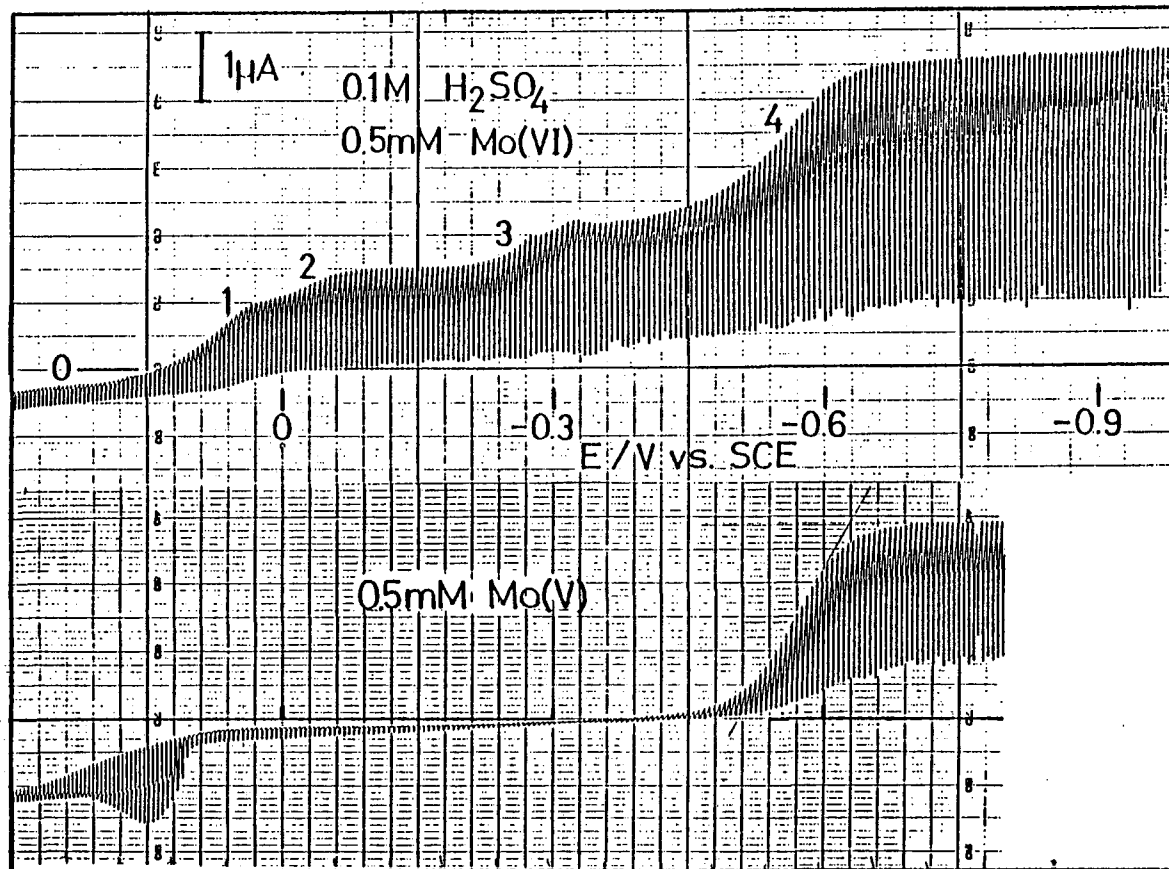


Fig.V-1. Dc polarograms for 0.5mM Mo(VI) and Mo(V) in 0.1M H<sub>2</sub>SO<sub>4</sub>.

wave height for Mo(V) in 0.1M H<sub>2</sub>SO<sub>4</sub> ( solution after one-electron reduction of Mo(VI) in 0.1M H<sub>2</sub>SO<sub>4</sub> ) on  $h^{1/2}$  is shown in Fig.V-2. The linearity indicates that the reduction of Mo(V) is diffusion controlled. Therefore, the reduction process at wave 4 of Mo(VI) solution is considered to contain the preceding chemical reaction.

Figure V-3 shows the cyclic voltammogram with HMDE for the same solution as for Fig.V-1. For Mo(VI) three cathodic peaks ( c(1) +0.14V, c(2) -0.48V, c(3) -0.68V vs. SCE ) and three anodic ones ( about +0.25V, -0.20V and -0.31V ) are observed. For Mo(V) a cathodic ( -0.65V ) and an anodic ( -0.21V ) peaks are observed. The dependence of the anodic peak current  $i_{pa}$  for Mo(VI) on switching potential  $P_s$  ( for example, -0.9V in Fig.V-3 ) is shown in Fig.V-4. When  $P_s$  is more positive than -0.2V, single anodic peak ( a(1) +0.20V ) is observed. Therefore, the c(1)-a(1) redox couple is one-electron reversible reaction. As  $P_s$  is changed from -0.30V to -0.60V,  $i_{pa}(-0.20V)$  and  $i_{pa}(-0.30V)$  are increased. And  $P_s$  is further increased from -0.60V to -0.90V,  $i_{pa}(-0.20V)$  is increased continuously while  $i_{pa}(-0.30V)$  levels off. That is,  $pa(-0.20V)$  corresponds to the oxidation of the reduction product of c(3) and  $pa(-0.30V)$  to c(2).  $pa(-0.20V)$  and  $pa(-0.30V)$  are expressed as a(3) and a(2) respectively. When  $P_s$  is more negative than -0.3V, a(1) is also increased, indicating that the reduction product of c(2)

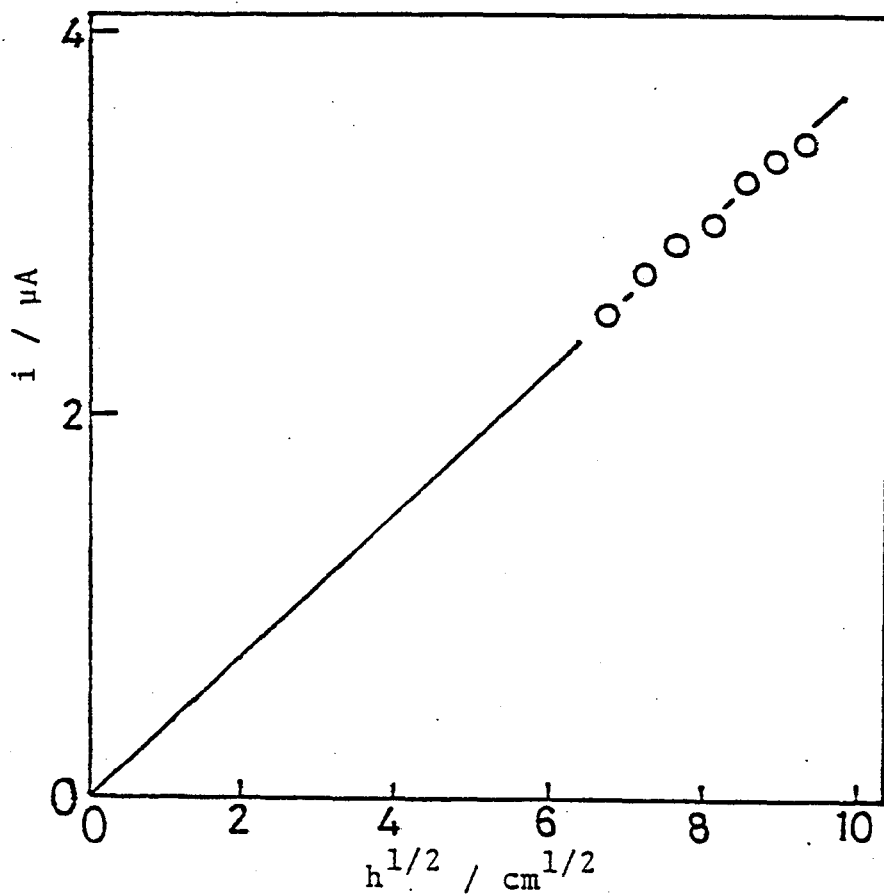


Fig.V-2. Dependence of the wave height for 0.5mM Mo(V) in 0.1M  $\text{H}_2\text{SO}_4$  on the square root of the mercury column height.

(16)

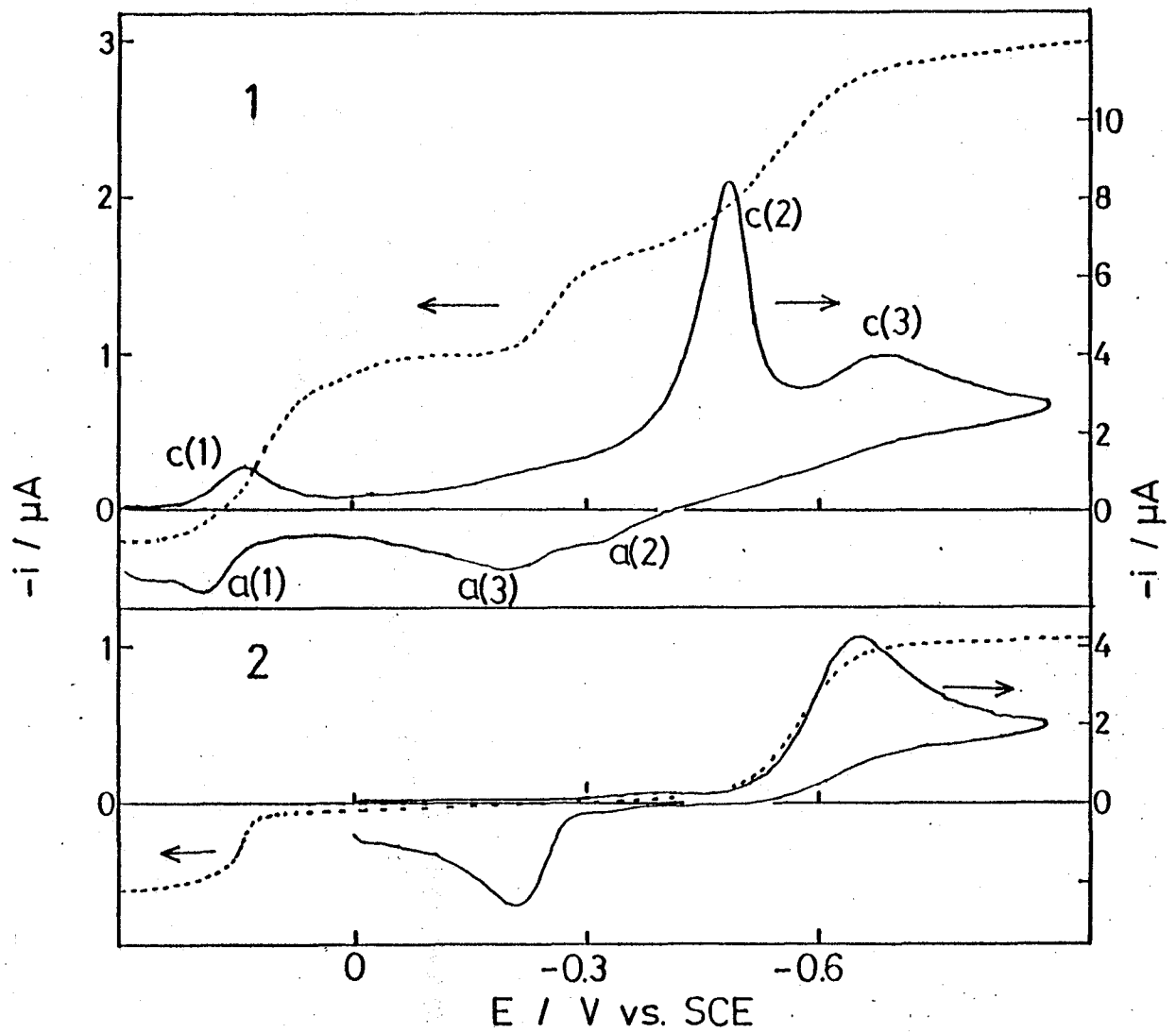


Fig.V-3. Dc (-----) and cyclic (——) voltammograms in 0.1M H<sub>2</sub>SO<sub>4</sub>. 1. 0.5mM Mo(VI); 2. 0.5mM Mo(V) ( scan rate: 0.1Vs<sup>-1</sup> ).  $m = 1.42\text{mgs}^{-1}$ ,  $t = 2.5\text{s}$



(92)

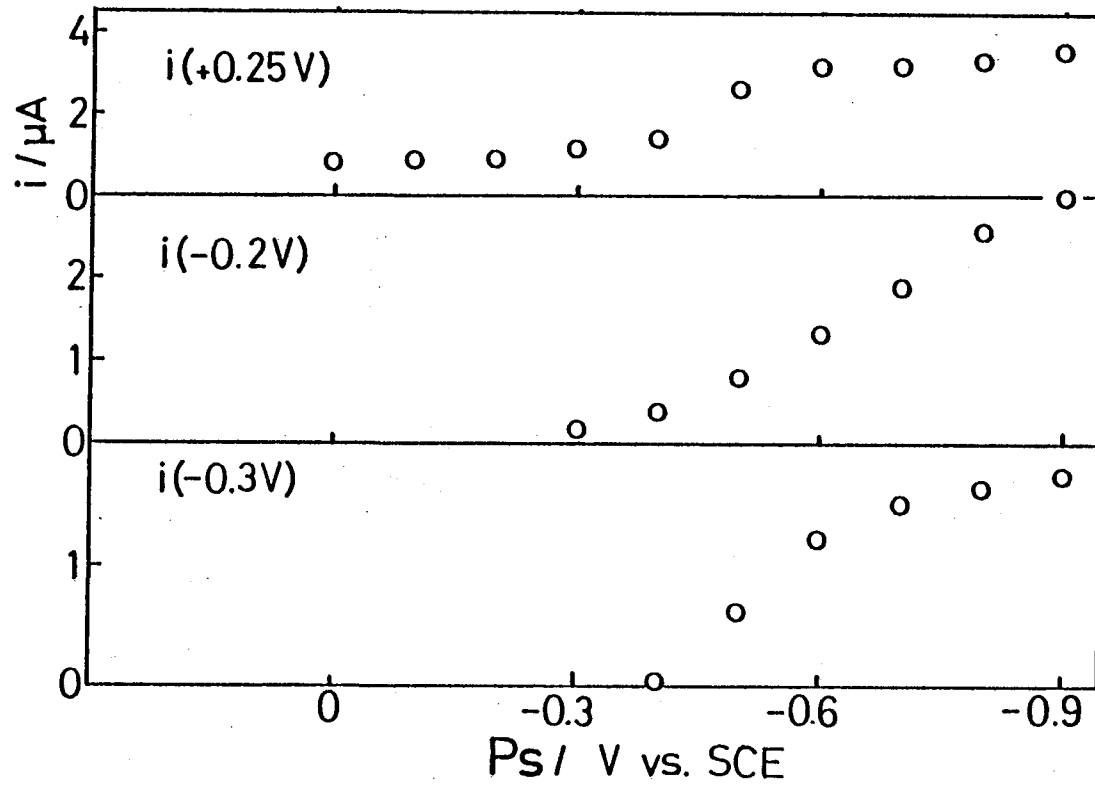


Fig.V-4. Dependence of the anodic peak current on the switching potential ( scan rate:  $0.1\text{Vs}^{-1}$  ).

is oxidized also at around  $E_{pa(1)}$ . Summarizing these phenomena, c(1) and c(2) correspond to the reduction of Mo(VI) to Mo(V) and c(3) to the reduction of Mo(V) to Mo(III). And a(1) and a(2) correspond to the oxidation of Mo(V) to Mo(VI) and a(3) to the oxidation of Mo(III). As compared with dc polarogram c(1) corresponds to wave 1, c(2) to wave 3 and c(3) to wave 4. The assignment of c(2) to wave 3 is supported by the evidence that  $i_{pc(2)}$  is enhanced catalytically in the presence of perchlorate.

In cyclic voltammetry with HMDE, the characteristics of the electrode reaction is often examined by the dependence of the peak current on the scan rate of the potential,  $\nu$ . When the peak current is controlled by the diffusion of electroactive species, the peak current is practically proportional to  $\nu^{1/2}$  [1]. And when the peak current is controlled by adsorption of electroactive species, the current is proportional to  $\nu$  [2]. The dependence of  $i_{pc(1)}$  on  $\nu$  is shown in Fig.V-5. The plot is linear for various concentration of Mo(VI), indicating that the reactant of the electrode reaction adsorbs to the electrode.

Figure V-6 shows the cyclic voltammogram for Mo(VI) solution measured with an amalgamated gold ring-disc electrode. Though the electrode is rotated, the voltammogram for the disc electrode consists of the peaks, indicating that the strong adsorption of reactant or product takes place. At +0.25V of

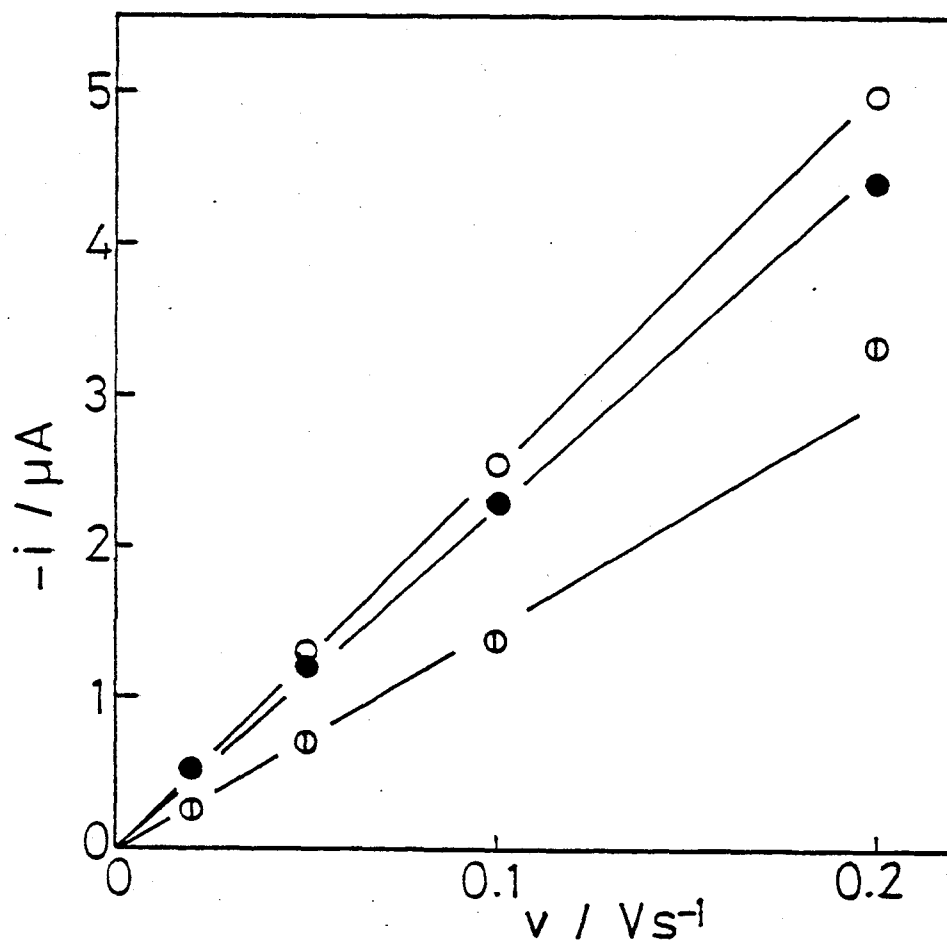


Fig.V-5. Dependence of  $i_{pc}(1)$  on the scan rate: (○) 2.0mM Mo(VI); (●) 0.5mM Mo(VI); (⊙) 0.1mM Mo(VI).

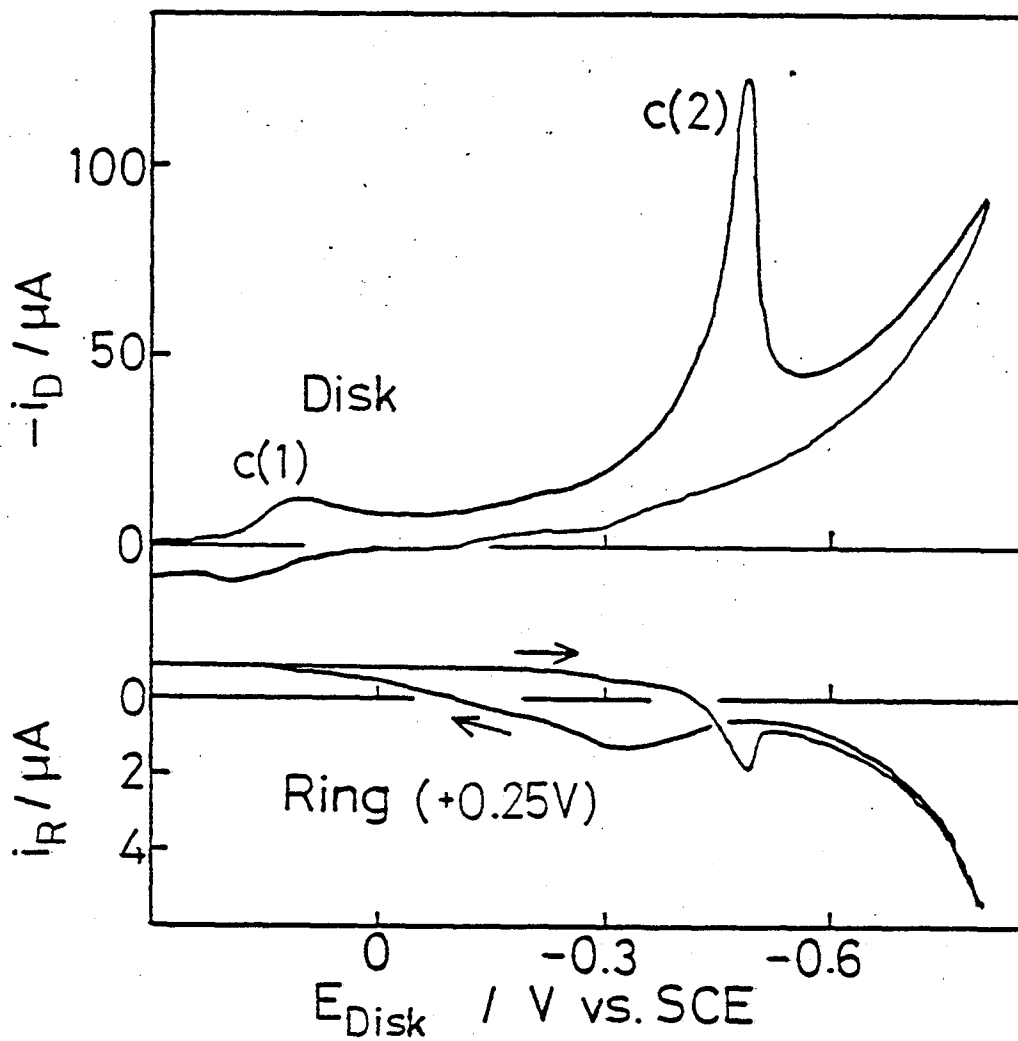


Fig.V-6. Cyclic voltammogram measured with amalgamated gold ring-disc electrode ( scan rate:  $0.1\text{Vs}^{-1}$ ; rotation speed: 2000rpm ).

the ring electrode no oxidation current is observed corresponding to a(1). Therefore, the reduction product at c(1) is fixed on the disc electrode. In fact, anodic current a(1) similar to that with HMDE is observed at the disc. The anodic current corresponding to a(2) is observed at the ring but the collection efficiency is quite small ( N is found to be about 0.07 when  $E_D$  is -0.47V ) compared with the theoretical one.

The cyclic voltammogram for 0.1mM Mo(VI) in 0.1M  $H_2SO_4$  is shown in Fig.V-7. For 0.5mM Mo(VI) c(2) is observed at more negative potential than that for wave 3 in dc polarogram ( Fig.V-3 ). While for 0.1mM Mo(VI), cathodic peak c(2)' ( -0.23V ) is observed at the potential of wave 3. It has been reported that the adsorption of the reactant causes the additional peak current at more negative potential than that for the diffusion current, and this peak is called post peak [2]. That is, c(2) is considered to be the post peak resulting from the adsorption of the reactant for wave 3. In fact,  $i_{pc(2)}$  is linearly dependent on  $v$ , while  $i_{pc(2)}'$  is not linearly dependent on both  $v$  and  $v^{1/2}$ , therefore, c(2)' is controlled by the competition of diffusion and adsorption of electroactive species as concluded for wave 3 in dc polarography ( chapter II ).

The dependence of  $i_{pc(3)}$  on  $v$  is shown in Fig.V-8. As  $v$  is increased the relative intensity of  $i_{pc(3)}$  to  $i_{pc(2)}$

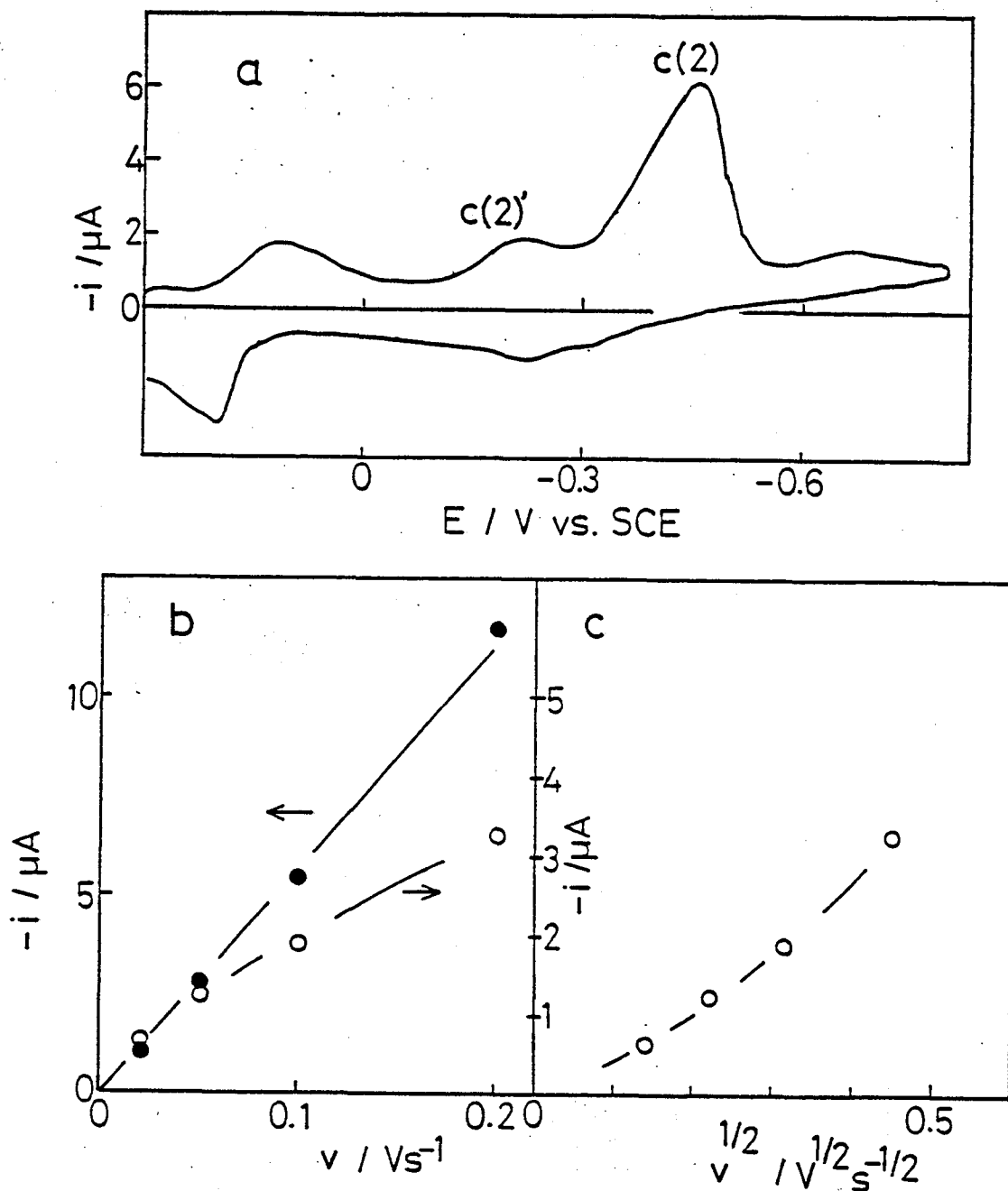


Fig.V-7. a. Cyclic voltammogram for 0.1mM Mo(VI) in 0.1M  $\text{H}_2\text{SO}_4$  ( scan rate:  $0.1Vs^{-1}$  ).  
 b. Dependence of the peak current on scan rate: ( $\bullet$ )  $i_{pc(2)}$ ; ( $\circ$ )  $i_{pc(2)}'$ .  
 c. Dependence of the peak current on a square root of scan rate: ( $\circ$ )  $i_{pc(2)}'$ .

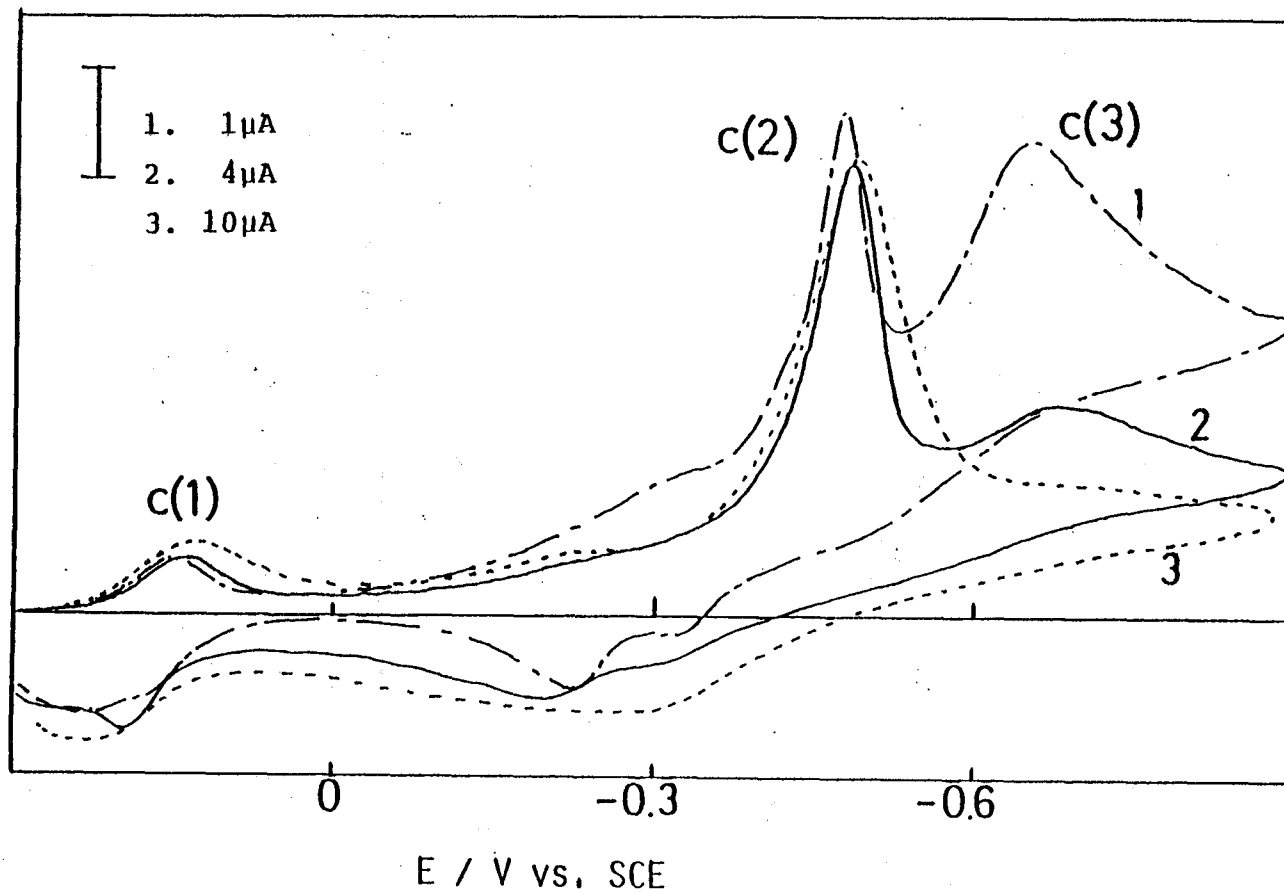


Fig.V-8. Cyclic voltammogram for 0.5mM Mo(VI) in 0.1M  $\text{H}_2\text{SO}_4$  for various scan rate: (1)  $0.02\text{Vs}^{-1}$ , (2)  $0.1\text{Vs}^{-1}$ ; (3)  $0.4\text{Vs}^{-1}$ .

is decreased. For Mo(V) solution, cathodic peak current corresponding to c(3) is linearly dependent on  $\nu^{1/2}$  as shown in Fig.V-9, indicating it is diffusion controlled. Therefore the reduction product of c(2) ( and c(2)' ) takes part in the preceding chemical reaction of wave 4. Fig.V-10 shows the DP polarograms of Mo(VI) and Mo(V). Peaks c(2) and c(3) correspond to the shoulder at about -0.5V and the peak at -0.60V for Mo(VI) respectively. In the presence of nitrate or perchlorate ion, the intensity of the shoulder is enhanced while that of the peak is slightly decreased. That is, the catalytically active species takes part in the preceding chemical reaction of wave 4.

Fig.V-11 shows the dependence of  $i_{pc}(2)$  and  $i_{pc}(3)$  on temperature. Fig.V-12 shows the temperature effect on the DP polarogram.  $i_{pc}(3)$  in the cyclic voltammogram and wave 4 in DP polarogram are extremely enhanced with temperature.

#### V-4 Discussion

The main object in this chapter is to elucidate the mechanism of the electrode reaction of wave 4. From the results obtained above, it is concluded that the preceding chemical reaction on wave 4 or c(3) is the transformation of the product of c(2). The reasons are as follows: (1) the



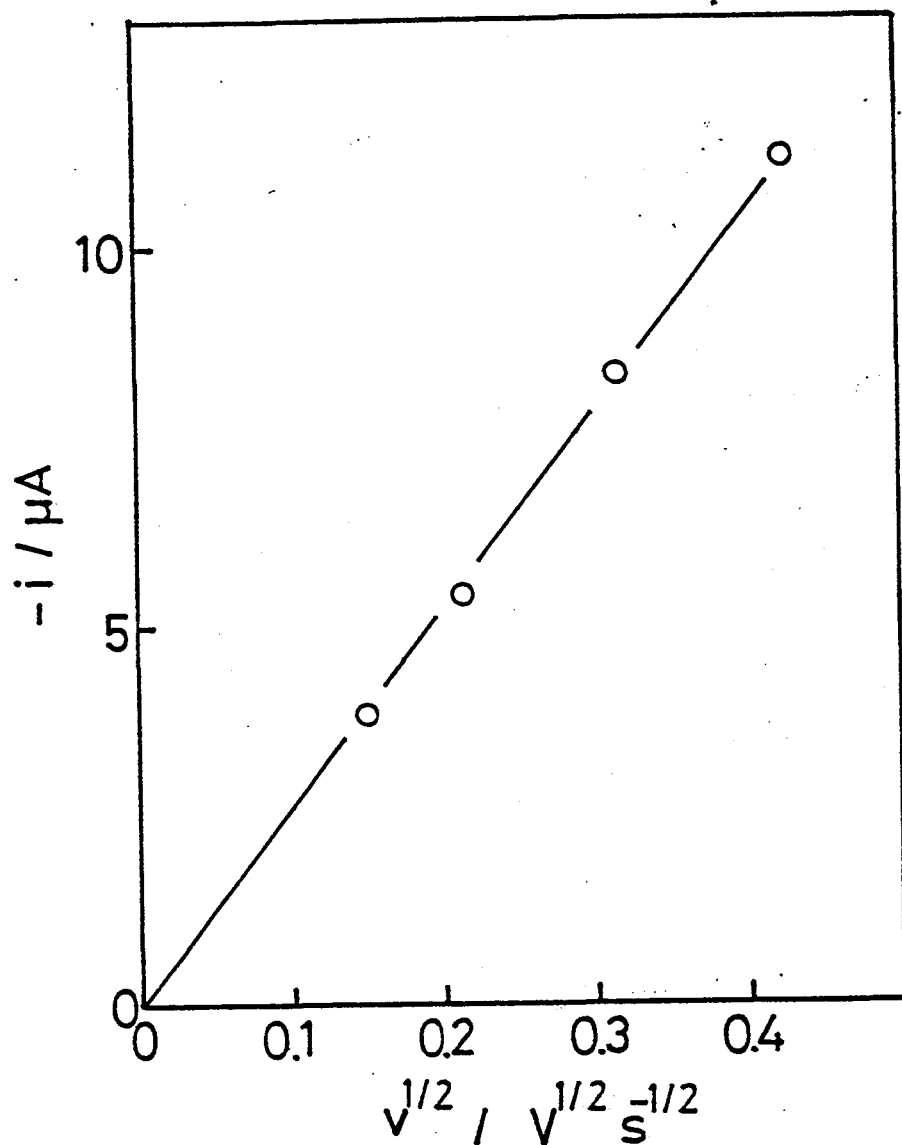


Fig.V-9. Dependence of  $i_{pc}$  for 0.5mM Mo(V) in 0.1M  $H_2SO_4$  on a square root of scan rate.

(101)

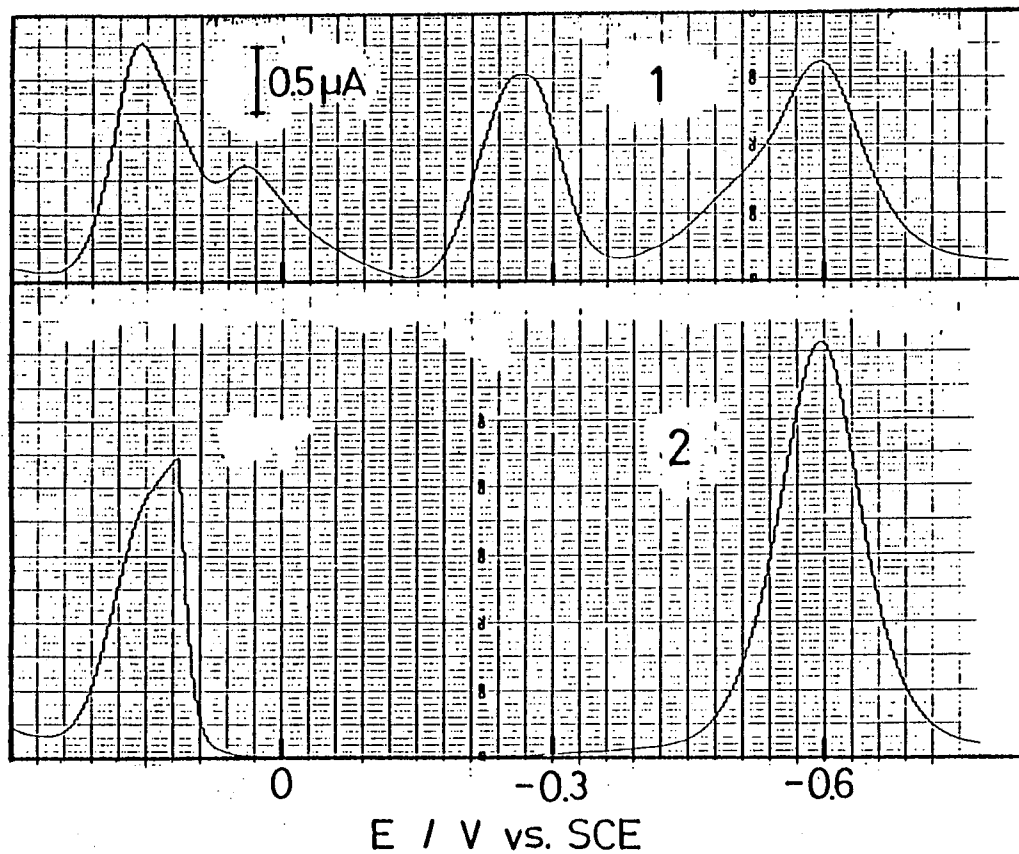


Fig.V-10. DP polarogram in  $0.1\text{M H}_2\text{SO}_4$ : (1)  $0.5\text{mM Mo(VI)}$ ;  
(2)  $0.5\text{mM Mo(V)}$ .  $t = 3.5\text{s}$

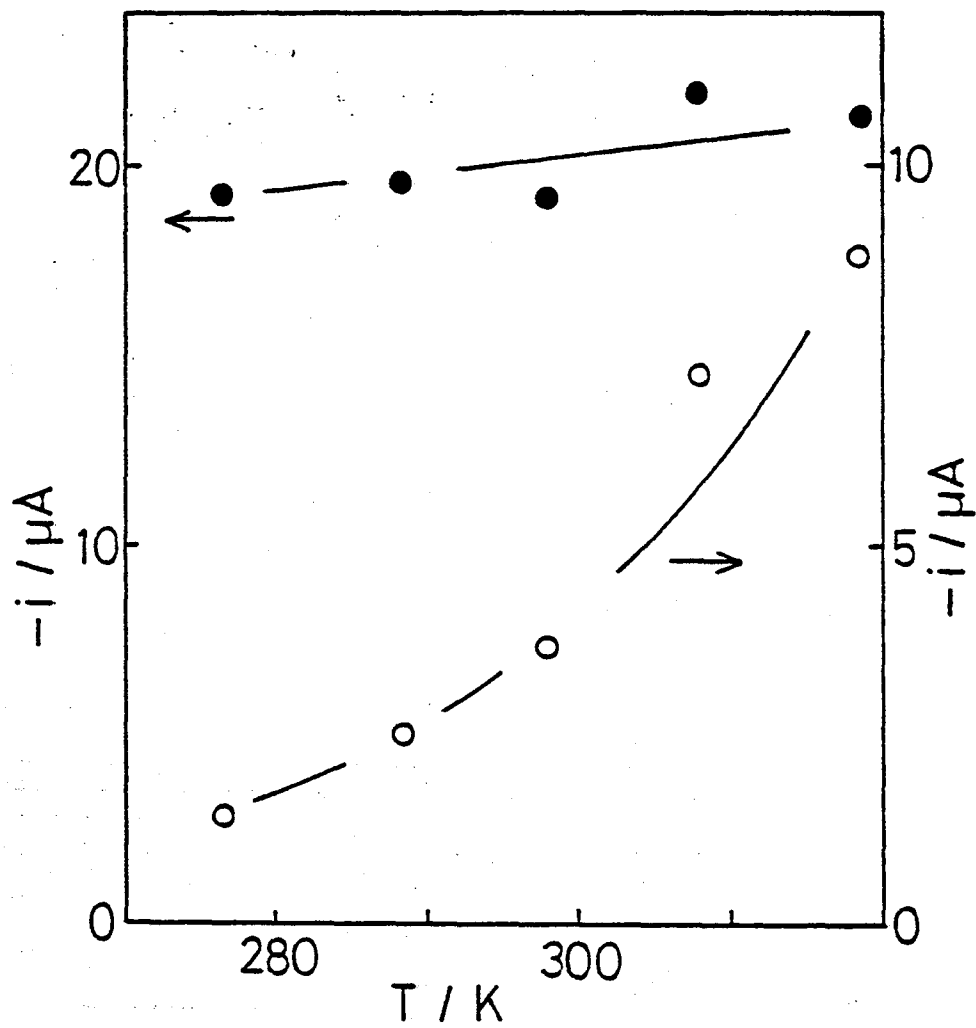


Fig.V-11. Dependence of peak height on temperature for 0.5mM Mo(VI) in 0.1M  $H_2SO_4$ : (●)  $i_{pc(2)}$ ; (○)  $i_{pc(3)}$ .

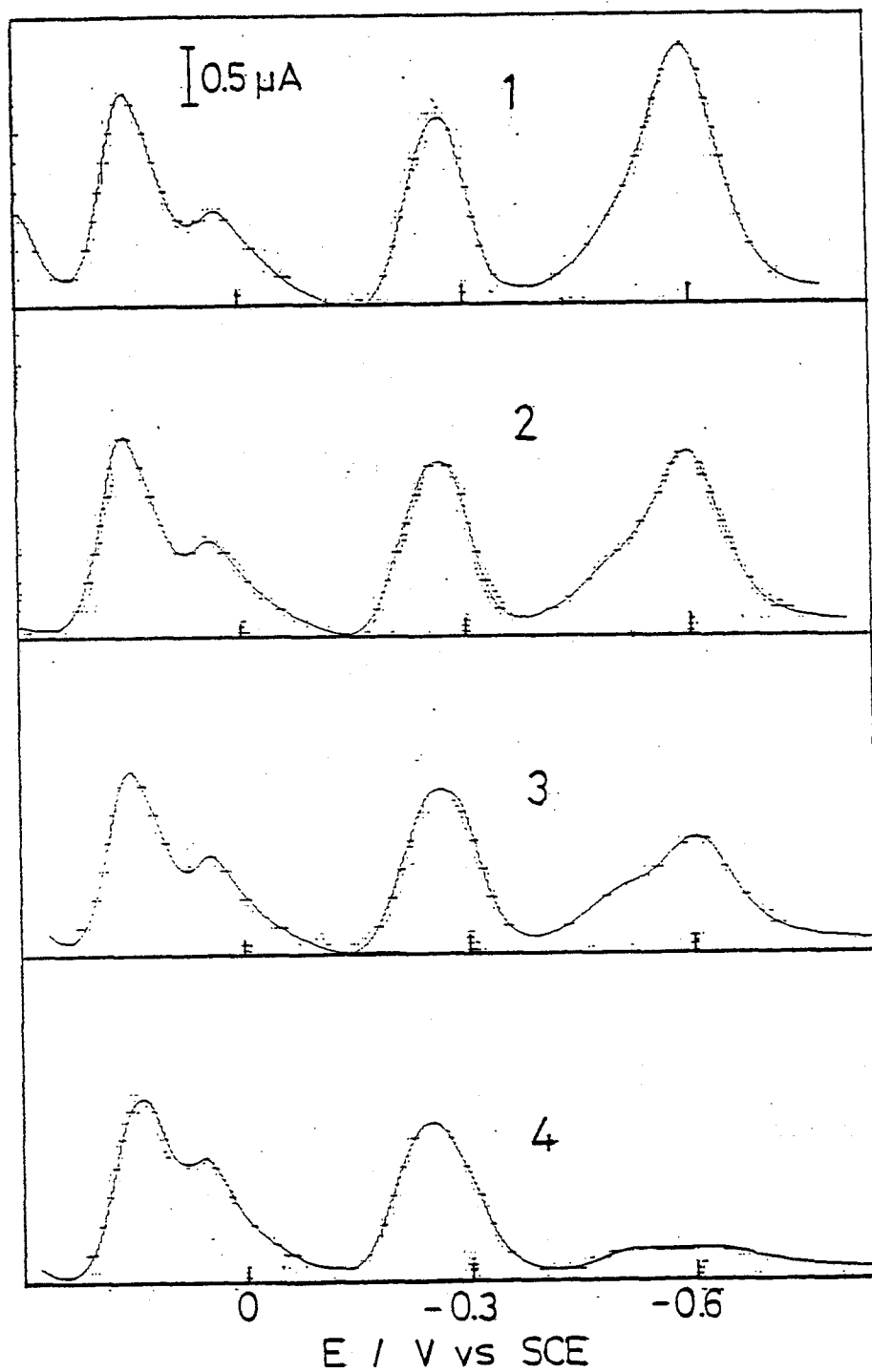
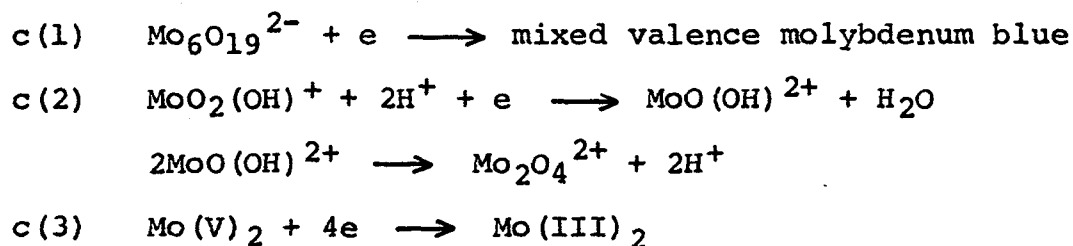


Fig.V-12. Effect of temperature on DP polarogram for 0.5mM Mo(VI) in 0.1M  $H_2SO_4$ : (1) 305K; (2) 298K; (3) 289.5K; (4) 273K.  $t = 3.5s$

reduction product of c(2) is Mo(V); (2) the reactant for c(3) is Mo(V) which is the same species as that existing as a stable species in 0.1M H<sub>2</sub>SO<sub>4</sub>; (3) in the presence of catalytic reaction on c(2), the height of wave 4 is decreased, because the production of the reactant for c(3) is prevented. It is known that the stable Mo(V) species in 0.1M H<sub>2</sub>SO<sub>4</sub> is of the dimeric form of Mo<sub>2</sub>O<sub>4</sub><sup>2+</sup> ( chapter IV ), while the reduction product on c(2) seems to be the monomeric form of MoO(OH)<sup>2+</sup> ( chapter III ). Therefore the preceding chemical reaction on wave 4 is the dimerization reaction of MoO(OH)<sup>2+</sup>. That is, the reaction from c(2) to c(3) proceeds in the form of ECE mechanism, electrochemical ( reduction on c(2) )-chemical ( dimerization )-electrochemical ( reduction on c(3) ). In differential pulse polarography, relative intensity of i<sub>p</sub>(4) to i<sub>p</sub>(3) gradually increases as C<sub>Mo(VI)</sub> is increased ( Fig.III-2 ). This phenomena is also considered to occur as the result of the second-order preceding chemical reaction of wave 4. The oxidant on c(1) is deduced to be Mo<sub>6</sub>O<sub>19</sub><sup>2-</sup> ( chapter II ), total reactions for c(1), c(2) and c(3) are described as follows:



From the data of Figs.V-3 and V-4, monomeric  $\text{MoO}(\text{OH})^{2+}$  and dimeric  $\text{Mo}_2\text{O}_4^{2+}$  are oxidized at  $-0.30\text{V}$  and about  $+0.2\text{V}$  respectively. These observations are consistent with the fact that oxidation of  $\text{MoO}(\text{OH})^{2+}$  with nitrate or perchlorate proceeds quite faster than that of  $\text{Mo}_2\text{O}_4^{2+}$  ( chapter IV ).

Dimerization of electrogenerated monomeric Mo(V) has been reported in tartrate buffer [3] and with catechol complex of Mo(V) [4]. In non-complexing acidic solutions ( in sulfuric acid [5] and in trifluoromethanesulfonic acid [6] ), different reaction mechanisms have been proposed about the most negative wave in dc polarogram ( wave 4 ) or the most cathodic peak in cyclic voltammogram ( c(3) ). One [5] is the reduction of Mo(VI) directly to Mo(III) and the other [6] is the reduction of dimeric Mo(V) to Mo(III) accompanying the the preceding reaction of dimerization of monomeric Mo(V). The work done in this chapter shows that the latter mechanism is most probable.

## Appendix 2    The rotating ring-disc electrode and the collection efficiency

Schematic illustrations of a ring-disc electrode is shown in Fig.2-1. The ring-disc electrode can be divided into three parts concentrically, i.e. the ring(A), insulator (B) and the disc(C). The radii,  $r_1$ ,  $r_2$  and  $r_3$  are as shown in the figure. The product of electrolysis at the disc electrode is transferred to the ring and then oxidized at the ring if the potential of the ring is fixed at sufficiently positive potential. In this case the collection efficiency,  $N$ , is defined the ratio of absolute value of the ring current to the disc current, i.e.  $i_R/i_D$ . When the electrode processes are rapid,  $N$  can be determined theoretically from the values of  $r_2/r_1$  and  $r_3/r_2$ . The value of  $N$  in the text is determined from the Table in ref.[7].

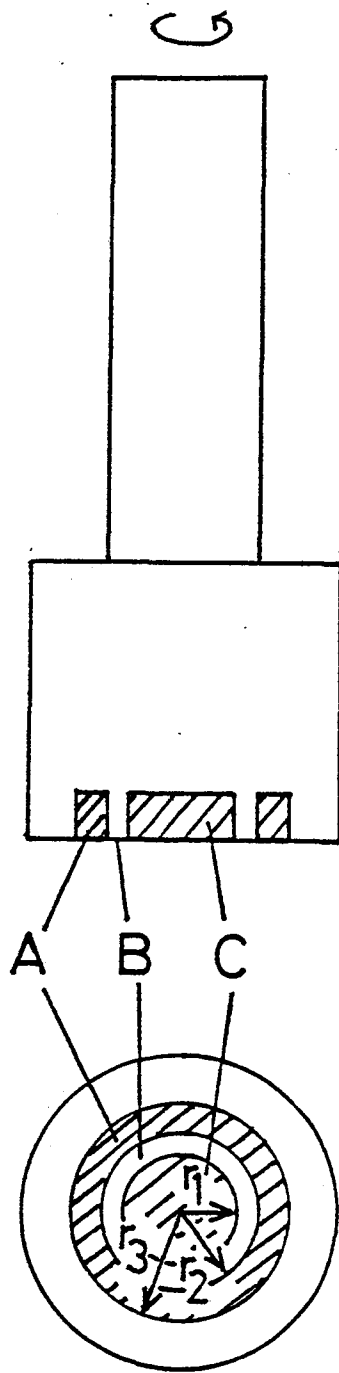


Fig.2-1. Schematic illustrations of a ring-disc electrode:  
(A) ring; (B) insulator; (C) disc.



V-5    References

1. R.H.Wopschall and I.Shain, *Anal.Chem.*, 39 (1967) 1514.
2. R.S.Nicholson and I.Shain, *Anal.Chem.*, 36 (1964) 706.
3. J.T.Spence and M.Heydanek, *Inorg.Chem.*, 6 (1967) 1489.
4. L.M.Charney and F.A.Schultz, *Inorg.Chem.*, 19 (1980) 1527.
5. M.N.Hull, *J.Electroanal.Chem.*, 51 (1974) 57.
6. M.T.Paffett and F.C.Anson, *Inorg.Chem.*, 20 (1981) 3967.
7. W.J.Albery and M.L.Hitchman, *Ring-Disc Electrode*, Clarendon Press, Oxford, 1971.

## VI Summary

The present investigation with respect to the electrode reaction of hexavalent molybdenum ion in sulfuric acid solution may be concluded:

(1) In 0.1M  $H_2SO_4$  four dc polarographic reduction waves ( waves 1-4 ) appear. Coulometric result indicates that the former three waves ( wave 1-3 ) correspond to the reduction of Mo(VI) to Mo(V) and the fourth ( wave 4 ) of Mo(V) to Mo(III). In the presence of nitrate or perchlorate the height of wave 3 is enhanced catalytically, and the catalytically active species is Mo(V). In 5M  $H_2SO_4$  three reduction waves appear, the first and the second waves correspond to the reduction of Mo(VI) and the third involves the reduction of Mo(VI) to Mo(V) and of Mo(V) to Mo(III).

(2) Tensammetric peak current based on the adsorption of Mo(VI) species is observed in DP and ac polarogram. The reactant of Mo(VI) on waves 1, 2 and 3 in 0.1M  $H_2SO_4$  are anionic, anionic and cationic respectively.

(3) In sulfuric acid solution as  $C_{H_2SO_4}$  is increased the stable species of Mo(V) is transformed from diamagnetic dimer,  $Mo_2O_4^{2+}$ , to paramagnetic dimer and to paramagnetic monomer. The oxidation reaction of the monomer with perchlorate proceeds more slowly than that of the catalytically active Mo(V), indicating that the electrogenerated catalytically

active Mo(V) is not the same species as the monomer in bulk solution.

(4) The reduction wave of Mo(V) to Mo(III) ( wave 4 ) for Mo(VI) solution accompanies the preceding chemical reaction. This chemical reaction is considered to be the dimerization of electrogenerated catalytically active Mo(V) to the stable dimeric form of  $\text{Mo}_2\text{O}_4^{2+}$ .

In the history of polarographic study of Mo(VI), many different conclusions have been proposed. Taking the coulometric results, the catalytic effect and the preceding chemical reaction into consideration, reasonable electrode reaction mechanisms for the polarography of Mo(VI) are obtained in this work.

## Acknowledgement

The author wishes to express his greatest gratitude to Professor Shigero Ikeda for his kind suggestion and support in coordinating this work.

The author also would like to express his hearty thanks to Dr. Iwao Watanabe for his helpful discussion and accurate instruction.

The author is grateful to Dr. Mikiharu Kamachi for obtaining the esr spectra.

The author is also grateful to many members of Ikeda laboratory for their helpful advice and assistance.

Papers relevant to the present study

- 1) Polarographic study of Mo(VI) in aqueous sulfuric acid solutions  
K.Yokoi, T.Ozeki, I.Watanabe and S.Ikeda,  
J.Electroanal.Chem., 132 (1982) 191.
  
- 2) Polarographic study of Mo(VI) in 0.1-5M sulfuric acid solutions  
K.Yokoi, T.Ozeki, I.Watanabe and S.Ikeda,  
J.Electroanal.Chem., 133 (1982) 73.
  
- 3) Differential pulse and alternating current polarographic study of Mo(VI) in sulfuric acid solutions  
K.Yokoi, N.Ogawa, I.Watanabe and S.Ikeda,  
J.Electroanal.Chem., 153 (1983) 255.
  
- 4) Kinetic studies on the oxidation of the electrogenerated Mo(V) and stable monomeric Mo(V) in sulfuric acid solution  
K.Yokoi, I.Watanabe and S.Ikeda,  
to be submitted.
  
- 5) ECE mechanism in electrochemistry of Mo(VI) in sulfuric acid solution  
K.Yokoi, I.Watanabe and S.Ikeda, to be submitted.